JUSTUS-LIEBIG-UNIVERSITÄT GIESSEN

Impact of polyunsaturated omega-6 and omega-3 fatty acids on cardiomyogenesis and vasculogenesis of mouse embryonic stem cells

Inaugural dissertation submitted to the Faculty of Medicine
in partial fulfillment of the doctoral degree in human biology at
Justus Liebig University Giessen

Submitted by

Amer Hussein Taha

From

Mosul, Iraq

Giessen 2022

From the Institute of Physiology
Faculty of Medicine of the Justus Liebig University Giessen

First Supervisor and Committee Member: **Prof. Dr. Heinrich Sauer**
Second Reviewer and Committee Member: **Jun.-Prof. Dr. Elie El Agha**

Date of Doctoral Defense: **03. 02. 2022**

Dedication

I am writing my thesis and would like to dedicate it to my parents. However, they passed away while I was studying. Also, I would like to dedicate it to:

my sons Ali, Majd, and Yaman.

my lovely wife Rasha.

Amer

Table of Contents

1. Introduction

1.1 Essential fatty acids

The term essential fatty acids (EFAs) refers to those polyunsaturated fatty acids (PUFAs) that have the necessity to be provided by food because they cannot be synthesized in the human body. PUFAs are important for health and may contribute significant advantages in addition to fundamental nutrition. There are two major families of EFAs, omega-3 (ω-3) (i.e. α-linolenic acid (ALA)) and omega-6 (ω-6) (i.e. linoleic acid (LA)). These EFAs produce very long-chain PUFAs (more than 22 C-atoms) during cascade of elongation reaction (Das, 2006; Kaur et al., 2014). In the late 1920s, they were first reported as essential in the diet (Shireman, 2003). Ω-3 and ω-6 PUFAs are beneficial elements of oils with specific dietary and functional characteristics. Their therapeutic and health-promoting impacts have already been discovered in several chronic inflammatory and autoimmune diseases through various mechanisms, including modifications in cell membrane lipid composition, gene expression, cellular metabolism, and signal transduction (Balić et al., 2020).

1.2 Fatty acid structure and classification

Fatty acids consist basically of chainlike structure with a methyl group at one end of the molecule (designated omega, ω) and a carboxyl group at the other. The second carbon atom located after the carboxyl group is called α-carbon atom, and the next one called β-carbon atom. According to the ω-x notation, the letter *n* indicates the position of the double bond nearest to the methyl end (ω) in carbon chains (figure 1.1). The nomenclature of fatty acids may also depend on the location of double bonds with a citation to the carboxyl group (Δ) (figure 1.2) (Rustan & Drevon, 2001).

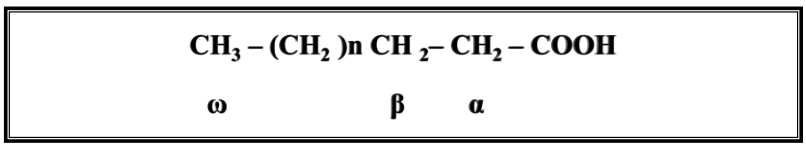

Figure 1.1: The basic structure of fatty acids. The fatty acid chain has two different ends, (COOH) refers to the carboxyl end, and the other end is a methyl group (CH_3) named by the last letter of the Greek alphabet (ω). The letter (*n*) indicates the location of the

double bond nearest to the ω methyl group. Figure adapted with permission from (Rustan & Drevon, 2001); copyright 2001 John Wiley and Sons.

Fatty acids present in two main groups: Saturated fatty acids, in which the carbon atoms are bound by hydrogen atoms. Most saturated fatty acids are straight hydrocarbon chain molecules, i.e. Palmitic acid (PA;16:0) and Stearic acid (18:0). PA is the most well-known saturated fatty acid estimating for 20–30% of total fatty acids in the human body, and can be obtained in the diet or synthesized endogenously through de novo lipogenesis. (Carta et al., 2017; Rustan & Drevon, 2001). The other group comprises of unsaturated fatty acids such as monounsaturated fatty acids (MUFAs), which have one carbon-carbon double bond. Their carbon-carbon double bond can occur in different positions. The most common monoenes have a double bond in cis configuration, which means that the hydrogen atoms on the same side of the double bond are oriented in the same direction. Cis configuration in the structure gives it a "kink" to form a different secondary structure, which may change their physical properties (Jump et al., 2012). PUFAs have more than one carbon-carbon double bond. There are two families of PUFAs, ω-3 and ω-6. **Ω**-3 fatty acids have in common a closing carbon-carbon double bond in the ω-3 position, the third bond from the methyl end of the fatty acid, while ω-6 fatty acids have it in the ω-6 position i.e. the sixth bond from the methyl end of the fatty acid (figure 1.2) (Kaur et al., 2014).

$^{\omega}$-characteristics	Methyl end Carboxyl end	Saturation	$^{\Delta}$-characteristics
PA 16;0	CH_3 COOH	saturated	16:0
Stearic 18;0	CH_3 COOH	saturated	18:0
Oleic 18:1, ω-9	CH_3 COOH	monoene	18:1 Δ9
LA 18:2, ω-6	CH_3 COOH	polyene	18:2 Δ9, 12
ALA 18:3, ω-3	CH_3 COOH	polyene	18:3 Δ9, 12, 15

Eicosapentaenoic acid (EPA) 20:5, ω-3	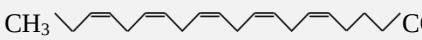	polyene	20:5 Δ5, 8, 11, 14, 17
Docosahexaenoic acid (DHA) 22:6, ω-3		polyene	22:6 Δ4, 7, 10, 13, 16, 19

Figure 1.2: Schematic overview of the structures of different unbranched fatty acids with a methyl and a carboxyl (acidic) end. Figure adapted with permission from (Rustan & Drevon, 2001); copyright 2001 John Wiley and Sons; Panel PA adapted from (Shah & Cox, 2009) licensed under Creative Commons Attribution 2.0 Generic (CC BY 2.0).

1.3 Metabolism of PUFAs

Ω-3 and ω-6 PUFAs are provided from different food sources in triglyceride form. When consumed in the diet, triglycerides undergo digestion in the small intestine, which allows absorption, transport via blood and assimilation in the different organs of the body like the brain, heart, and other tissue. These fatty acids can be metabolized in different metabolic pathways:

(1) β-oxidation to give energy in adenosine triphosphate (ATP) form.

(2) Esterification into various cellular lipids as triglycerides, cholesterol ester and phospholipids.

(3) Transformation into longer chain and more unsaturated products, which are formed by a series of desaturation and elongation reactions. This process takes place mainly in the liver and to a minor degree in other tissues (Kaur et al., 2014).

LA and ALA can be only obtained from dietary sources because the human body lacks the enzymes delta-Δ12 and delta-Δ15-desaturase, which are present in plants and are necessary for *de novo* synthesis of PUFAs (Kaur et al., 2014; Wallis et al., 2002). Hence, the LA and ALA undergo a series of desaturation and elongation reactions (Jump et al., 2012; Nakamura & Nara, 2004). Desaturation is the addition of a double bond to the fatty acid structure by the presence of fatty acid desaturase enzymes (FADS), i.e., delta-5 desaturase (D5D) FADS1 (Δ^5-desaturase) and delta-6 desaturase (D6D) FADS2 (Δ^6-desaturase) which perform acyl chain desaturation of PUFAs. Elongation is a condensation reaction, which is catalyzed by elongase enzymes referred to as elongation of very long-chain fatty

acids (ELOVLs) which add two carbon atoms. Elongation is required for the generation of very long-chain fatty acids (VLCFAs) (Denic & Weissman, 2007; Lee et al., 2019; Moon et al., 2001; Oh et al., 1997). There are three types of (ELOVLs): ELOVL2, ELOVL4, and ELOVL5 being selective for PUFAs (Agbaga et al., 2008; Kitazawa et al., 2009; Leonard et al., 2000; Moon et al., 2001; Tamura et al., 2009; Tvrdik et al., 2000; Wang et al., 2005). LA and ALA are digested by desaturase and elongase enzymes during metabolic reactions, and both serve as precursors to produce essential longer PUFAs such as ω-6 gamma-linolenic acid (GLA), dihomo-gamma-linolenic acid (DGLA**)**, arachidonic acid (AA) and docosapentaenoic acid (DPA) from LA, while ω-3 stearidonic acid (SDA), eicosatetraenoic acid (ETA), and EPA from ALA, which play an essential roles in the physiological metabolism (figure 1.3) (Jump, 2002; Jump et al., 2012; Nakamura & Nara, 2004).

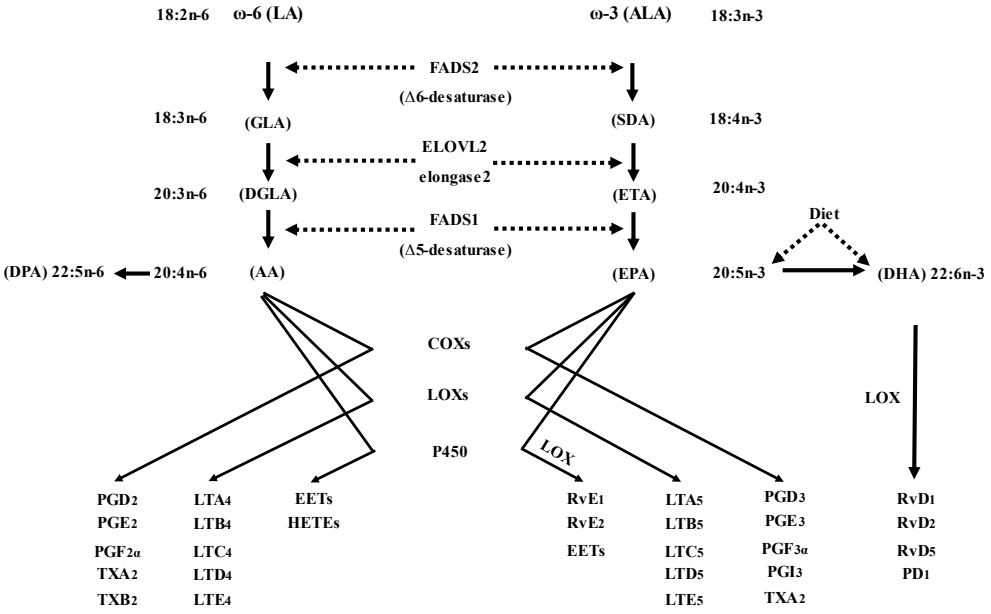

Figure 1.3: Long chain unsaturated fatty acid synthesis from the EFAs such as LA and ALA in mammalians. Eicosanoids such as prostaglandins (PGs), leukotrienes (LTs), thromboxanes (TXs), resolvins (Rvs), epoxyeicosatrienoic acids (EETs) and 5-hydroxyeicosatetraenoic acids (HETEs) are synthesised from AA and EPA by lipoxygenases (LOXs), cyclooxygenases (COXs) and cytochrome P450 (CYP) enzymes. Furthermore, Rv, as well as protectins D1 (PD1), are synthesised from DHA. Figure adapted with permission from (Kang et al., 2014); copyright John Wiley and Sons.

1.4 Sources of PUFAs

1.4.1 Sources of ω-3 as EPA

ALA is plentiful in flaxseed as well as in hemp, walnut, soybean, and canola oil (Hunter, 1990). It is mainly present in the chloroplast of green leafy vegetables. Furthermore, ALA can be converted during metabolism into other important PUFAs such as EPA. Fish and fish oil are major sources for EPA, the content of EPA in fresh and saltwater fish can be estimated to 39%-50%. Additionally, EPA is considered as a parent of series 3-eicosanoid hormones. DHA is also present in red-brown algae. The human brain consists of 65% fat, half of this is DHA (Kinsella, 1990).

1.4.2 Sources of ω-6 as LA

LA is plenteous in safflower, sunflower, and corn, while medium amounts are present in soybean, sesame and almonds. Canola, peanut and olive oils contain LA in small amounts, and coconut and palm kernel contain only very low amounts. LA can be converted to other ω-6 fatty acids depending on the body's requirements (Kaur et al., 2014). Evening primrose oil contains GLA, which is one of the products of LA metabolism, to about 7-10%, (Høy et al., 1983). Black currant and borage contain (15–20g/100g) and (18–26g/100g), respectively (Lawson & Hughes, 1988). Organ meat and breast milk contain a small quantity of it. AA is produced in more LA's metabolism. It is present in meat, eggs and dairy products. (Horrobin, 1990).

1.5 Stem cells

Stem cells are undifferentiated cells that can renew and give daughter cells by keeping their properties as stem cells or use the process of differentiation dependent on signals taken from their neighborhood. They have two main properties, first: they have the potential to retain their self-renewal infinitely, that means, keeping their undifferentiated state through infinite cycles of cell division, and second: differentiation potency, their potential to convert into different organo-typic cells (Friel et al., 2005).

1.5.1 Classification of stem cells based on their differentiation potency

Dependent on the differentiation potential of stem cells, they can be classified into different types. Therefore, the classes of stem cells regarding their plasticity are: Totipotent, pluripotent, multipotent, oligopotent and unipotent (figure 1.4) (Majo et al., 2008; Niwa, 2007; Rajabzadeh et al., 2019).

Totipotent stem cells: these stem cells are capable of developing into a complete organism or in other words, these cells can differentiate into any cell or tissue (Condic, 2013). Totipotent are cells that arise from zygotes (a one-cell embryo) and exist until the morula stage of embryogenesis (early stage of the blastocyst). A totipotent cell is also a one-cell embryo; that is, a cell that is capable of generating a globally coordinated developmental sequence (Condic, 2013; Niwa, 2007). Somatic stem/progenitor cells and primitive germ-line stem cells originate from totipotent stem cells (Weissman, 2000; Zakrzewski et al., 2019).

Pluripotent stem cells: Pluripotent stem cells have the potential to generate many but not all types of cells, because some of their differentiation potency has been lost. They arise from totipotent stem cells and exist in the inner cells mass (ICM) (Niwa, 2007). Pluripotent stem cells can differentiate into approximately all cells, i.e., cells derived from any of the three germ layers (ectoderm, mesoderm and endoderm), and these pluripotent cells are considered true stem cells because they own self-renewal and differentiation potential for all cell types of the adult organism (Baker & Pera, 2018; Horie et al., 2011). For example, embryonic stem cells (ES cells) have been listed within this classification. Therefore, human pluripotent stem cells are an invaluable tool for *in vitro* studies of human embryogenesis (Shamblott et al., 1998).

Multipotent stem cells: Multipotent stem cells are characterized by the capability of self-renewal, and differentiate into various types of cells. They can only differentiate into closely related cells in a specific tissue, organ or system (Niwa, 2007). Furthermore, multipotent stem cells can only differentiate into a limited number of cell types, for example, hematopoietic stem cells. Moreover, multipotent stem cell produce multiple

blood cell progenitors (Quintana & Grosveld, 2011). Additionally, adipose tissue is considered as one of the sources for multipotent stem cells (Zuk et al., 2002).

Oligopotent stem cells: Oligopotent stem cells can differentiate into only very few cell types, including stem cells residing on the mammalian ocular surface (Majo et al., 2008).

Unipotent stem cells: Unipotent stem cells are capable to generate cells with only one lineage differentiation, example is: muscle stem cells (Kalra & Tomar, 2014). They have self-renewal property as well. Most epithelial tissues self-renew throughout adult life due to the presence of unipotent progenitor cells (Blanpain et al., 2007).

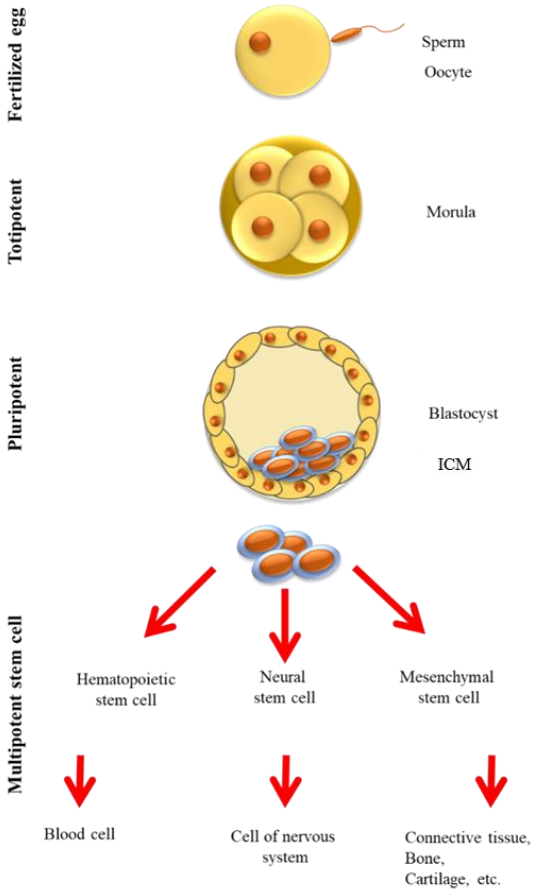

Figure 1.4: Diagram overview of stem cells types regarding their potency. This figure was modified from (Rajabzadeh et al., 2019).

1.5.2 ES cells

ES cells are pluripotent stem cells, which have a high capability to undergo unlimited proliferation and self-renewal *in vitro* for an extended time period, and differentiate into all cell types in the body. Thus, they have potential for the therapy of various degenerative diseases (Khan et al., 2018; Papatsenko et al., 2018). Their pluripotent states can be maintained *in vitro* by a network of signaling, transcriptional and epigenetic regulatory synergies known as the pluripotency gene regulatory network (PGRN) (Davidson et al., 2015; Papatsenko et al., 2018). In cell culture conditions, cytokines and other factors have been demonstrated to preserve stem cell pluripotency by activation of specific transcriptional and epigenetic regulators (Morey et al., 2015). PGRN has been described as a series of hierarchical levels, determined according to the propagation of biological signals in ES cells, which are initiated with cell signaling to transcription and epigenetic factors (figure 1.5) (Papatsenko et al., 2018).

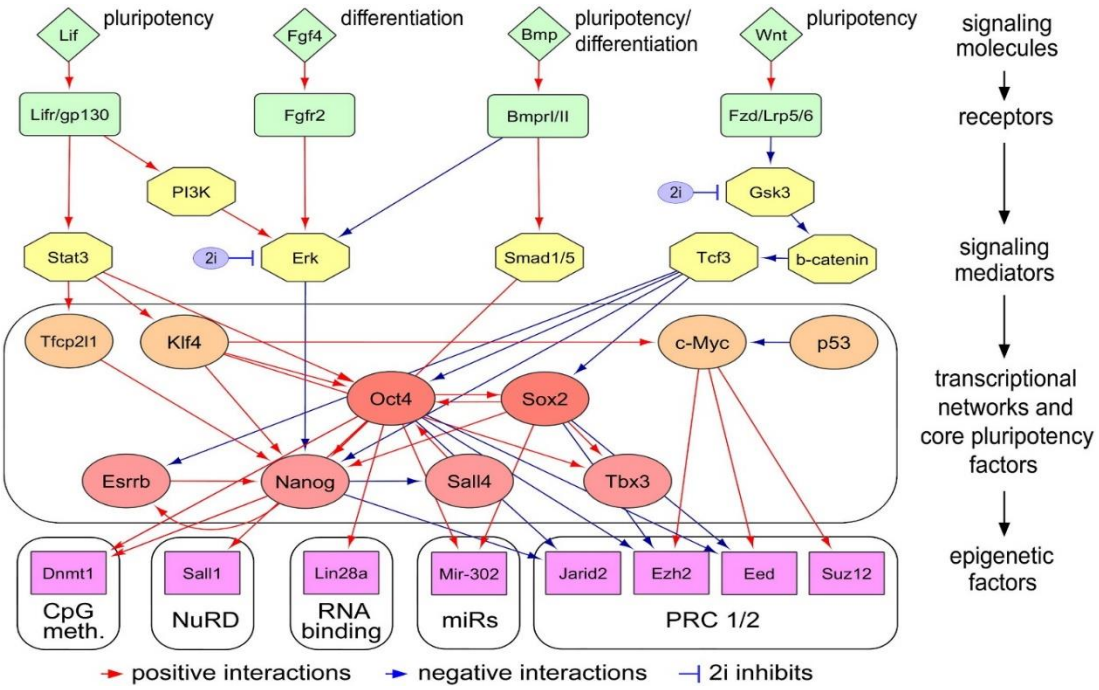

Figure 1.5: Hierarchical organization of the PGRN. Signal pathways represent the first hierarchical level (in green). Signal pathway mediators (in yellow) represent the second hierarchical level. Components of the transcriptional pluripotency network (red) represent the following levels. Lowest levels of the pluripotency network (in violet) include components of epigenetic complexes involved in chromatin modification, DNA

methylation and regulation at posttranscriptional levels, as indicated. Red and blue arrows show positive and negative interactions correspondingly; blue T-arrows show targets of inhibitors for "2i" conditions. Figure adapted from (Papatsenko et al., 2018) licensed under Creative Commons Attribution Non-Commercial No Derivatives (CC-BY-NC-ND).

ES cells are able to remain in pluripotency state by providing them with nutrients and cytokines, such as leukemia inhibitory factor (LIF) and respond to WNT, bone morphogenetic protein (BMP) and fibroblast growth factors (FGF). (Itoh et al., 2014; Lakatos et al., 2014; Malaguti et al., 2013). The first responses to extracellular signals are mediated by cellular receptors such as LIF, WNT, BMP, and FGF. Therefore, these molecules may be supposed as the top hierarchical level, which downstream transfers the input information within the PGRN (Papatsenko et al., 2018). The second hierarchical level is initiated by factors such as signal transducer and activator of transcription 3 (Stat3), Smads, β-catenin, and extracellular signal-regulated kinase (Erk) which are effectors of LIF, BMP, WNT and FGF signaling pathways, respectively (Itoh et al., 2014; Lakatos et al., 2014; Tai & Ying, 2013; Van Oosten et al., 2012). Signals from the effectors are forwarded to many downstream targets, including the core pluripotency network (CPN), which includes transcription factors such as octamer-binding transcription factor 4 (Oct4), Sex-determining region Y/Box 2 (Sox2), nanog homeobox protein (Nanog), estrogen-related receptor beta (Esrrb), T-box transcription factor 3 (Tbx3), c-Myc and others, which control inputs from signaling systems and perform decisions associated with self-renewal or differentiation (Boyer et al., 2005; Dunn et al., 2014; Xu et al., 2014), The lower position in the PGRN network is occupied by the epigenetic regulation. Moreover, the transcription events of pluripotency include changes in the epigenetic landscape, including chromatin remodeling and deoxyribonucleic acid (DNA) methylation (figure 1.5) (Kobayashi & Kikyo, 2015). Recently, evidence has been provided, that in addition to growth factors and extracellular matrix cues, many metabolic pathways definitively provide essential signals for the self-renewal and differentiation potential of stem cells (Hu et al., 2016). Historically, murine ES cells were isolated and established in 1981 (Evans & Kaufman, 1981). Later, in 1998, Thomson and his team were the first to derive human embryonic stem cells (hESCs) from human blastocysts (Thomson et al., 1998). After a few years, in 2006, Takahashi and Yamanaka demonstrated

transdifferentiation of pluripotent stem cells from mouse embryonic or adult fibroblasts by introducing four factors, Oct3/4, Sox2, c-Myc, and kruppel-like factor 4 (Klf4), under ES cell culture states. These cells were called induced pluripotent stem cells (iPSCs) (Takahashi & Yamanaka, 2006).

1.6 Vasculogenesis

The creation of new blood vessels is a necessary step in the development of tissues. During embryogenesis and in *in vitro* models, the blood vessels provide the growing tissue with nutrients and oxygen. They remove waste products, transport macromolecules (e.g. hormones, growth factors and cytokines), exchange liquids between tissues and organs, and transport immune cells to sites of inflammation or infection. Other functions of blood vessels are the maintenance of steady body temperature and pH to keep homeostasis. (Adams & Alitalo, 2007; Aird, 2006; Jakobsson et al., 2007; Sweeney & Foldes, 2018). Vasculogenesis refers to *de novo* blood vessel formation from progenitor cells, while angiogenesis denotes migration, branching, and remodelling of pre-existing blood vessels to form complex vascular networks and capillary beds (figure 1.6) (Risau & Flamme, 1995). Endothelial cells are the basic unit of blood vessels, and are capable of creating a tube-like structure (Stratman et al., 2009; Sweeney & Foldes, 2018). Doetschman and his colleagues demonstrated in 1985, that endothelial cell development and subsequent vascular morphogenesis in differentiating ES cells cultures occurs in an *in vivo*-like fashion (Doetschman et al., 1985). During embryogenesis, blood vessel formation takes place in the yolk sac originating from groups of cells, which are called primitive endothelial cells and express endothelial markers such as vascular endothelial growth factor receptors (VEGFRs), vascular endothelial cadherin (VE-Cadherin), and cluster of differentiation 31 (CD31) (Platelet endothelial cell adhesion molecule (PECAM-1)) (Breier et al., 1996; Risau & Flamme, 1995). During the first steps of vasculogenesis primitive endothelial cells derive from the mesodermal layer of the embryo, migrate to form blood islands and differentiate into either hematopoietic cells in the central core or angioblastic cells (the precursors of endothelial cells) at the periphery of the blood islands (Gonzalez-Crussi, 1971). Angioblasts flatten and create intercellular connections to form a circumferential

layer of primitive endothelial cells (figure 1.6) (Heinke et al., 2012; Risau & Flamme, 1995). Vascular development in differentiated ES cell cultures progresses through the same steps of vasculogenesis and angiogenesis as in the *in vivo* situation (Risau, 1997).

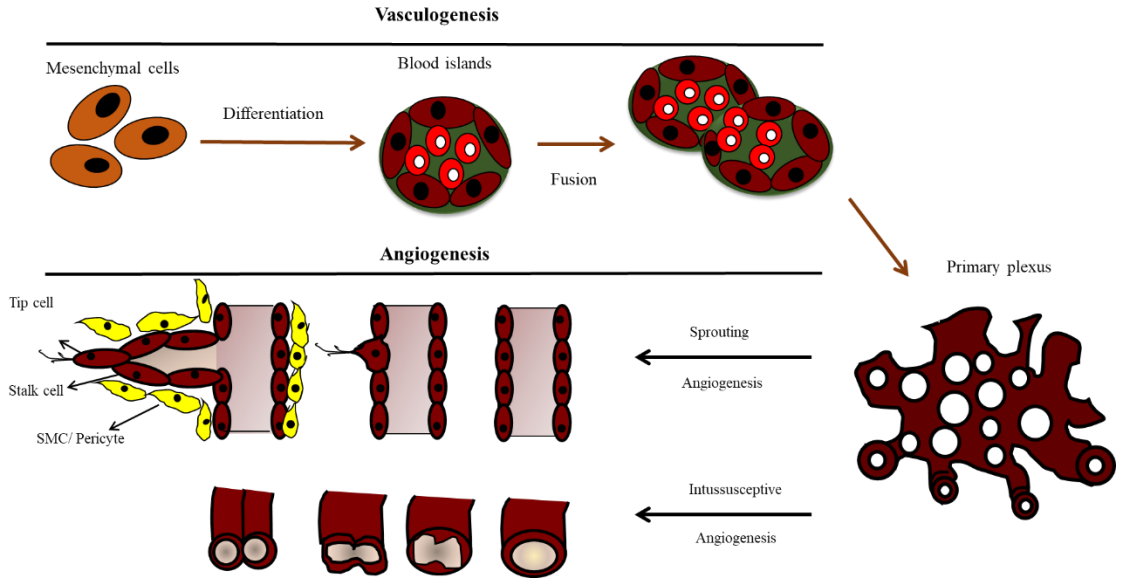

Figure 1.6: Illustration of vasculogenesis and angiogenesis during blood vessel formation. Vasculogenesis requires the differentiation of endothelial cells from angioblast cells to form a primitive vascular plexus. Mesodermal cells differentiate toward haemangioblasts, which more progress into angioblast. Developing processes of these pre-existing vessels is termed angiogenesis, which occurs in two manners: Intussusceptive angiogenesis and/or sprouting angiogenesis. Figure adapted with permission from (Heinke et al., 2012); copyright 2012 Frontiers in Bioscience.

Angiogenesis occurs by two fundamental mechanisms: i) non-sprouting (intussusceptive) angiogenesis, which involves splitting of existing blood vessels by the creation of translumen pillars and growing of vessels. ii) Sprouting angiogenesis, where in growing branches of blood vessels, endothelial cells proliferate behind tip cells in response to cytokines, and lumens are formed by vacuole fusion. Angiogenesis requires the recruitment of smooth muscle cells (SMCs) or pericytes to fix the nascent vessels (Heinke et al., 2012; Risau, 1997).

1.7 Cardiomyogenesis

Cardiomyocytes arise from differentiation of pluripotent ES cells. These cells include all specialized cell types of the heart, such as atrial-like, ventricular-like and sinus nodal-like

cells. The process of cardiomyogenic differentiation occurs in early stages of embryo development and is called cardiomyogenesis (Boheler et al., 2002). During the early stage of differentiation within a three-dimensional tissue of ES cells, named embryoid body (EB), the cardiomyocyte is characterized by single nucleus with a small and round shape which expresses on day 3 of differentiation the cardiac transcription factors Nkx2.5, myocyte enhancer factor 2C (MEF2C) and GATA4 (Wei et al., 2005). Growing myofibrils are sparse and irregularly organized. During further differentiation parallel bundles of myofibrils showing A and I bands are occurring (Westfall et al., 1997). During maturation cardiomyocytes become elongated with well-developed myofibrils and sarcomeres. Spontaneously contracting cardiomyocytes contain cell-cell junctions and are primarily mononucleated and rod-shaped (Westfall et al., 1997). In the final stage of differentiation, the bundles of myofibrils are densely packed and well-organized, and A, I bands and Z disks are organized into sarcomeres (Fassler et al., 1996; Westfall et al., 1997). In addition, cardiac-specific genes and proteins are expressed in parallel with ion channels (Boheler et al., 2002). Transcription factors such as zinc-finger GATA (GATA-4) protein and Nkx-2.5 regulate heart development together with several factors and signaling molecules (Sachinidis et al., 2003). Cardiac cell formation is organized by the sequential expression of multiple signal transduction proteins and transcription factors operating in a combinatory manner. Numerous studies have reported that Wnts/Nodal, BMPs, and FGFs are implicated in the development of specialized cardiac subtypes (figure 1.7) (Marvin et al., 2001; Zhang & Bradley, 1996).

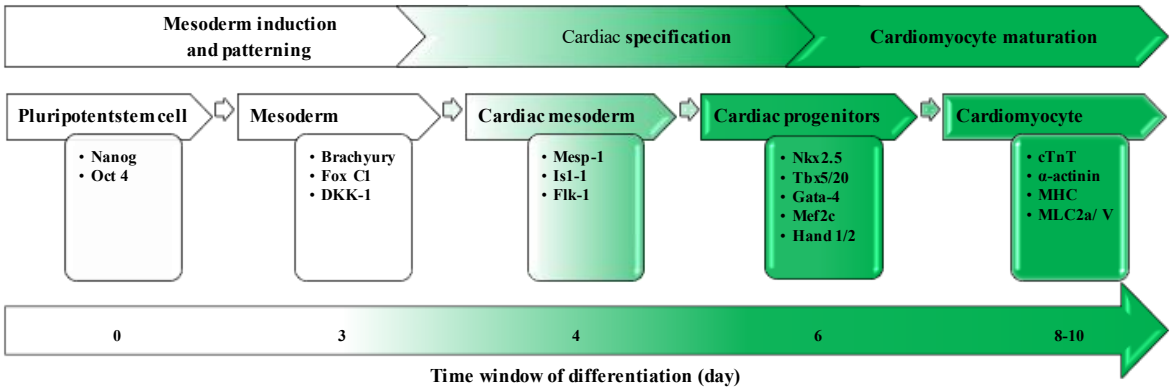

Figure 1.7: Sequential steps within the differentiation time window of pluripotent ES cells to obtain maturated cardiomyocytes. The figure was modified from (Rajala et al., 2011; Willems et al., 2009).

1.8 Reactive oxygen species

Stem cell function during development and tissue homeostasis throughout life is regulated by fitting balance between self-renewal and differentiation. Recently, stem cell studies suggested that this balance is partly regulated by reactive oxygen species (ROS), which are reactive molecules that play significant roles in the regulation of several cell functions and biological processes (Bigarella et al., 2014; Chen et al., 2018). On the other hand, ROS play an important role in stem cell fate. Low concentration of ROS is required for stem cells to undergo self-renewal and proliferation. Increasing ROS generation reduces self-renewal of stem cells by enhancing stem cell proliferation and differentiation, and a further increase in ROS generation can cause stem cell senescence and apoptosis. Furthermore, excess ROS production is involved in development of pathological states and diseases by causing stem cell damage. Hence, stem cell self-renewal, proliferation, differentiation, senescence, and apoptosis are regulated dose-dependent by ROS (figure 1.8) (Chen et al., 2018; Ezashi et al., 2005; Juntilla et al., 2010; Kinder et al., 2010; Lewandowski et al., 2010; Owusu-Ansah & Banerjee, 2009; Sauer & Wartenberg, 2005; Wong et al., 2004; Zhou et al., 2014). Moreover, increased generation of ROS by various NOXs plays a critical role in cardiovascular differentiation of ES cells (Li et al., 2006; Sauer & Wartenberg, 2005; Schmelter et al., 2006). Peroxisome proliferator-activated receptor alpha (PPAR-α) is a ligand for many fatty acids and plays a vital role in several physiological functions such as regulation of vascular tone, inflammation, and glucose homoeostasis (Krey et al., 1997). Activation of PPAR-α is necessary for cardiomyogenesis of ES cells, which is associated with ROS-generation (Sharifpanah et al., 2008). Also, AA-induced vasculogenesis of ES cells is dependent on ROS generation (Huang et al., 2016). In summary, ROS play a very significant role in the fate decision of various stem cells in a concentration-dependent manner.

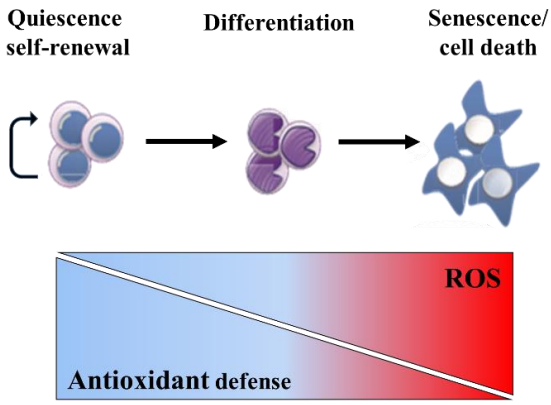

Figure 1.8: Effects of the intracellular ROS level on stem cell fate. Figure adapted with permission from (Bigarella et al., 2014); copyright 2014 The Company of Biologists.

Chemically, ROS are small molecules, which refer to a number of reactive molecules and free radicals derived from molecular oxygen. Intracellular ROS comprise of three different forms: superoxide anions ($O_2^{\cdot -}$), hydrogen peroxide (H_2O_2) and hydroxyl radicals ($OH^{\cdot}$). H_2O_2 is involved in many intracellular signal pathways and acts as a second messenger, integrating and delivering exogenous inducers to the downstream signal transduction cascade (Holmström & Finkel, 2014). H_2O_2 forms through the rapid reduction of superoxide anion by the antioxidant enzyme superoxide dismutase (SOD). H_2O_2 is further reduced to H_2O and O_2 by catalase and various cellular antioxidants (figure 1.9 B). H_2O_2 has a longer half-life and is able to produce other forms of ROS via diffusion through membranes (Holmström & Finkel, 2014).

1.9 Sources of ROS

Mitochondria have been considered as the main source of ROS in the cell. About ~0.1-0.2% of O_2 consumed during mitochondrial respiration by electron transport chain (ETC) activity forms ROS through leak electron flow to O_2. The main role of the ETC is to produce the proton motive force for to ATP production. This occurs through ATP synthase in a process known as oxidative phosphorylation. ROS are produced in the ETC complexes I and III (figure 1.9 A) (Tahara et al., 2009). The amount of ROS generation may differ greatly depending on the cell type, environment and the activity of mitochondria (Murphy, 2009). Another major source of ROS formation are membrane-bound nicotinamide

adenine dinucleotide phosphate (NADPH) oxidases (NOXs). They are enzymes responsible for ROS generation and regulate many redox-dependent signaling pathways. Furthermore, they contribute to a variety of cell processes such as cell differentiation, growth, proliferation, and embryonic development (figure 1.9 B) (Forrester et al., 2018; Nathan & Cunningham-Bussel, 2013; Skonieczna et al., 2017).

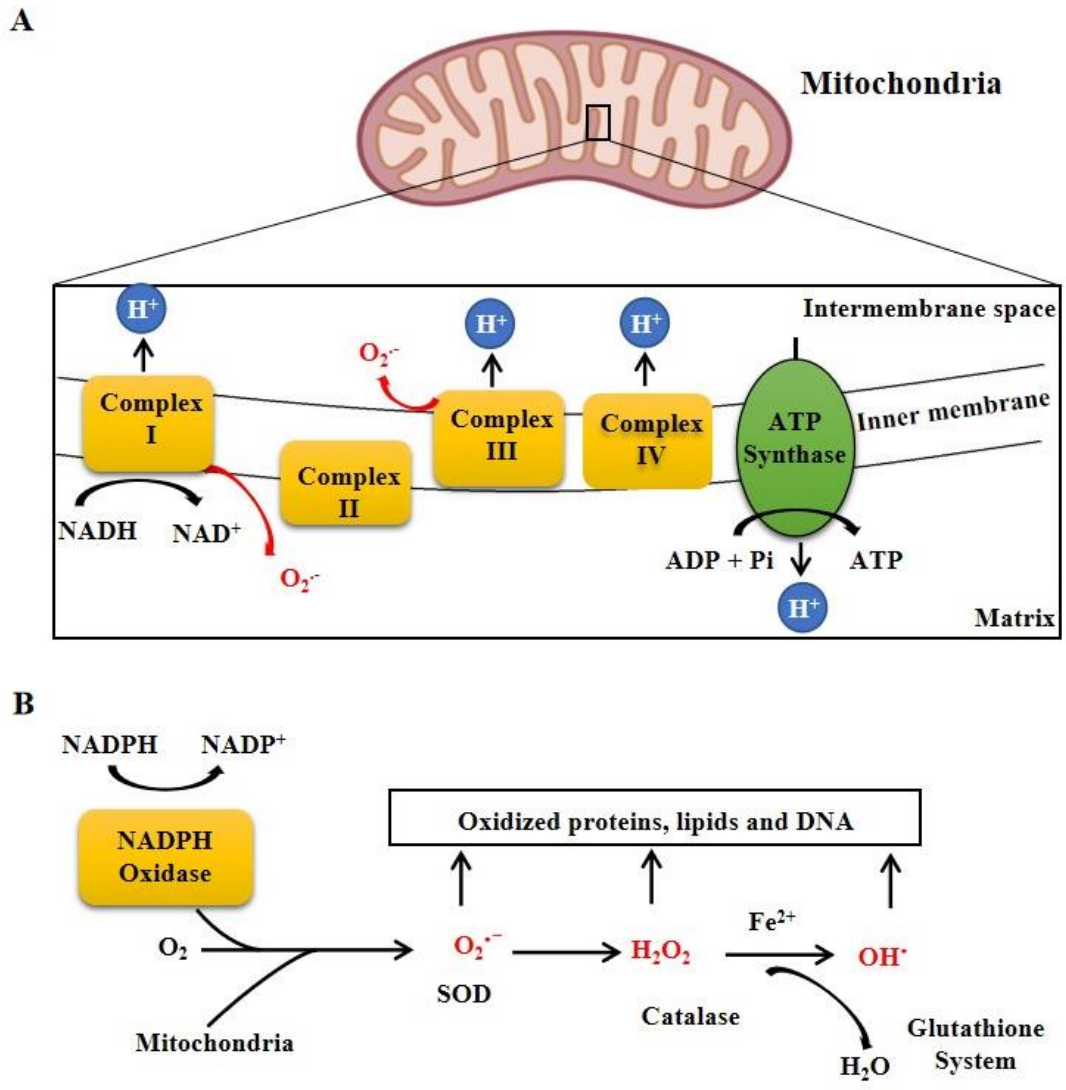

Figure 1.9: Intracellular ROS generation. The schemes display the formation of three different isoforms of intracellular ROS: superoxide ($O_2^{\cdot-}$), hydrogen peroxide (H_2O_2) and

the highly reactive hydroxyl radical ($OH^{\cdot}$) from various sources including: (A), mitochondria and (B), NADPH oxidase. Figure adapted with permission from (Bigarella et al., 2014) copyright 2014 The Company of Biologists.

NOX enzymes have the ability to modulate the proliferation and differentiation of stem cells. Therefore, they play an essential role in stem cell therapies, tissue engineering and regenerative medicine. Several studies have been reported that NOX-mediated redox signaling played an important role in neovascularization *in vivo*, which is required for the generation of functional tissues (Elsa C Chan et al., 2009; Jiang et al., 2008; Lee et al., 2014; Skonieczna et al., 2017). The NOX family is a transmembrane protein group, participating in ROS generation (i.e. superoxide anion ($O_2^{\cdot -}$) and hydrogen peroxide (H_2O_2)) via reducing oxygen by transport electrons from NADPH (Bedard & Krause, 2007). There are seven NOX isoforms in mammals NOX1-NOX5 and the others two are Duox1 (dual oxidase 1) and Duox2. Rat and mice lack the NOX5 (figure 1.10) (Holterman et al., 2014). NOX isoforms distribute in cell membranes such as the plasma membrane, endoplasmic reticulum, mitochondrial membrane, and nuclear membrane, as well as in specialized membrane microdomains like caveolae and lipid rafts, focal adhesions, and invadopodia (BelAiba et al., 2007; Block & Gorin, 2012). Although mitochondria and NADPH oxidase are considered major sources of ROS, there are other potential sources such as (CYP), xanthine oxidase (XO), or nitric oxide synthase (NOS) which also contribute to the redox potential (Roy et al., 2015). Moreover, intracellular ROS can be generated by other organelles within the cell such as peroxisomes, which are very dynamic and metabolically active organelles. Peroxisomes have the potential to rapidly generate and scavenge H_2O_2 and $O_2^{\cdot -}$, which enables to regulate dynamic shifts in ROS levels (Sandalio et al., 2013).

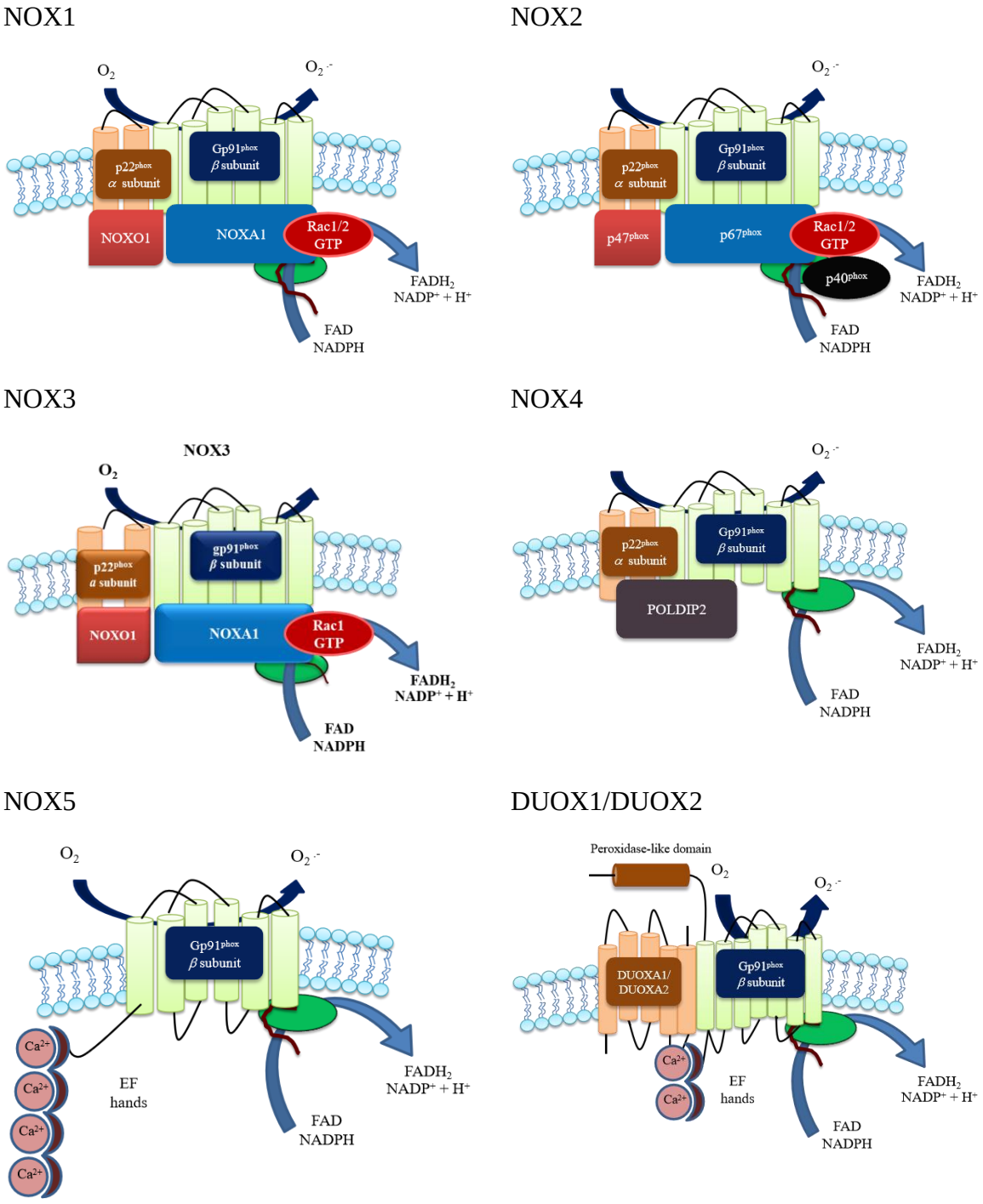

Figure 1.10: Structure of NOX isoforms (NOX1 to NOX5) and (DUOX1 and DUOX2). Figure adapted with permission from (Skonieczna et al., 2017); copyright 2017 Hindawi.

1.10 Nitric oxide

Nitric oxide (NO) is a short-lived free radical, synthesized enzymatically from the amino acid L-arginine. There are three NOS isoforms: neuronal NOS-1 (nNOS), inducible NOS-2 (iNOS), and endothelial NOS-3 (eNOS). (Marletta, 1994; Rochette et al., 2013; Tejedo et al., 2010). NO interacts with molecules such as oxygen, superoxide or metals, nucleic acids, and proteins (Cosby et al., 2003). NO serves as a second messenger and has numerous biological effects related to a variety of physiological functions in mammals, such as the regulation of blood pressure via smooth muscle relaxation and restraint of platelet aggregation (Enikolopov et al., 1999; Y Kots et al., 2011). It has been determined that it changes gene expression at the level of transcription and translation and regulates cell survival and proliferation in different cell types. In addition, NO is involved in growth, survival, proliferation, differentiation. Moreover, NO plays a significant role in the maintenance of fundamental features required for embryonic development and expansion of ES cells. In ES cells, NO has a dual function: it controls differentiation, survival, and pluripotency (Beltran-Povea et al., 2015; Caballano-Infantes et al., 2017; Tejedo et al., 2012), and promotes ES cell differentiation. Notably, it increases cardiac differentiation of mouse embryonic stem cell (mES cell) by positive and negative selection (Kanno et al., 2004; Padmasekar et al., 2011). The effects of NO on cellular processes are dose-dependent. Lower concentration of NO has been proposed to stimulate cell proliferation and survival processes, while a higher concentration of NO exerts oxidative and nitrosative stress (Alderton et al., 2001; Lundberg & Weitzberg, 2009; Thomas et al., 2008). In addition, it has been shown in ES cells, that lower concentrations of NO maintains pluripotency and enhances mitochondrial biogenesis, whereas at high concentrations, NO is a potential differentiation agent in several cell lines (Caballano-Infantes et al., 2017). Nitrate and nitrite form quickly by oxidation of NO and are now considered as non-inert end products because they are a source of NO through their reduction by a reverse pathway that describes an alternative source of NO while the endogenous L-arginine/NOS pathway is dysfunctional (Cosby et al., 2003). NOS-1 and NOS-3 are expressed in ES cells, and they produce a low level of NO. Cyclic guanosine monophosphate (cGMP) synthesis and protein kinase G (PKG-1) are inhibited in case of the low expression of the NO receptor

gene. These changes in gene expression promote pluripotency, self-renewal and cell survival. Low doses of exogenous NO can stimulate differentiation by activation of soluble guanylate cyclase (sGC) and subsequent synthesis of cGMP. When ES cells are treated with high doses of NO apoptosis and changes in mitochondrial metabolism and tissue-specific gene regulation occur which depend on culture conditions and differentiation protocols (figure 1.11) (Mora-Castilla et al., 2010; Tejedo et al., 2010; Tejedo et al., 2012).

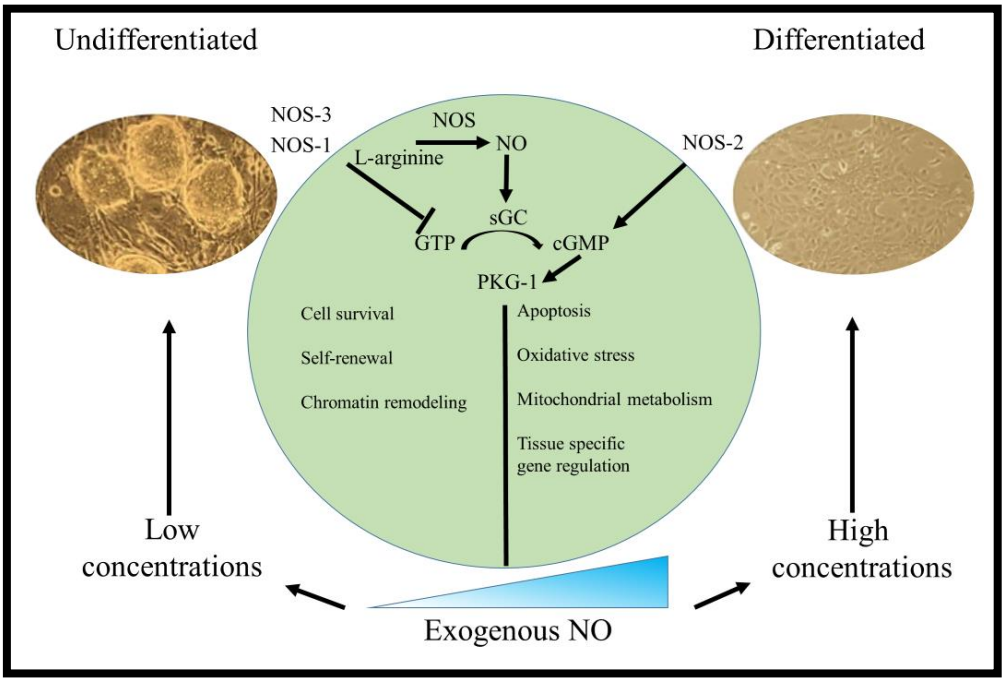

Figure 1.11: NO signaling in ES cells. Exogenous and endogenous NO effect on the ES cell status depend on the concentration. Low concentration of NO promotes pluripotency, self-renewal, and cell survival, while high concentration of NO leads to activation of apoptosis, mitochondrial metabolism and tissue-specific gene regulation. Figure adapted with permission from (Tejedo et al., 2012); copyright 2012 Springer Nature.

1.11 Intracellular calcium

The Intracellular calcium (Ca^{2+}) ion is the crucial second messenger in extra/intracellular signaling cascades. Transient changes in intracellular Ca^{2+} concentration $[Ca^{2+}]_i$, occur in microseconds (µs) or s, and Ca^{2+} can diffuse through cells and tissues. Spontaneous events

or regulated signal transduction cascades control free intracellular Ca^{2+} levels, and these signalling networks operate in different ways to contribute to various differentiation stages and stem cell fates. Moreover, Ca^{2+} plays an essential role in cellular functions such as muscle contraction, secretion, metabolism, gene expression, cell survival, as well as in cell life and death decisions. (Bootman et al., 2001; Görlach et al., 2015; Sun et al., 2007; Tonelli et al., 2012). There are two ways to increase intracellular Ca^{2+}: either by the flow of Ca^{2+} across the plasma membrane or release from intracellular stores of both the endoplasmic reticulum (ER) and sarcoplasmic reticulum (SR) in muscle. Ca^{2+} release takes place via activation of inositol trisphosphate (IP3) receptors or ryanodine receptors (RyRs) either by chemical or mechanical interaction between receptors/ion channels in the plasma membrane and Ca^{2+} stores (Berridge et al., 1999; Tumelty et al., 2007).

1.12 Scavenger receptor class B member 3 or CD36 receptor

Scavenger receptor class B member 3 (SCARB3) or CD36 is a widely expressed transmembrane glycoprotein. It belongs to the class B of the scavenger receptor family (i.e., scavenger receptors with two transmembrane domains), which includes scavenger receptor-B1 (SR-B1) that is involved in binding of low-density lipoprotein (LDL) and high-density lipoprotein (HDL) particles, and lysosomal integral membrane protein II (LIMP2) (SR-B3). CD36 is now officially designated as SR-B2. CD36 consists of two major transmembrane domains, the large extracellular loop and the small cytoplasmic tails. The extracellular part has 9 *N*-linked glycosylation sites (positions 79, 102, 134, 205, 220, 231, 235, 247 and 417) and 2 phosphorylation sites (positions 92 and 237). Disulfide bonds linked between extracellular cysteines, which are present between amino acid residues243–311, 272–333, and 313–323 (figure 1.12). Basically, in heart and muscle, CD36 is participating in long-chain fatty acid uptake across the plasma membrane. This occurs by vesicle-mediated reversible trafficking between intracellular membrane compartments and the cell surface (Luiken et al., 2016; PrabhuDas et al., 2014). Furthermore, CD36 has been involved in dysregulated fatty acid and lipid metabolism in pathophysiological conditions, especially in high-fat diet-induced insulin resistance and diabetic cardiomyopathy. (Glatz & Luiken, 2018). There is some evidence that CD36 facilitated transport of EPA, and DHA. CD36 also mediates fatty acid-induced signaling to increase intracellular Ca^{2+} in

various cell types. The membrane-impermeable sulfo-N-succinimidyl oleate (SSO) irreversibly binds CD36 and has been extensively utilized to inhibit CD36-dependent fatty acid uptake and its effect on Ca^{2+} signaling (Franekova et al., 2014; Glatz & Luiken, 2015; Kuda et al., 2013).

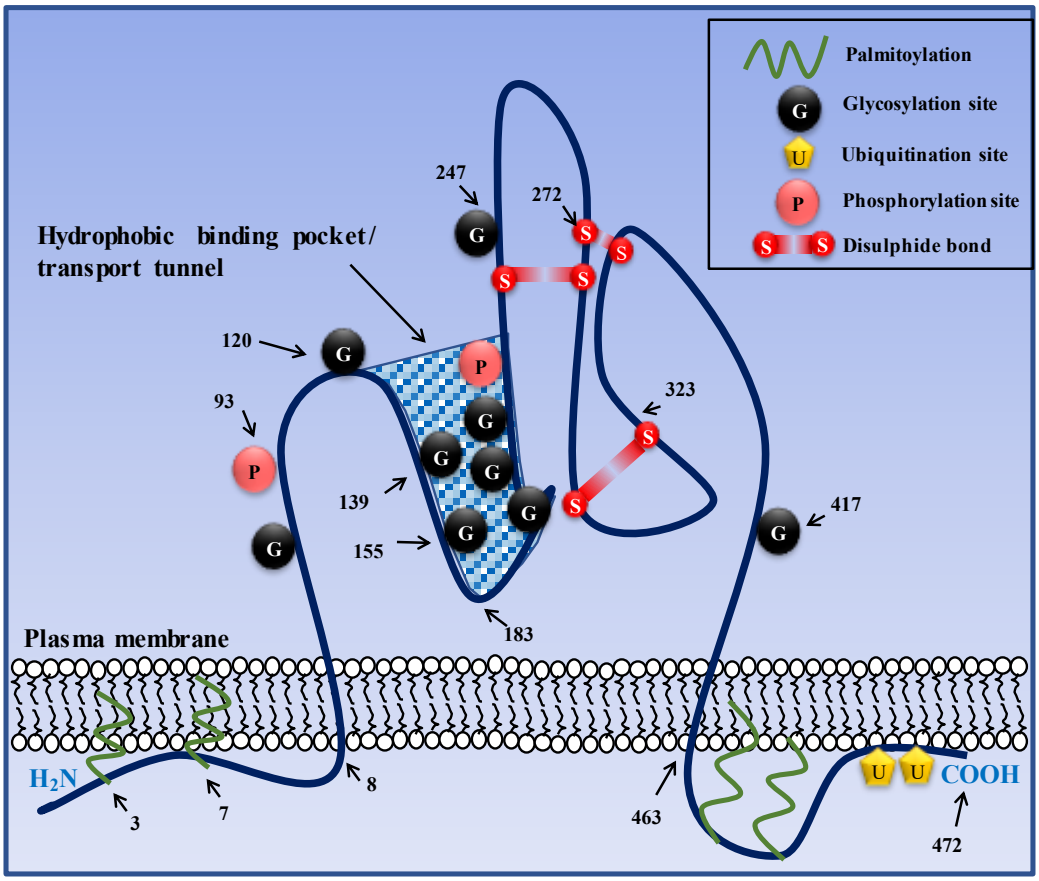

Figure 1.12: Two-dimensional structure and membrane topology of glycoprotein CD36. Figure adapted from (Glatz & Luiken, 2018) licensed under Creative Commons Attribution 4.0 International (CC BY 4.0) and with permission from (Luiken et al., 2016); copyright 2016 Elsevier.

1.13 5' adenosine monophosphate-activated protein kinase

5' adenosine monophosphate-activated protein kinase (AMPK) is a serine/threonine-protein kinase. It is a master energy sensor, that regulates cellular metabolism in response

to nutritional and environmental variations, and plays an important role in energy homeostasis. It activates and induces energy production via stimulation of glucose uptake and lipid oxidation during a deficit in the nutrient condition. It reestablishes energy balance by turning off energy-consuming processes including glucose and lipid production while activating energy-producing processes. Moreover, AMPK regulates glucose homeostasis in multiple tissues in the body such as skeletal muscle, liver, adipose tissue, and pancreatic β cells and assists as an inter-tissue signal integrator by responding to various hormonal signals including leptin and adiponectin (Long & Zierath, 2006; Lyons & Roche, 2018). AMPK is a heterotrimeric protein complex which consists of a catalytic α subunit, a scaffolding β subunit, and a regulatory γ subunit. The α and β subunit is encoded by two genes (α1 and α2 or β1 and β2), while three genes encode the γ subunit (γ1, γ2, and γ3) (Cheung et al., 2000; Stapleton et al., 1996; Thornton et al., 1998). AMPK acts as a nutrient sensor, which is activated by a low energy state. ATP is an energy source, which is broken down to produce adenosine diphosphate (ADP) and then adenosine monophosphate (AMP), respectively. When the ADP:AMP ratio is higher and ATP level is lower, AMPK activates pathways that produce ATP through glucose, lipid and mitochondrial metabolism pathways, consequently increasing ATP levels. Conversely, pathways that deplete ATP are inhibited by AMPK (figure 1.13) (Garcia & Shaw, 2017; Hardie, 2015; Lyons & Roche, 2018; Ma et al., 2012). AMPK can be activated in two ways: i) directly, by binding with its activators (e.g. 5-aminoimidazole-4-carboxamide riboside (AICAR)), which stimulate structural changes in the AMPK complex through direct interaction with a specific subunit of AMPK. This takes place without any significant change in cellular ATP, ADP, or AMP levels, ii) indirectly (e.g. metformin or ALA) by accumulation of AMP and calcium (Kim et al., 2016). AMPK activity is principally determined by intracellular energy levels and is very sensible to the cellular ROS level (Choi et al., 2001). ROS can induce AMPK activity even without a reduction in cellular ATP (Quintero et al., 2006; Wu et al., 2012). Oxidative modification of the AMPK-α subunit seems to be an essential mechanism by which AMPK is stimulated under states of oxidative stress. Hence, every modulator which is able to cause intracellular ROS generation can activate AMPK without an associated decrease in ATP levels (Zmijewski et al., 2010).

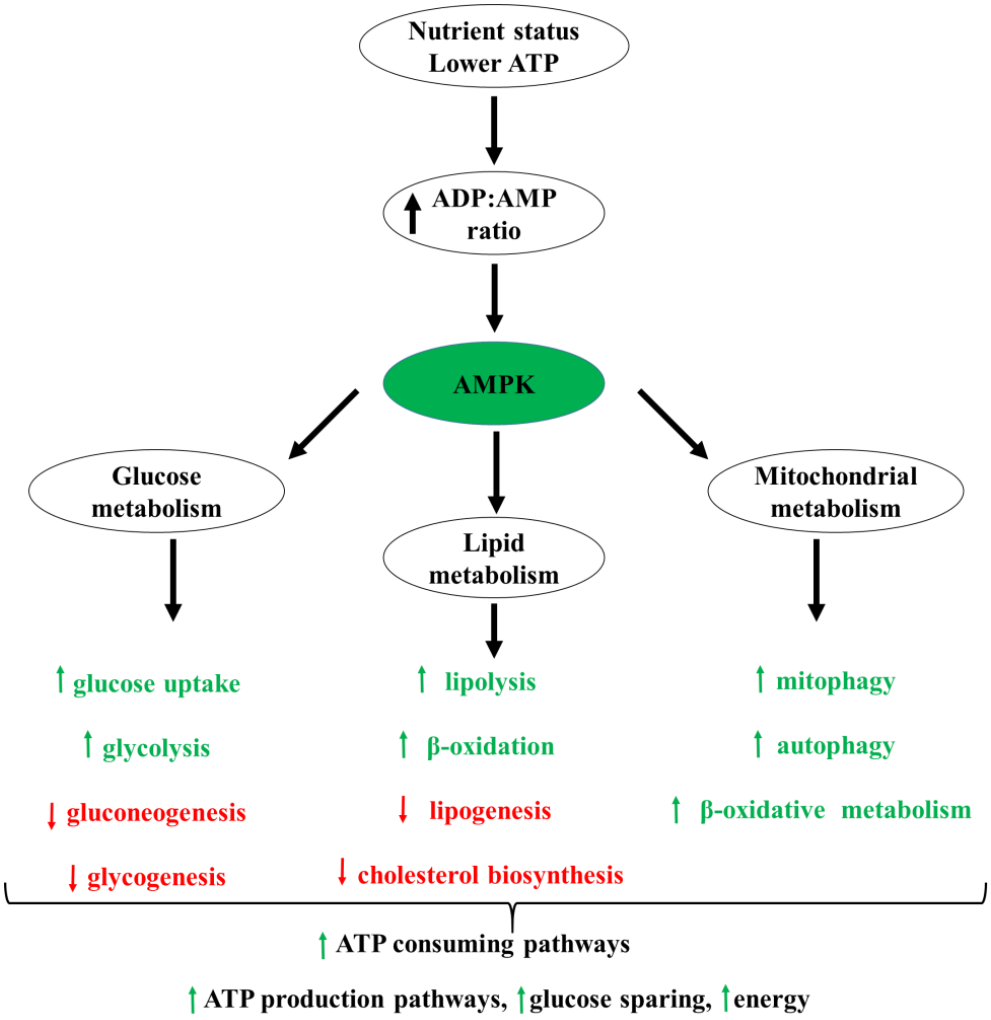

Figure 1.13: Overview of AMPK in cellular metabolism. Green arrows represent upregulated processes, red arrows represent downregulated processes. Figure adapted from (Lyons & Roche, 2018) licensed under (CC BY 4.0).

1.14 PPAR-α

PPAR-α is a ligand-activated transcription factor which belongs to the nuclear receptor family of PPARs. This nuclear receptor family consists of the subfamily receptors PPAR-β and PPAR-γ (Kersten, 2014; Lee et al., 2009). Several PPAR-α target genes are associated with fatty acid metabolism. PPAR-α is highly expressed in a variety of tissues with high energy demand such as the liver, heart, skeletal muscle, brown adipose tissue, and kidney. It is also expressed in other tissues like intestine, vascular endothelium, smooth muscle and

immune cells like monocytes, macrophages, and lymphocytes. It is significantly increased during cardiomyogenesis in ES cells (Ding et al., 2007; Pawlak et al., 2015). PPAR-α regulates the genes encoding mitochondrial fatty acid β-oxidation enzymes during cardiac developmental processes and under physiological/pathophysiological conditions. Additionally, inhibition of PPAR-α diminishes expression of cardiac sarcomeric proteins and specific genes during cardiac differentiation (Ding et al., 2007). PPAR-α is a nutritional sensor; thus PPAR-α plays a significant role in metabolic regulation and modifies the rates of fatty acid catabolism and lipogenesis (Hashimoto et al., 2000; Kersten, 2014; Lee et al., 2009). PPAR-α is a transcriptional regulator of genes implicated in peroxisomal and mitochondrial β-oxidation as well as fatty acid transport (J. Xu et al., 2002). The development and progression of atherosclerosis, plaque rupture, and thrombus formation could be abolished via activation of PPAR-α by its ligands in the cardiovascular system (Marx et al., 2001; Zandbergen & Plutzky, 2007). PPARs are required for multiple physiological functions (Kota et al., 2005), that are controlled by a lot of endogenous and exogenous compounds, including fatty acids (e.g. n-3 and n-6 fatty acids) and their metabolites. Eicosanoids and some endocannabinoids and phospholipids have been classified as endogenous ligands of PPARs. These PPAR-α activators include 8-epoxyeicosatrienoic acids (8-EETs), the AA lipoxygenase metabolite leukotriene B4 (LTB4), and the arachidonate monooxygenase metabolites EETs (Cowart et al., 2002; Guan, 2002). Exogenous PPAR ligands e.g. clofibrate, gemfibrozil, fenofibrate, bezafibrate, and ciprofibrate have been developed and applied in experimental studies and clinical applications. For example, fibrates, which are PPAR-α ligands, are utilised to ameliorate microvascular risks associated with metabolic syndrome (Fidaleo & Sartori, 2008; Liss & Finck, 2017; Wang et al., 2013).

Aims of the study

PUFAs regulate many cellular functions, such as proliferation, cell growth, and differentiation via a complicated network of signaling pathways. Nevertheless, the role of PUFAs in the differentiation of ES cells into the cardiovascular lineage, e.g. cardiomyocytes and endothelial cells remains unexplored.

In detail, the goals of this study are:

- To unravel the impact of PUFAs, i.e. LA (ω-6) and EPA (ω-3) on cardiovascular lineage differentiation of ES cells.
- To identify intracellular messengers in the PUFA-induced signal transduction cascade such as ROS, NO and intracellular calcium (Ca^{2+}), which have been identified in previous studies to play an important role in the regulation of ES cell differentiation into the cardiovascular lineage.
- To investigate, how ROS, NO, and Ca^{2+} raised by PUFAs interfere and interact with energy sensing molecules such as PPAR-α, and AMPK-α.

2. Materials and methods

2.1 Materials

2.1.1 Companies

Table 1: Company list

Company	Address
Abcam	Cambridge, UK
Abnova	Heidelberg, Germany
Air Liquide	Vitry-sur-Seine, France
Amsbio	Abingdon, UK
Ansell	Brussels, Belgium
AppliChem	Darmstadt, Germany
Aqua B. Braun Melsungen AG	Melsungen, Germany
BD Biosciences	Heidelberg, Germany
BD Falcon	New York, USA
Bemis Flexible Packaging	Neenah, USA
Biochrom	Berlin, Germany
BioLegend	Koblenz, Germany
Biometra	Göttingen, Germany
Biorbyt-Biozol	Eching, Germany
Biotec-Fischer	Reiskirchen, Germany
BioVision	Milpitas, USA
Biozym Scientific	Hessisch Oldendorf, Germany
Boehringer, Ingelheim,	Ingelheim am Rhein, Germany
Brand	Wertheim, Germany
Calbiochem	San Diego, USA
Carl Roth	Karlsruhe, Germany

Carl Zeiss	Göttingen, Germany
Castel MAC SpA	Castelfranco Veneto, Italy
Cayman	Ann Arbor MI, USA
Cell Signaling Technology	Danvers, USA
Chemicon	Hampshire, UK
Corning	New York, USA
Edmund Bühler	Hechingen, Germany
Enzo	Farmingdale NY, USA
Eppendorf	Germany
Falcon	Franklin Lakes, USA
Fisher Scientific	Schwerte, Germany
Focus Biomolecules LLC	Plymouth Meeting, USA
Gentaur	Aachen, Germany
Gilson	Middleton, USA
Greiner bio-one	Frickenhausen , Germany
Hanna Instruments	Kehl am Rhein, Germany
Heirler-Cenovis	Radolfzell, Germany
Heraeus	Hanau, Germany
HLC BioTech	Bovenden Germany
Holzner	Nussloch, Germany
IKA	Wilmington, USA
Integra Biosciences	Fernwald, Germany
Integra Biosciences	Fernwald, Germany
Invitrogen by Life Technologies	Darmstadt, Germany
Invitrogen by Thermo Fisher Scientific	Dreieich, Germany
InvivoGen	San Diego, USA
ISO Lab	Wertheim, Germany
Jackson ImmunoResearch,	Cambridgeshire, UK

Labexchange	Burladingen-Hausen, Germany
Lauda	Lauda-Königshofen, Germany
LeicaMicrosystems	Wetzlar, Germany
Life Technologies	Darmstadt, Germany
Lonza	Rockland, USA
Merck-Millipore	Darmstadt, Germany
Mettler Toledo	Greifensee, Switzerland
Millipore	Darmstadt, Germany
PAA	Cölbe, Germany
Peqlab Biotechnologie	Erlangen, Germany
R. Langenbrinck	Emmendingen, Germany
Sarstedt	Nümbrecht, Germany
Sartorius	Göttingen, Germany
Schleicher & Schuell	Dassel, Germany
Siemens	Munich, Germany
Sigma-Aldrich	Steinheim, Germany
Southern Biotech	Birmingham, USA
Stuart	London, UK
Tecan	Männedorf, Switzerland
Thermo Fisher Scientific	Dreieich, Germany
Tocris	Nordenstadt, Germany
Vasopharm	Würzburg, Germany
VWR International	Darmstadt, Germany

2.1.2 Materials

Table 2: Materials list

Materials	Supporting Company
24-well cell culture plate	Sarstedt
96-well ELISA plate	Falcon
Bacterial culture dish 100, suspension	Greiner bio-one
Blotting chamber Xcell II Blot module	Invitrogen by Life Technologies
Cellspin spinner flask stirrer	Integra Biosciences
Conical flasks	Fisher Scientific
Conical tubes 15ml & 50ml	BD Falcon
CryoPure Tube 1.8ml	Sarstedt
Filter paper circles	Schleicher & Schuell
Filter paper for blotting	Biotec-Fischer
Filtropur S 0.2	Sarstedt
Gel electrophoresis chamber	Invitrogen by Life Technologies
Gel electrophoresis power supply	Invitrogen by Life Technologies
Glass Pasteur pipettes	VWR International
Magnetic stirrer	IKA
Magnetic stirrer for spinner flask	Integra Biosciences
Micropipettes	Gilson and Eppendorf
Microscope Cover Slips	Fisher Scientific
Microscope slides, ground edges	R. Langenbrinck
Micro-tubes 0.5ml &1.5ml	Sarstedt
Nalgene Mr. Frosty	Thermo Fisher Scientific
Nitrile gloves	Ansell
PAGEr EX Gels	Lonza, Rockland
Parafilm	Bemis Flexible Packaging
Pipette filter tips	Biozym Scientific

Pipette tips	Sarstedt
PVDF Millipore transfer membrane	Merck-Millipore
Serological glass pipettes	ISO Lab
Serological pipettes wide tip	Corning
Serological plastic pipettes	Greiner Bio-One
Spinner flask	Integra Biosciences
Sponge Pad for blotting	Invitrogen® by Life Technologies
Tissue culture treated dish 100, standard	Sarstedt
Tissue culture treated dish 60, standard	Sarstedt
Tissue culture treated dish 60, suspension	Sarstedt

2.1.3 Instruments

Table 3: Instruments list

Instruments	Supporting Company
+4 ºC refrigerator	Siemens
-20 ºC freezer	Thermo Fisher Scientific
-80 ºC freezer	Heraeus
Analogue tube rollers	Stuart
Autoclave	Holzner
Cell culture bench	Heraeus
Cell culture incubators	Heraeus
Centrifuge 1S-R	Heraeus
Centrifuge 5417C	Eppendorf
Chemiluminescence imaging system	Peqlab Biotechnologie
Confocal laser scanning microscope (CLSM) TCS-SP2, AOBS	LeicaMicrosystems
ELISA reader	Tecan
Heating block	Biometra
Homogenizer	Sigma-Aldrich

Ice machine	Castel MAC SpA
Inverted light microscope (Zeiss Axiovert 40 C)	Carl Zeiss
Liquid nitrogen tank	Air Liquide
Microscope heating stage TRZ 3700	Labexchange®
Milli-Q Advantage A10 System	Millipore
Pellet pestle 1.5 ml	Fisher Scientific
pH-meter	Hanna Instruments
Safety Bunsen burner	Integra Biosciences
Shaker	Stuart and Edmund Bühler, Hechingen
Vacuum pump	HLC BioTech
Vortex-Genie®	VWR International
Water bath	Lauda
Weighing machine-AB265S	Mettler Toledo
Weighing machine-TE153S	Sartorius

2.1.4 Chemicals

Table 4: Chemicals list

Materials	Supporting Company
1,5-bis (2-(di-methylamino) ethylamino)-4,8-dihydroxyanthracene-9,10-dione (DRAQ5)	Cell Signaling Technology
2´7´-dichlorodihydrofluorescein diacetate (H_2DCF-DA)	Thermo Fisher Scientific
4-(6-Acetoxymethoxy-2,7-difluoro-3-oxo-9-xanthenyl)-4′-methyl-2,2′-(ethylenedioxy) dianiline-N,N,N′,N′-tetraacetic acid tetrakis (acetoxymethyl) ester (Fluo-4-AM)	Thermo Fisher Scientific
4-amino-5-methylamino-2′,7′ dichlorofluorescein diacetate (DAF-FM) diacetate	Thermo Fisher Scientific
Acetic acid	Sigma-Aldrich
Bovine serum albumins (BSA) (powder)	Sigma-Aldrich

Collagenase B	Boehringer, Ingelheim
Copper sulfate	Sigma-Aldrich
Dimethyl sulfoxide (DMSO)	Millipore
Di-Sodium hydrogen phosphate dihydrate	Carl Roth
Dulbecco's modified Eagle medium (DMEM) high glucose medium	Biochrom
Dulbecco's 1xphosphate buffered saline (PBS) without Ca^{2+} & Mg^{2+} ions	PAA
EmbryoMax® 0.1% gelatin solution	Merck-Millipore
EPA	Focus Biomolecules LLC and Tocris
ESGRO® LIF (107 units)	Chemicon
Ethanol	Carl Roth
Ethylenediaminetetraacetic acid (EDTA)	Carl Roth
Fetal calf serum (FCS)	Sigma-Aldrich
Fluoromount-G®	Southern Biotech
Folin-ciocalteau reagent	Sigma-Aldrich
Hydrochloric acid (HCl)	Sigma-Aldrich
Hydrogen peroxide solution (30%)	Sigma-Aldrich
Iscove's basal medium	Biochrom
LA	Enzo
L-glutamine (200mM)	Biochrom
Luminol	Sigma-Aldrich
Methanol	Carl Roth
Mitomycin-C	Calbiochem
Non-essential amino acids (NEAA) (100X)	Biochrom
Non-fat dried milk powder	Heirler-Cenovis
Nonidet P-40	AppliChem
Novex® Sharp Pre-stained protein standard	Life Technologies
NuPAGE Antioxidant	Invitrogen by Thermo Fisher Scientific

NuPAGE® LDS sample buffer (4x)	Invitrogen by Thermo Fisher Scientific
NuPAGE® Sample reducing agent (10x)	Invitrogen by Thermo Fisher Scientific
P-Coumaric acid	Sigma-Aldrich
Penicillin-Streptomycin (100X)	Biochrom
Phosphatase inhibitor cocktail 3	Sigma-Aldrich
Plasmocin™ Prophylactic 25mg/ml	InvivoGen
Ponceau-S	AppliChem
Potassium chloride	Carl Roth
Potassium dihydrogen phosphate	Carl Roth
Potassium sodium tartrate tetrahydrate	Merck-Millipore
ProSieve EX- running buffer	Lonza
ProSieve EX- transfer buffer	Lonza
Protease inhibitor cocktail	BioVision
Restore Western blot stripping buffer	Thermo Fisher Scientific
Sigmacote®	Sigma-Aldrich
Sodium carbonate	Carl Roth
Sodium chloride	Carl Roth
Sodium deoxycholate	Sigma-Aldrich
Sodium dodecyl sulfate (SDS)	Sigma-Aldrich
Sodium hydroxide	Carl Roth
Sodium pyruvate (100mM)	Biochrom
Sterile distilled water (DW)	Aqua B. Braun Melsungen AG
Tris	Sigma-Aldrich
Triton® X-100	Sigma-Aldrich
Trypsin/EDTA (1x)	Life Technologies
Tween-20	Sigma-Aldrich
β-Mercaptoethanol	Sigma-Aldrich

2.1.5 Buffer compositions

Table 5: Buffers and solutions compositions

Stock Buffers			
Buffers	**Volum**	**The final molar concentrations of the 1x solution are:**	**Materials**
10x PBS	1 Liter	2.7mM 2.0mM 137mM 10.0mM	KCl KH_2PO_4 NaCl Na_2HPO_4. $2H_2O$
10xTBS	1 Liter	25mM 137mM	Tris base NaCl
Radioimmunopr-ecipitation assay (RIPA)-Buffer	1 Liter	50mM 150mM 1% 0.5% 0.5%	Tris. pH 7.4 NaCl Nonidet P-40 SDS Sodium deoxycholate (excluded in the Phosphoprotein assay)
1xTris–HCl	1 Liter	100mM	Adjust pH at 7.4 using concentrated HCl
Mix-ups Dissolve the materials in 800ml distilled H_2O, adjust pH to 7.4, complete volume to 1L with additional distilled H_2O, and then sterilize by autoclaving.			
Washing Buffers			
1xPBS	100ml of 10x PBS diluted in 900ml distilled H_2O		
0.01% PBS-Triton X-100	100µl of Triton X-100 added to 1000ml 1x PBS		
0.1% TBS-Tween20	(100ml of 10xTBS) + (1ml of Tween20) diluted in 900ml distilled H_2O		
Permeabilization buffer			
1% PBS-Triton X-100	1ml of Triton X-100 added to 100ml 1x PBS		
Blocking buffers			
10% FCS	1ml of FCS added to 10ml 0.01% PBST		
10% Non-fat dry milk	1g of milk dissolved in 10ml 0.01% PBST		
5% Non-fat dry milk	5g of milk dissolved in 100ml 1xTBS-Tween20		
Protein extraction buffers			

Protein extraction buffer	RIPA buffer with sodium deoxycholate	1x
	Protease inhibitor cocktail	1x
Phospho-protein extraction buffer	RIPA buffer without sodium deoxycholate	1x
	Protease inhibitor cocktail (500x)	1x
	Phosphatase inhibitor cocktail (100x)	1x
	EDTA (pH 8)	1mM
	Glycerophosphate	1mM
Ponceau-S staining solution		
Ponceau-S staining (w/v)		0.1%
Acetic acid (v/v)		5%
Enhanced chemiluminescence (ECL) detection solution		
Luminol		1.25mM
p-Coumaric acid		225µM
Hydrogen peroxide solution (30%) (v/v)		3mM
Tris-HCl (pH 8.5)		100mM
Lowry solutions		
Solution A: 2% Sodium carbonate (w/v) in 0.1N sodium hydroxide solution		
Solution B: 1.25% Copper sulphate (w/v)		
Solution C: 3.37% Potassium sodium tartrate tetrahydrate (w/v)		
Solution D: Solution A, solution B, and solution C mixed-up in the ratio 100:1:1		
Solution E:1N Sodium hydroxide solution		
Solution F: 2N Folin & ciocalteu's phenol reagent		

2.1.6 Cell culture media components

Table 6: Media composition

MEF medium	Final concentration
DMEM high glucose medium	1x
Heat-inactivated (FCS)	10%
β- mercaptoethanol	0.1mM
Sodium pyruvate (100mM)	1.0mM

L-glutamine (200mM)	2.0mM
NEAA (100mM)	0.1mM
Penicillin-Streptomycin (10000U/ml)	50U/ml
LIF-Plasmocin-Prophylactic (LIF-pLpro) medium	**Final concentration**
Iscove's basal medium	1x
Heat-inactivated (FCS)	16%
β- mercaptoethanol	0.1mM
Sodium pyruvate (100mM)	1.0mM
L-glutamine (200mM)	2.0mM
NEAA (100mM)	0.1mM
Plasmocin Prophylactic	2.5µg/ml
LIF	1000U/ml
CCE differentiation medium	**Final concentration**
Iscove's basal medium	1x
Heat-inactivated (FCS)	16%
β-mercaptoethanol	0.1mM
Sodium pyruvate (100mM)	1.0mM
L-glutamine (200mM)	2.0mM
NEAA (100mM)	0.1mM
Penicillin-Streptomycin (10000U/ml)	50U/ml
Freezing Medium	**Final concentration**
MEF medium	50%
Heat-inactivated (FCS)	40%
DMSO	10%

2.1.7 Cell lines

Mouse embryonic fibroblasts (MEFs) (Amsbio).

CCE S103 cell line: Mouse ES cell line isolated from mouse embryos strain129/sv (Robertson et al., 1986).

2.1.8 Immunocytochemistry antibodies

Table 7: Immunocytochemistry antibodies

Primary antibody	**Animal**	**Concentration**	**Supporting Company/ Catalog Number (Cat. No.)**
Anti-α-actinin	Mouse	1:100	Abcam/ ab9465
Anti-CD31	Rat	1:100	Merck-Millipore/ CBL1337
Anti-phospho PPAR-α (S12)	Rabbit	1:200	Abcam/ ab3484
Secondary antibody	**Animal**	**Concentration**	**Supporting Company/ Cat. No.**
Alexa Fluor 488 anti-rat IgG	Donkey	1:100	Life Technologies/ A-21208
Alexa Fluor 647 anti-mouse IgG	Sheep	1:100	Jackson ImmunoResearch/ 515-605-072
Alexa Fluor 488 anti-rabbit IgG	Donkey	1:100	Life Technologies/ A-21206
Alexa Fluor 488 anti-rat IgG	Donkey	1:100	Jackson ImmunoResearch/ 712-546-153
DyLight 650 anti-rat IgG	Goat	1:100	Abcam/ ab98408

2.1.9 Western blot antibodies

Table 8: Western blot antibodies

Primary antibody	**Animal**	**Concentration**	**Supporting Company/ Cat. No**	**KDa**
Endothelial cell markers				
Anti-VE-Cadherin (CD144)	Rat	1:1000	BD Biosciences/ 555289	115
Anti-PECAM1 (CD31)	Goat	1:1000	BioLegend/ 910003	130
Progenitor marker				
Anti-fetal liver kinase-1(FLK-1)	Rabbit	1:1000	Cell Signaling Technology/ 9698	230
Cardiac protein markers				
Anti-α-actinin	Mouse	1:1000	Sigma-Aldrich /A 5044	107
Anti-Myosin regulatory	Mouse	1:1000	Thermo Fisher	19

light chain 2, atrial isoform (MLC2a)			Scientific/PA5-30789	
Phosphoproteins				
Anti-p-AMPK-α (Thr172)	Rabbit	1:1000	Cell Signaling Technology/2535S	62
Anti-p-eNOS (Ser1177)	Rabbit	1:1000	Cell Signaling Technology/9571S	140
Anti-p-PPAR-α (pSer12)	Rabbit	1:1000	Abcam/ab3484	52
Housekeeping proteins				
Anti-GAPDH	Rabbit	1:1000	Abcam/ab9485	36
Anti-Vinculin	Mouse	1:1000	Sigma-Aldrich/V9131	116
Anti-β-actin	Rabbit	1:2000	BioLegend/622102	45
Secondary antibody	**Animal**	**Concentration**	**Supporting Company/ Cat. No**	
HRP anti-Rat	Goat	1:1000	Cell Signaling Technology/7077	
HRP anti-Rabbit	Goat	1:1000	Abcam/ab205722	
HRP anti-Mouse	Horse	1:1000	Cell Signaling Technology/7076	
HRP anti-Goat	Donkey	1:1000	Abnova/PAB10570	

2.1.10 Substances

2.1.10.1 Preparing PUFAs and mES cell treatment

The PUFAs were supplied as minimum purity >99% and were prepared by dissolving in DMSO (final concentration of DMSO $\leq$ 0.1% in the culture medium). Once prepared, PUFAs were stored at -20 °C as recommended in datasheets. To obtain dose-response relations, physiological concentrations of 1, 5, 10, 50, and 100µM PUFAs were applied. In vehicle (DMSO) groups, the identical concentration of DMSO as included in PUFA treated samples was added to the culture medium.

2.1.10.2 Fluorescence substances

2.1.10.2.1 H_2DCF-DA

H_2DCF-DA is an apolar, nonfluorescent, cell-permeable substance and serves as an indicator of various ROS. After diffusion into the cell, the diacetate moiety is cleaved by intracellular esterases. The resulting polar DCFH is nonfluorescent and cell-impermeable and is rapidly oxidized to the highly fluorescent 2´,7´-dichlorofluorescein (DCF) by

intracellular ROS. The fluorescence intensity of DCF, which is excited at 488 nanometer (nm) wavelength, serves as an indicator for the intracellular amount of ROS, the fluorescence emission is detected at a wavelength of ≥540 nm (Bass et al., 1983).

2.1.10.2.2 DAF-FM DA

The fluorescent marker DAF-FM DA is an indicator for the measurement of intracellular NO. The cell-permeable diacetate, DAF-FM can passively diffuse across the cell membrane into the cell. Once in the cell, the diacetate group is cleaved by cell-specific esterases. The resulting product DAF-FM is weakly fluorescent. It cannot leave the cell and reacts in the presence of NO to a highly fluorescent benzotriazole derivative, which can fluoresce up to 160-fold more intense than DAF-FM (Kojima et al., 2001). Maximum excitation wavelength of the oxidized form is at 495nm, and fluorescence emission is detected at wavelengths ≥ 515nm. DAF–FM is dissolved in DMSO.

2.1.10.2.3 Fluo-4-AM

For the visualization (imaging) of intracellular Ca^{2+} transients in living cells, the cell-permeable dye Fluo-4- acetoxymethyl ester (Fluo-4-AM) was used. Fluo-4-AM diffuses into the cell, in which cell-derived esterases split off the AM group to trap the compound in the cells. On the other hand, the hydrolysis is necessary to enable calcium-binding and fluorescence emission of the dye. Fluorescence intensity is dependent on the amount of bound calcium and therefore suitable for quantitative measurements. Fluo-4-AM is used to quantify calcium concentrations ranging from 100nM to 1μM. The absorption maximum of the green fluorescent Fluo-4 is 494 nm; the emission maximum at 516 nm (Gee et al., 2000).

2.1.10.2.4 DRAQ5

DRAQ5 is a cell-permeable far-red fluorescent DNA dye that can be used in fixed or non-fixed live cells. DRAQ5 staining can be applied in flow cytometry, live-cell imaging, and cell-based assays. DRAQ5 is excited at 633nm, and emission is recorded at > 655nm (Cheedipudi et al., 2019).

2.1.10.3 Inhibitors

To determine the impact of PUFAs and their metabolism on vasculogenesis and cardiomyogenesis, differentiating ES cells were pre-incubated from day 3 to 10 with specific inhibitors at the indicated concentrations (Table 9) either in presence or absence of PUFAs. Subsequently, generation of signaling molecules, protein expression and activation of enzymes, transcription factors, and cardiovascular proteins were evaluated by microfluorometry, immunocytochemistry and western blot.

Table 9: Inhibitors used in detection of signaling pathways

Inhibitor	Target	Final concentration	Soluble in	MW	Supporting Company/ Cat. No.
BAPTA-AM	Calcium chelator	10µM	DMSO	764.7	Abcam/ ab120503
GW6471	PPAR-α inhibitor	5µM	DMSO	619.67	Tocris/ 4618
Nω-Nitro-L-arginine methyl ester (L-NAME)	NO-Synthase	100µM	DW	269.7	Sigma-Aldrich/ N5751
N-(2-mercaptopropionyl)-glycine (NMPG)	Radical scavenger	100µM	DMSO	163.2	Sigma-Aldrich/ M6635
Trolox	Radical scavenger	100µM	DMSO	264.3	Sigma-Aldrich/ 93510
VAS2870	NOX inhibitor	50µM	DMSO	360.3	Vasopharm/ F3395
SSO	SCARB3	200µM	DMSO	482.6	Cayman/ 11211
CD36 antibody	SCARB3	2-3µg/ml	-	-	Antibodies-Online.com/abin343926

2.1.11 Softwares

1- Adobe Acrobat Reader DC, version 2020.013.20064 (San Jose, USA)
2- ChemiCapt 500-Western blot imaging software version 15.01a, Vilber Smart Imaging, (Peqlab Biotechnologie, Eberhardzell, Germany).
3- Cisco AnyConnect Cisco Secure Mobility Client 4.1.0401 (Cisco Systems, San Jose, USA).
4- Endnote X9 [Bld. 12062], (Clarivate Analytics, Boston, USA).
5- GraphPad Prism 8-Statistical analysis software (GraphPad Software, San Diego, USA).
6- Image J-Western blot analysis software (National Institutes of Health (NIH), Bethesda, USA).
7- Leica Application Suite Advanced Fluorescence (Leica Microsystems, Wetzlar, Germany).
8- Metamorph Microscopy Automation & Image Analysis Software (Molecular Devices, San José, USA).
9- Microsoft Office 2013-2016 - Data documentation (Microsoft, Seattle, USA).
10- Tecan Magellan - ELISA Software (Tecan, Männedorf, Switzerland).

2.2 Methods

2.2.1 Cell culture methods

2.2.1.1 Preparing MEFs

MEFs have been used in this study as feeder layer cells for ES cells culture. Cultivation on feeder layers is important for maintenance of ES cells in a stemness state (Park et al., 2015), and promotes ES cell proliferation by providing the cell culture medium with extracellular secreted growth factors and LIF (Llames et al., 2015). The MEFs are stored in liquid nitrogen (-196 °C). MEFs were thawed in a water bath at 37 °C with gently shaking, till a small piece of ice in the tube was left. Immediately, they were transferred to a falcon tube containing 20ml pre-warmed MEF medium at 37 °C. Subsequently, the tube was centrifuged for 5 min at 209*g*. After centrifugation, the washing medium was aspirated, and cells were cultivated at a density of 5 x 10^5 cells in 5 ml MEF medium per Petri dish (diameter 60mm). Feeder cells were cultivated at a temperature of 37 °C, 5% CO_2, and relative humidity of 95%. Upon 80-90% confluency the feeder cell layer was a mitotically inactivated by incubation with fresh MEF medium containing 10µg/ml Mitomycin-C for 2-3h in a dark incubator at 37 °C, 5% CO_2. This step was important to avoid overgrowth of cells in the culture. Subsequently, the inactivation medium was removed, cells were washed three times with MEF medium and further incubated with pre-warmed fresh MEF medium. The washing step is critical to remove the rest of Mitomycin-C, which is a bioreductive alkylating agent, derived from *Streptomyces lavendulae* bacteria and has been clinically used as an antibiotic drug and in antitumor therapy (Mao et al., 1999). Mitomycin-C has the ability to crosslink with double strand-DNA and blocks DNA synthesis and nucleus division (Verweij & Pinedo, 1990). The MEF medium was changed every two days. Inactivated feeder layers can be stored under cell culture conditions for a maximum of one week.

2.2.1.2 Cultivation and maintenance of ES cells.

In this study the CCE-S103 mES cells line derived directly from mouse embryos was used (Robertson et al., 1986). ES cells were cultivated on mitotically inactivated MEFs to keep their stemness properties in presence of LIF. LIF is a member of the interleukin-6 (IL-6)

family of cytokines, and keeps mES cells in pluripotency and undifferentiated state, thus enabling long-term culture (Nicola & Babon, 2015). mES cells stored in liquid nitrogen tank (-196 °C) were thawed in water bath 37 °C for few seconds. Then the cell suspension was transferred to a conical tube containing 15ml CCE medium and centrifuged for 5 min at 209*g* to remove freezing medium. The freezing medium was aspirated and 200µl of LIF-pLpro medium was added to the pellet and resuspended by gently pipetting up and down. mES cells were then seeded on an inactivated MEF feeder cell layer, which was previously prepared. The mES cells were cultivated at a temperature of 37 °C, 5% CO_2, and relative humidity of 95%. The mES cells were passaged regularity every 2-3 days to avoid any extra-confluence, stress and unfavorable differentiation processes. For each passage, the mES cells were enzymatically dissociated, and transferred to a new plate on a layer of MEF feeder cells. For differentiation experiments, mES cells were seeded into spinner flasks at a density of 3 x 10^6 cells/ml, which contained CCE differentiation medium. This system allows the mES cells to form a small, spherical three-dimensional structure called the EBs (Ali et al., 2018)

2.2.1.3 Surface coating of tissue culture plates and spinner flasks

Gelatin was used to enhance mES cell and EB attachment on the surface of tissue culture plates or coverslips. Incubation with gelatin 0.1% in PBS was performed for 1h at 37 °C. Subsequently, gelatin was removed and coated tissue culture plates or coverslips were dried in the clean bench. Spinner flasks and magnetic stirring bars were coated with 10ml of Sigmacote, which is a silicone solution, coating glass surfaces with microscopically thin silicone film to prevent attachment of mES cells to spinner flasks and stirring bars. After coating, the spinner flasks and magnetic stirring bars were dried in an oven at 60 °C for 1h, washed for three times with DW, and autoclaved.

2.2.1.4 Trypsinization of mES cells, spinner flask preparation, and EB formation

The mES cells were passaged every 2-3 days, when confluence reached about 80-90% (figure 2.1A). Briefly, mES cells in 60mm tissue culture plates were washed for one time with PBS and incubated with 2ml pre-warmed trypsin/EDTA solution for 2 min at 37 °C. Subsequently, mES cell colonies were further dissociated by gently pulling up and down

with a 1ml pipette tip to obtain a single cell suspension. Subsequently, 9 x 10^4 single mES cells/ml were seeded onto MEF feeder cell layers in fresh LIF-pLpro pre-warmed medium.

To generate EBs mES cells were enzymatically dissociated as described and seeded at a density of 3 x 10^6 cells/ml into siliconized spinner flasks containing 125 ml of CCE differentiation medium (figure 2.1B). The speed of the magnetic stirrer system was adjusted to 20 rotations per min. After 4 rotation rounds the direction of rotation was changed to avoid EB agglomeration. After 24h, 125ml CCE differentiation medium was added to give a final volume of 250ml. Every day 125 ml of culture medium was exchanged for fresh medium. After 3 days of cell culture in spinner flasks EBs were transferred into 100mm bacteriological plates to be used in experiments on cardiovascular differentiation (figure 2.1C).

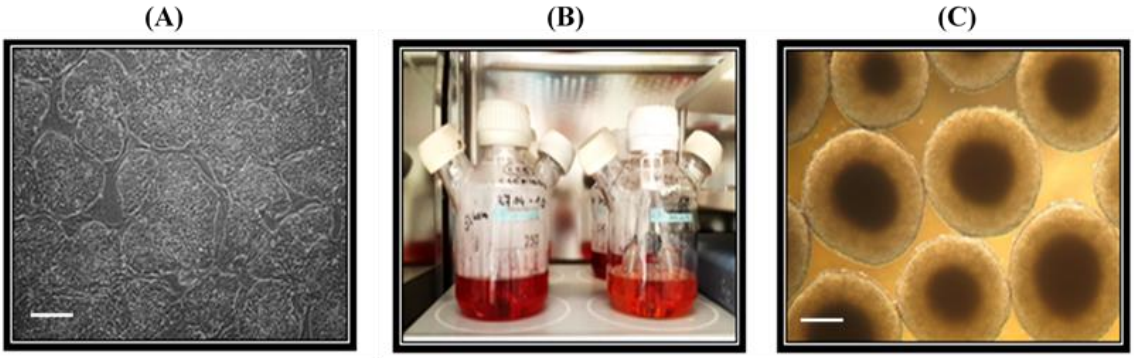

Figure 2.1: EB formation from differentiating mES cells. (A): Transmission image of undifferentiated ES cells cultivated on mitotically inactivated MEF feeder layers. (B): Spinner flask culture for EBs derived from mES cells. (C): Transmission image of EBs. The scale bars represent 200µm.

2.2.1.5 Protocol of PUFA treatment

For each, experiment approximately 25-30 EBs (3-day-old) were transferred to 60mm bacteriological tissue culture dishes. EBs were treated with series of physiological concentrations of LA as well as EPA, ranging from 1 to 100µM or were treated with appropriate concentrations of DMSO (vehicle). Petri dishes with EBs were placed on the shaker inside the incubator. The cell culture medium supplemented with PUFAs was changed every 24h. For investigation of signaling events upon PUFA treatment 5-day-old

EBs were collected. For immunofluorescence or protein extraction, EBs were treated with PUFAs until day 10 of cell culture. The beating frequency of spontaneously beating cardiomyocyte clusters (foci) within EBs as well as the number of contracting EBs were recorded from day 7 to day10 of cell culture using an inverted light microscope (Zeiss Axiovert 40 C), which was connected with a microscope heating stage TRZ 3700 and equipped with a 5x/0.12 objective (figure 2.2).

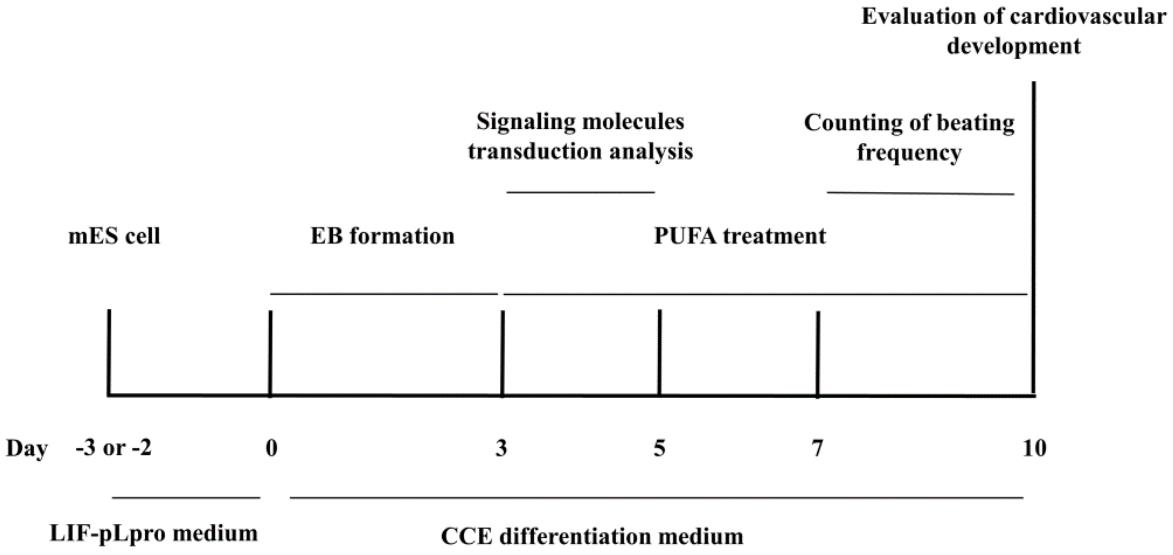

Figure 2.2: Schematic overview on the experimental setup

2.2.1.6 Freezing mES cells

mES cells were frozen upon confluency of 70-80%. Briefly the mES cells were washed with PBS and incubated with 2ml pre-warmed trypsin/EDTA for 2 min at 37 °C. The cells were dissociated by gently pipetting. Subsequently the suspension of mES was transferred into Falcon tubes containing 20ml CCE differentiation medium to stop enzymatic digestion. Then the tube was centrifuged for 5 min at 209*g*. The supernatant was aspirated, and the pellet was cooled down on the ice (+4°C), 1ml of the freezing medium was added slowly and re-suspended gently. Finally, the suspension was transferred to pre-cooled

1.8ml CryoPur tubes and stored at -80 °C overnight. The next day frozen mES cells were transferred to a liquid nitrogen tank for long-term storage.

2.2.2 Immunocytochemistry

EBs grown in suspension culture or cultivated on coverslips were collected, washed with PBS, and fixed in ice-cold methanol for 20 min at -20 °C. Subsequently, methanol was removed and the samples were washed 3-4 times with 0.01% PBST buffer. For permeabilization EBs were incubated in permeabilization buffer containing 1% PBS-Triton X-100 for 10 min at room temperature (RT). Then EBs were washed 3-4 times with 0.01% PBST buffer and incubated in blocking buffer containing 10% non-fat dry milk at RT for 60 min. EBs were incubated at RT for 120 min or overnight with primary antibodies, which were freshly prepared. Anti-CD31 was diluted with 10% non-fat dry milk and anti-α-actinin with 10% FCS. Primary antibodies were diluted 1:100. After incubation with primary antibodies EBs were washed 3-4 times with 0.01% PBST buffer and incubated with secondary antibody, which was prepared in blocking buffer, and incubated in a dark place at RT for 60 min. After that, the secondary antibody was removed, and EBs were washed 4-5 times with 0.01% PBST buffer, and kept in the same buffer at +4°C till immunofluorescence analysis. For long-term storage tissues were fixed and sealed in Fluoromount-G® solution. (Table 10).

Table 10: Immunocytochemistry protocol for staining of cardiomyocytes and endothelial cells within EBs

Steps	Specimen	Duration	Solutions and reagents	Temperature
Washing	Endothelial cells	~1 min	1xPBS	RT
	Cardiomyocytes			
Fixation	Endothelial cells	≥20 min	ice-cold 100% methanol	-20 °C
	Cardiomyocytes			
Permeabilization	Endothelial cells	10 min	1% PBST	RT
	Cardiomyocytes			
Blocking	Endothelial cells	60 min	10% nonfat- dry milk	RT
	Cardiomyocytes		10% FCS	

Primary antibody	Endothelial cells	60 min	Anti-CD31 diluted in 10% non-fat dry milk 1:100	+4°C
	Cardiomyocytes	overnight	Anti-α-actinin diluted in 10% FCS 1:100	
Secondary antibody	Endothelial cells	60 min	Diluted in 10% non-fat dry milk 1:100	RT
	Cardiomyocytes	60 min	Diluted in 10% FCS 1:100	RT

Fluorescence recordings were performed by means of a confocal laser scanning setup (Leica SP2 AOBS) connected to an inverted microscope. The confocal setup was equipped with a 5 milliwatt (mW) helium/neon laser, single excitation 633 nm, and an argon–ion laser, single excitation 488 nm. Emission was recorded using the band-pass filter BP 515-550 and long-pass LP 650 filter sets, respectively. For the analysis, a 10×, numerical aperture (NA) 0.5 objective was used. The pinhole settings of the confocal setup were adjusted to give a full-width half maximum of 5µm. For the quantification of capillary areas within EBs an optical sectioning routine based on CLSM was used. Images (512 × 512 pixels) were acquired from CD31-stained EBs using the extended depth of focus algorithm of the confocal setup. In brief, 10 full frame images, separated by a distance of 10µm in z-direction, were recorded. The obtained images included information of the capillary area and spatial organization of CD31-positive cell structures in a tissue slice 100µm thick. The acquired images were processed to generate a single in-focus image projection of vascular structures in the scanned tissue slice. By use of an image analysis software (Metamorph), the branching points of vascular structures within the three-dimensional projection were identified and counted in relation to the size of the respective EB. Moreover, other settings of CLSM were used to identify α-actinin-positive cardiac cell areas **(**figure 2.3**)**.

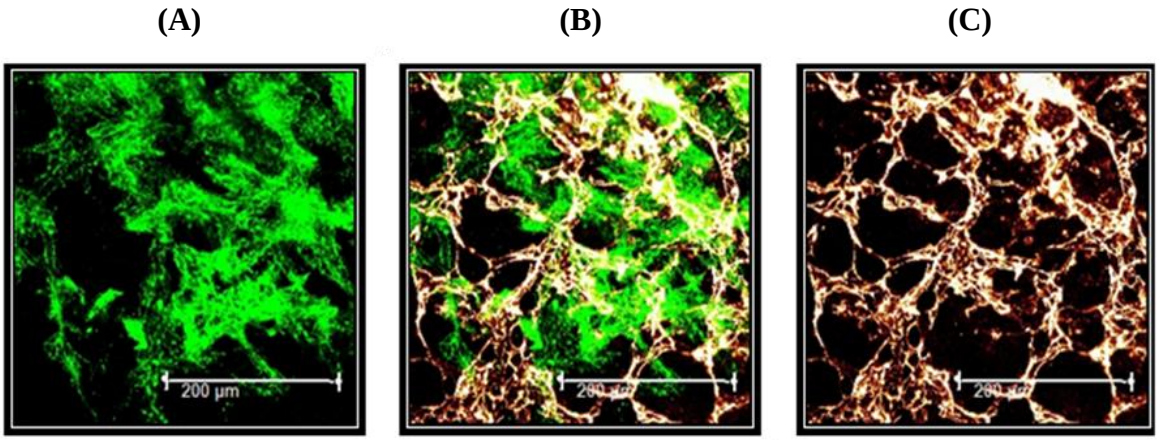

Figure 2.3: Cardiovascular differentiation of mES cells. (A): Cardiac cell structure stained with an antibody directed against α-actinin. (C): Vascular cell structures labeled with an antibody directed against vascular CD31. (B): Overlay image of cardiac (green) and vascular (white) cell structures. The scales bar in A, B, and C represents 200µm.

2.2.3 Measurement of ROS generation

Intracellular ROS generation was quantified using H_2DCF-DA, which is the most widely used cell-permeable dye for analysis of the intracellular redox state. Intracellularly, H_2DCF-DA is hydrolyzed by cellular esterases to yield the DCFH carboxylate anion, which is trapped in the cells. DCFH is rapidly oxidized into the fluorescent product (DCF) 2, 7-dichlorofluorescein by intracellular ROS. To measure intracellular ROS, the EBs were incubated with 20µM H_2DCF-DA for 30 min in the dark on a shaker at 37 °C, 5% CO_2. After staining EBs were washed once with fresh serum-free Iscove's basal medium and immediately transferred into the slide chamber and monitored using CLSM. Fluorescence excitation was performed using the 488nm line of an argon-ion laser, and emission was recorded at 515-550nm (Bartsch et al., 2011; Sharifpanah et al., 2016).

2.2.4 Measurement of NO generation

To evaluate the intracellular NO concentration within EBs, the EBs were loaded with 10µM of the cell-permeable specific fluorescent NO indicator DAF-FM DA and incubated for 30 min on a shaker in the dark at 37 °C, 5% CO_2. Subsequently, the EBs were washed with serum-free Iscove's basal medium and further incubated for 30 min. The EBs were

transferred to the slide chamber which was fixed on the stage of the CLSM. DAF fluorescence was excited at 488nm and emission recorded at 515-550nm (Mascheck et al., 2015; Sharifpanah et al., 2019).

2.2.5 Recording of the intracellular calcium concentration

To measure intracellular calcium transients, single cells were loaded with the cell-permeable dye Fluo-4-AM. Initially, 3-day-old EBs were enzymatically dissociated by using PBS containing 2 mg/ml of collagenase B for 30 min at 37 °C. Single cells were seeded on (0.1%) gelatin-coated coverslips in 24-well cell culture plates and incubated in CCE differentiation medium at 37 °C, 5% CO_2 and relative humidity of 95%. After 24h, single cells were attached, and were then incubated in serum-free Iscove's basal medium containing 5µM Fluo-4-AM at 37 °C, 5% CO_2 for 30 min. Subsequently, the coverslips were transferred to an incubation slide chamber containing fresh serum-free Iscove's Basal Medium, and then transferred to the stage of the CLSM. Cells were superfused with PUFAs after 300 s of recording. For fluorescence excitation the 488 nm a wavelength of an argon laser was used. Emission was recorded at 500–550nm. Fluorescence images were acquired every 3 s (Mascheck et al., 2015; Sharifpanah et al., 2016).

2.2.6 Western blot assay

Western blotting is the most common and widely used assay to detect protein expression qualitatively and quantitatively in biological specimen such as cells or tissues. Western blotting was performed according to a previously published protocol (Ali et al., 2018).

2.2.6.1 Protein extraction

After the EBs were prepared, they were collected in 1.5ml micro-tubes, the medium was aspirated and EBs were washed with ice-cold PBS to remove the rest of cell culture medium. Subsequently 100µl of protein extraction buffer (lysis-buffer) was added, which was prepared freshly. The EBs were grinded with a pellet pestle in the 1.5ml micro-tube, incubated for 20 min on ice, then the cells were homogenized again. Subsequently, the micro-tube was centrifuged in a pre-cooled centrifuge for 10 min at +4 °C at 35395*g*.

Finally, the supernatant was transferred to another 0.5ml micro-tube and stored at -80 °C till use.

2.2.6.2 Lowry protein assay

Lowry protein assay (Lowry et al., 1951) is a biochemical assay, which is used to quantify protein levels in biological samples. This method is dependent on color change of the solution, which can be measured by colorimetric techniques. The sample was prepared by mix-up of solution D, solution E, DW, and protein sample in the ratio 1000:100:100:10, respectively. In parallel, a concentration series of BSA protein standards was prepared. The mixed solutions were incubated for 10 min at RT, then 200µl of solution F was added to 1000µl of the mixed solutions, and then incubated for an additional 30 min at 37 °C. The solutions were centrifuged for 30 min at RT and 35395g. Finally, 200µl of solutions were transferred to a 96-well ELISA plate and absorbance measured by using an ELISA reader (Tecan Infinite m200 Microplate reader) and a wavelength of 578nm.

2.2.6.3 Gel electrophoresis

Protein electrophoresis refers to the migration of charged proteins in polyacrylamide gels in an electric field. This leads to protein separation depending on the respective molecular weight. In the present study semi-quantitative western blot was performed. An amount of 20µg of the protein sample was mixed with 1xNuPAGE LDS buffer and 1xNuPAGE reducing agent. Subsequently, the protein sample was denatured by heating for 10 min at 70 °C. The protein samples were loaded into the pockets of 4% stacking PAGEr EX polyacrylamide gels, which were mounted in the electrophoresis chamber. A volume of 500µl antioxidant solution was added to the electrophoresis chamber, which was filled with 0.67x of ProSieve EX running buffer. The chamber was connected with the power supply, and 200 voltage (V) and 120 milliampere (mA) were applied for 45-55min.

2.2.6.4 Protein transfer from the gel to the PVDF membrane

After completion of gel, electrophoresis proteins were transferred to PVDF membranes with a pore size of 0.2µM. PVDF membranes were wetted for 1 min with methanol, washed with DW, and then transferred to 1xProSieve EX transfer buffer. Additionally,

filter papers and sponges were soaked in transfer buffer. Subsequently, the transfer sandwich was prepared as illustrated below (figure 2.4). The transfer sandwich was inserted in the blotting chamber (Xcell II Blot module). The chamber was connected with the power supply, which was adjusted at 25V and 375mA for 60-90 min.

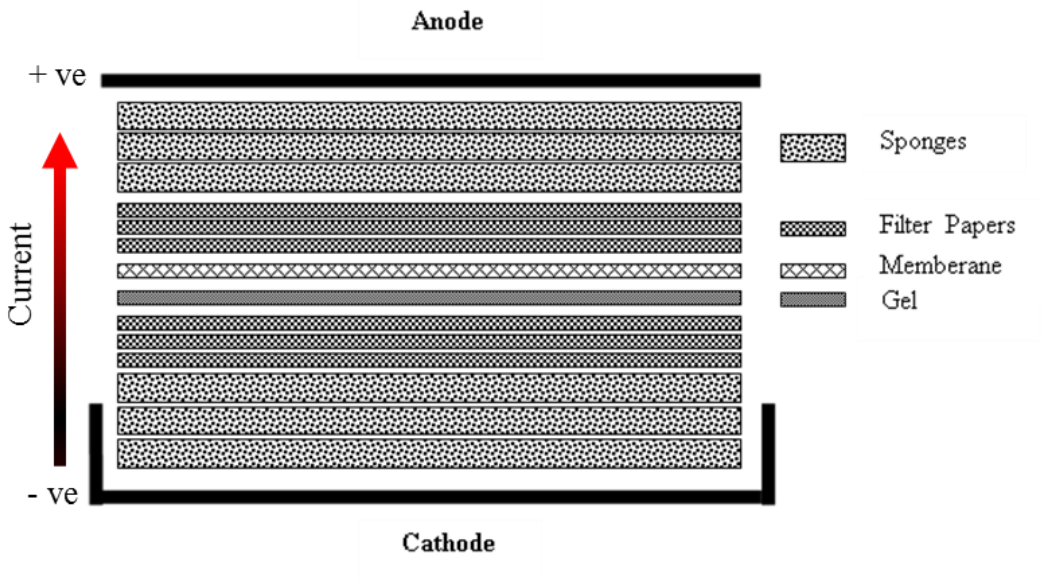

Figure 2.4: Example of sandwich preparation for western blot analysis.

2.2.6.5 Ponceau-S staining.

Ponceau-S staining is utilized to detect successful protein transfer onto the PVDF membrane. The membrane was soaked in the Ponceau-S staining solution for 5 min to visualize protein bands.

2.2.6.6 Protein detection

In this step, the target protein bands were detected on the membrane by immune-staining with specific antibodies. Ponceau-S staining solution was removed by washing the membrane with 0.1%TBST for blocking nonspecific protein binding. The membrane was incubated in blocking buffer (5% nonfat- dry milk in 0.1% TBS-Tween) at RT for 60 min on a shaker. After that, the membrane was incubated on a shaker overnight in primary antibody solution at +4 °C, and then for 60 min at RT with secondary antibody. The primary and secondary antibodies were previously diluted with 5% BSA in ratio as

described in 2-1-9. Between incubation with primary and secondary antibody the membranes were washed at least 3 times for 5 min with 0.1% TBS-Tween (Table 11).

Table 11: Summary of the antibody staining protocol on PVDF membranes

Step	Solution	Duration	Temperature
Washing	0.1%TBS- Tween	3x5 min	RT
Blocking	5% nonfat- dry milk	60 min	RT
Primary antibody	Diluted in 5% BSA	Overnight	+4 °C
Secondary antibody	Diluted in 5% BSA	60 min	RT

2.2.6.7 ECL detection

ECL detection is a method depending on an enzymatic reaction between horseradish peroxidase (HRP)-labelled secondary antibody and substrate, which consists of a stable peroxide solution and an enhanced luminol solution. This reaction generates a light signal which can be detected using a chemiluminescence imaging system. The PVDF membrane with labelled proteins was soaked in 10ml of freshly prepared ECL detection solution for ~1 min with gentle agitation. Subsequently, the membrane was wrapped in a plastic container, filled with ECL detection solution, and placed into the chemiluminescence imaging system. The luminescence light signal of the membranes was recorded under darkroom conditions, and saved as tagged image file format (TIFF).

2.2.6.8 Densitometry image analysis

The image was analyzed using the densitometry. Densitometric signal strength depends on the grey level intensity of protein bands in images. The signal intensity of protein expression in images was converted into a digital value by use of the Java software Image J. The value for relative specific protein expression was normalized with the internal loading control, which is an endogenous protein and is unaffected by experimental conditions or treatments.

2.2.6.9 Stripping and reprobing

Stripping refers to removal of the primary and secondary antibody from the western blot membrane by using the stripping buffer. This method was used for investigating more than one protein on the same blot membrane. The membrane was soaked in restore western blot stripping buffer for 20 min at RT with gently shaking. Subsequently, the membrane was washed with 0.1%TBS-Tween three times for 5 min. After this procedure, the membrane is ready for re-staining with another antibody by the same steps as mentioned in 2-2-6-6.

2.2.7 Statistical analysis

For statistical analysis, PRISM statistics software (GraphPad Software, San Diego, CA) was used. Data are given as mean ± standard deviation (SD), with *n* denoting the number of experiments performed with independent ES cell cultures. In each experiment, at least 20 culture objects were analyzed unless otherwise indicated. Student's t-test for unpaired data and one-way analysis of variance (ANOVA) (Tukey or Dunnett multiple comparison tests) were applied as appropriate for statistical analysis. A value of $P \leq 0.05$ (*) or (#) was considered significant.

3. Results

3.1 Vasculogenesis upon PUFA treatment in EBs

3.1.1 LA and EPA stimulated vasculogenesis in ES cell-derived EBs

Vasculogenesis refers to the differentiation of endothelial cells from angioblasts and endothelial precursor cells, in addition to the *de novo* formation of a primitive vascular network (Kolte et al., 2016). According to our working hypothesis, PUFAs may regulate ES cell differentiation towards the cardiovascular lineage. The effect of PUFAs and PA on vascular sprout formation was evaluated. EBs were formed in spinner flask culture, and were transferred on day 3 of cell culture to bacteriological plates. EBs were incubated with either EPA or LA in concentrations ranging from 1 to 100µM, and vascular structure formation as well as protein expression of the vascular markers PECAM-1 and VE-Cadherin were investigated. EPA as well as LA treatment dose-dependent significantly increased vascular structure formation (figure 3.1A–C) and the expression of vascular markers (figure 3.1E–H). In contrast, treatment with PA (10, 50, 100µM) did not affect vasculogenesis as compared with the untreated and the vehicle control (figure 3.1D). Optimum effects on vasculogenesis were achieved with 10–50µM EPA and LA. Moreover, increased expression of FLK-1, which is an early marker of vascular progenitor cells, was observed upon either EPA or LA treatment (figure 3.1I, J), suggesting stimulation of vasculogenesis in ES cells upon incubation with PUFAs.

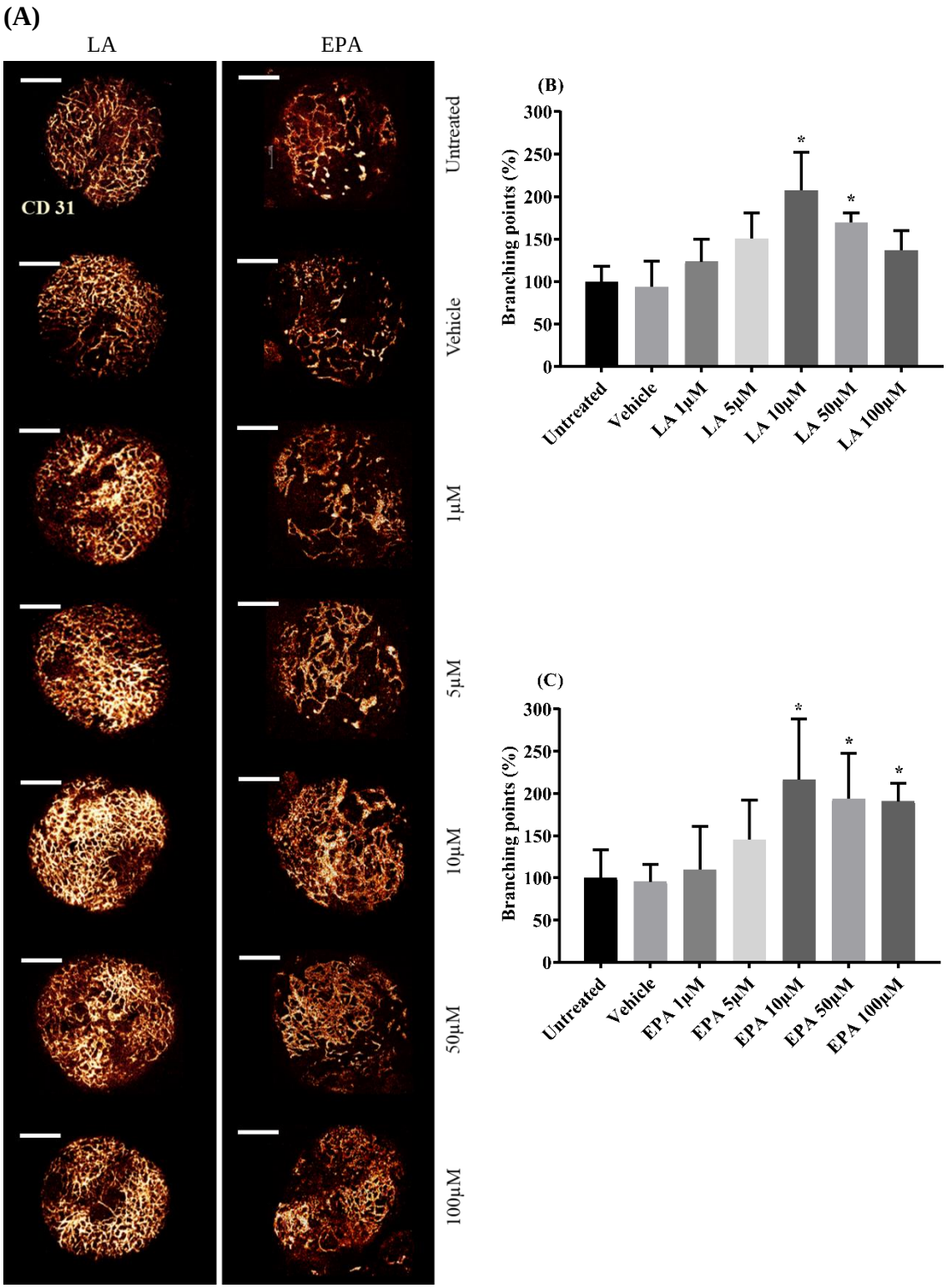
(A)
LA
EPA
CD 31
Untreated
Vehicle
1µM
5µM
10µM
50µM
100µM
(B)
Branching points (%)
300
250
200
150
100
50
0
Untreated
Vehicle
LA 1µM
LA 5µM
LA 10µM
LA 50µM
LA 100µM
(C)
Branching points (%)
300
250
200
150
100
50
0
Untreated
Vehicle
EPA 1µM
EPA 5µM
EPA 10µM
EPA 50µM
EPA 100µM

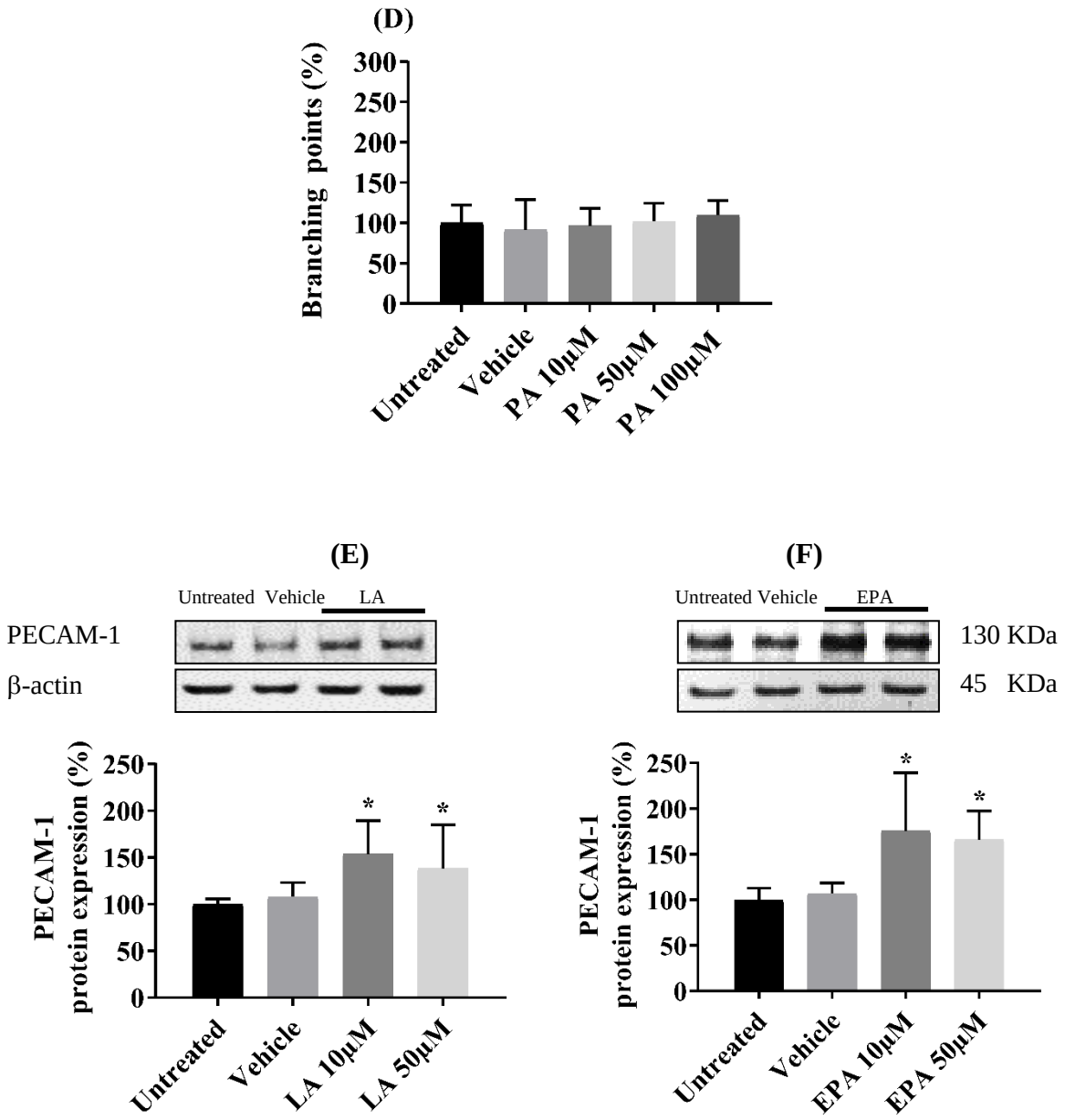
(D)
Branching points (%)
300
250
200
150
100
50
0
Untreated
Vehicle
PA 10μM
PA 50μM
PA 100μM
(E)
Untreated Vehicle LA
PECAM-1
β-actin
PECAM-1 protein expression (%)
250
200
150
100
50
0
*
*
Untreated
Vehicle
LA 10μM
LA 50μM
(F)
Untreated Vehicle EPA
130 KDa
45 KDa
PECAM-1 protein expression (%)
250
200
150
100
50
0
*
*
Untreated
Vehicle
EPA 10μM
EPA 50μM

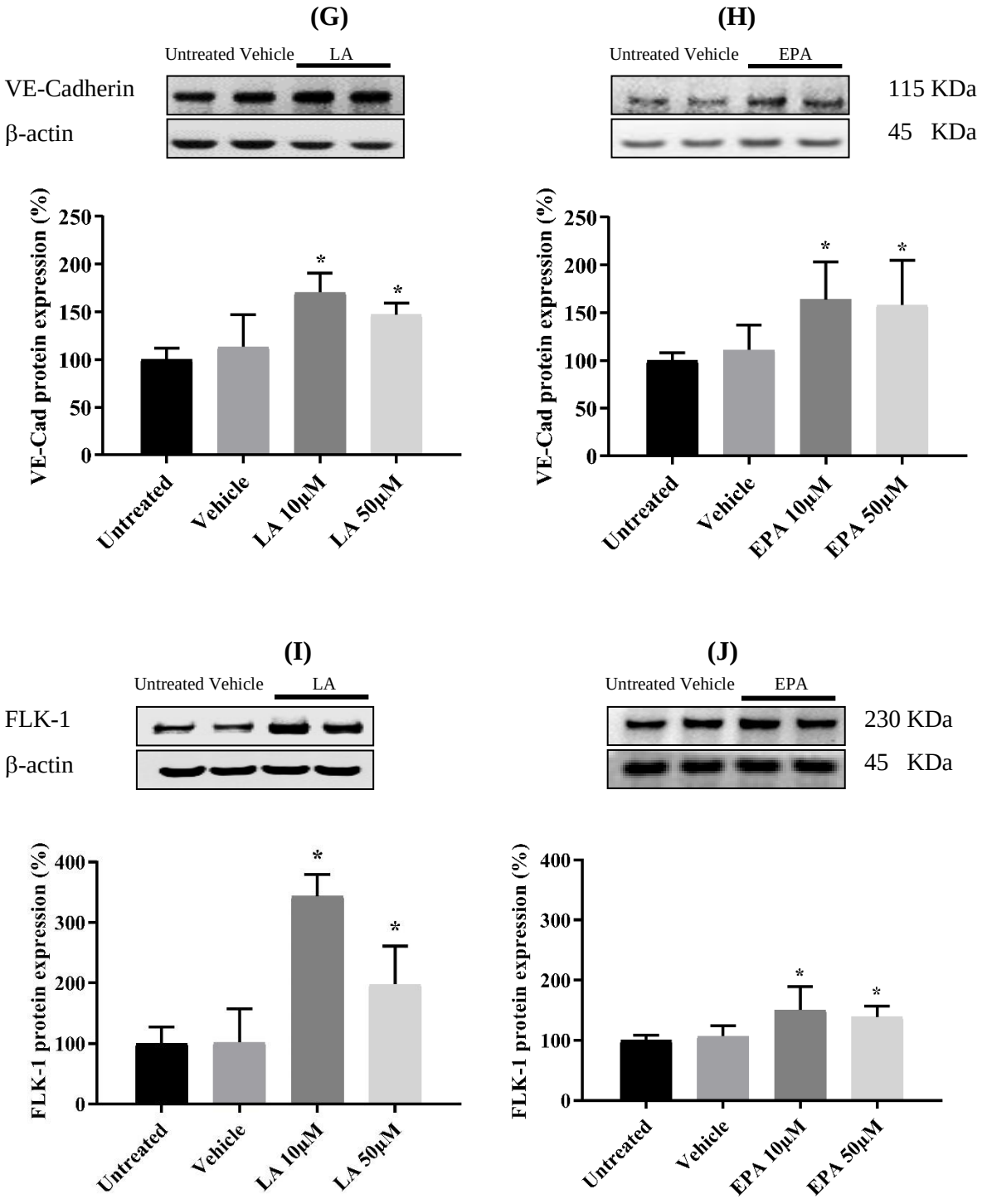

Figure 3.1: Stimulation of vasculogenesis and vascular marker expression by EPA and LA. ES cells differentiating within EBs were treated from day 3 to 10 of cell culture with increasing concentrations (1–100μM) of either EPA or LA, remained untreated or were treated with vehicle (DMSO). Vascular structures were stained with an anti-PECAM-1 antibody, and branching points were analyzed by computer-assisted image

analysis. (A) Representative PECAM-1 labeled EBs. The bar represents 300µm. (B–D) Quantitative presentation of branching points (%) following incubation with different concentrations of (B) LA (n = 3), (C) EPA (n = 6) or (D) PA (n = 3). (E and F) Western blot analysis of PECAM-1 expression upon treatment with either (E) 10 or 50µM LA (n = 9) or (F) EPA (n = 7). (G and H) Western blot analysis of VE-Cadherin expression upon treatment with either (G) 10 or 50µM LA (n = 4) or (H) EPA (n = 7). (I and J) Western blot analysis of fetal liver kinase-1 (FLK-1) expression upon treatment with either (I) 10 or 50µM LA (n = 4) or (J) EPA (n = 6). *P ≤ .05, significantly different to the vehicle and control.

3.1.2 PUFAs-induced signaling pathway elements in ES cells.

3.1.2.1 Generation of ROS and NO upon treatment of ES cells with PUFAs

Previous studies of us and others have demonstrated that cardiovascular differentiation of ES cells is dependent on ROS and NO, acting as signaling molecules in intracellular signal transduction pathways (Ali et al., 2018; Cencioni et al., 2018; Sharifpanah et al., 2016). We therefore assessed ROS generation using the ROS-sensitive indicator H_2DCF-DA as well as the NO-sensitive indicator DAF-FM for ROS and NO determination, respectively. Moreover, activation of eNOS was evaluated upon treatment with either EPA or LA. It was observed that treatment with EPA and LA (10 and 50µM) increased ROS generation (figure 3.2A, B). Investigation of the time course of ROS generation by LA revealed that ROS production occurred within few min after PUFA administration and remained on an elevated plateau for at least 24h (figure 3.2C). Coadministration of EPA and LA with the free radical scavengers Trolox (100µM) and NMPG (100µM) completely abolished the stimulation of vascular structure formation obtained upon PUFA treatment (figure 3.2D-F). Moreover, the stimulation of vasculogenesis by PUFAs was significantly inhibited in presence of the NADPH oxidase inhibitor VAS2870 (50µM; figure 3.2D–F). PUFA treatment of differentiating ES cells likewise increased NO generation (figure 3.3A–C) and increased eNOS phosphorylation at residue Ser1177 within few min (figure 3.3D, E). The phosphorylation of eNOS as well as vascular structure formation were completely blunted in presence of the NOS inhibitor L-NAME (figure 3.3F, G), indicating the importance of NO in parallel to ROS for the induction of vasculogenesis by PUFAs.

(A)

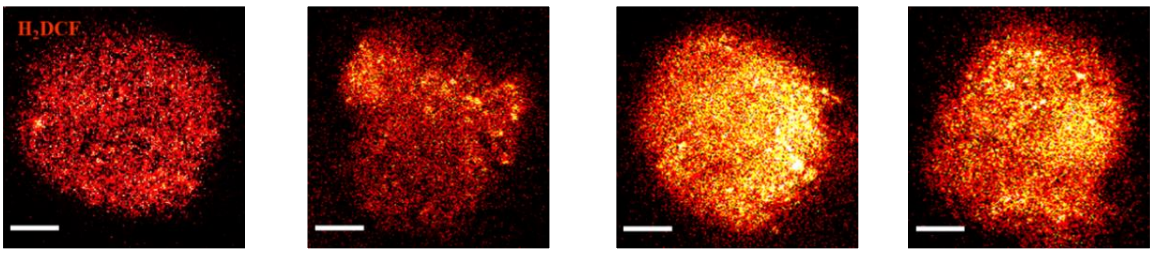

Untreated Vehicle LA 10µM LA 50µM

(B)

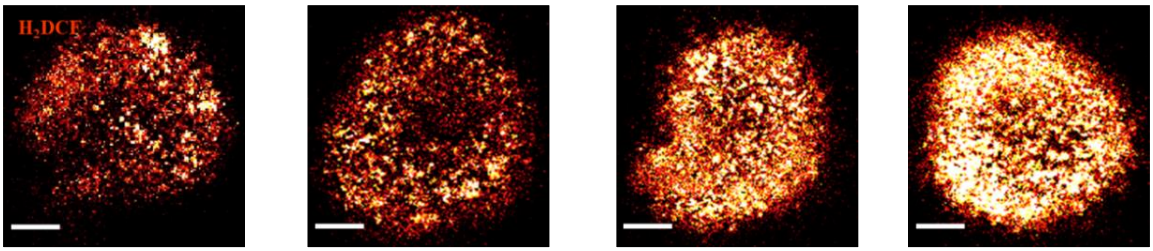

Untreated Vehicle EPA 10µM EPA 50µM

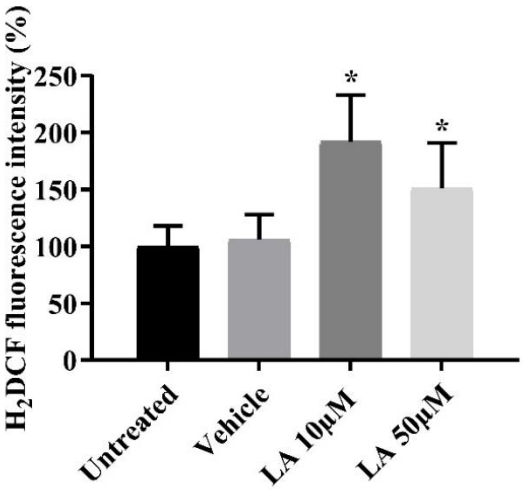

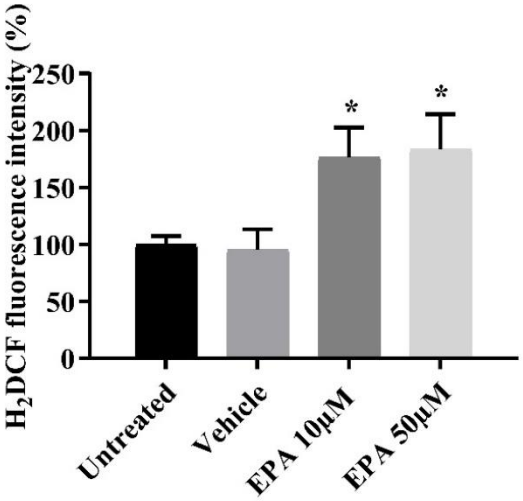

(C)

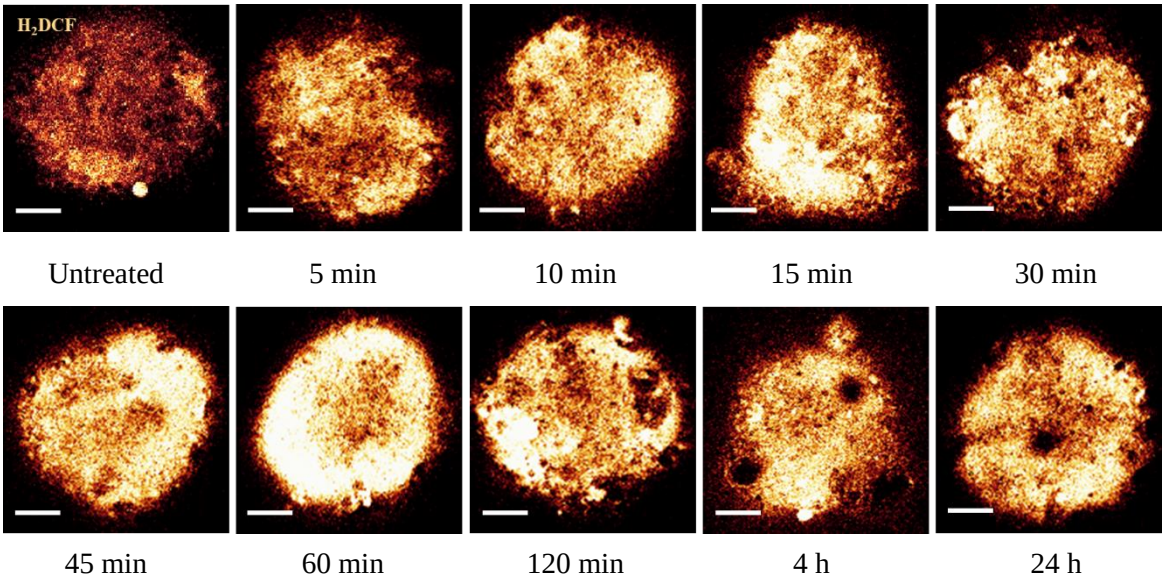
H2DCF
Untreated
5 min
10 min
15 min
30 min
45 min
60 min
120 min
4 h
24 h

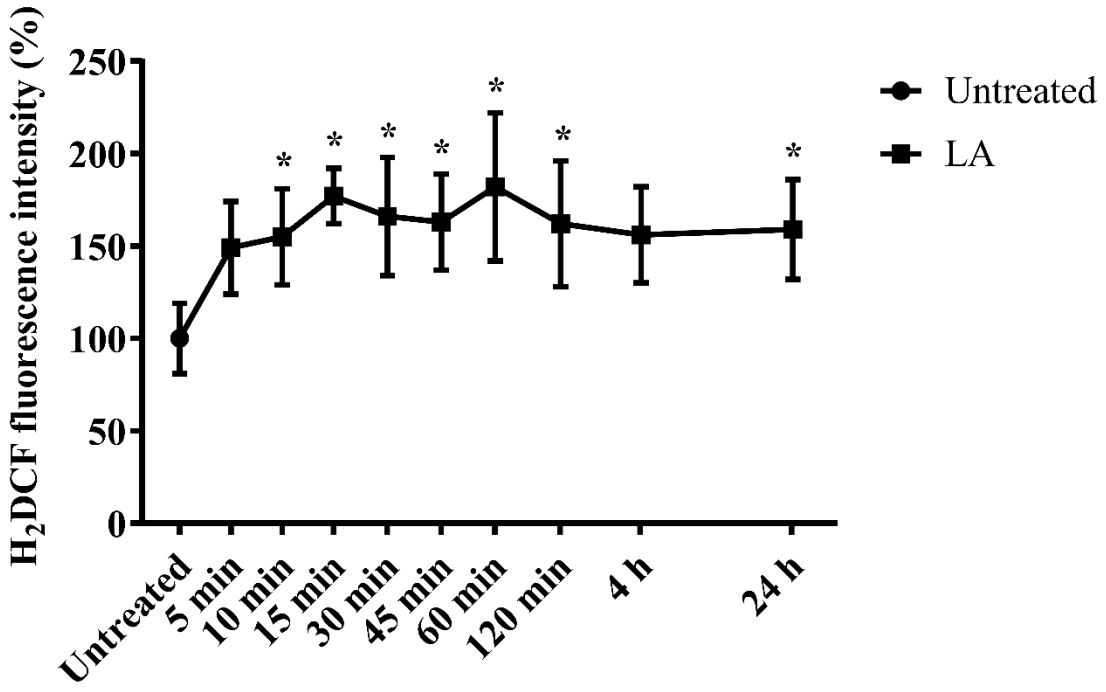
H2DCF fluorescence intensity (%)
250
200
150
100
50
0
Untreated
LA
Untreated
5 min
10 min
15 min
30 min
45 min
60 min
120 min
4 h
24 h

(D)

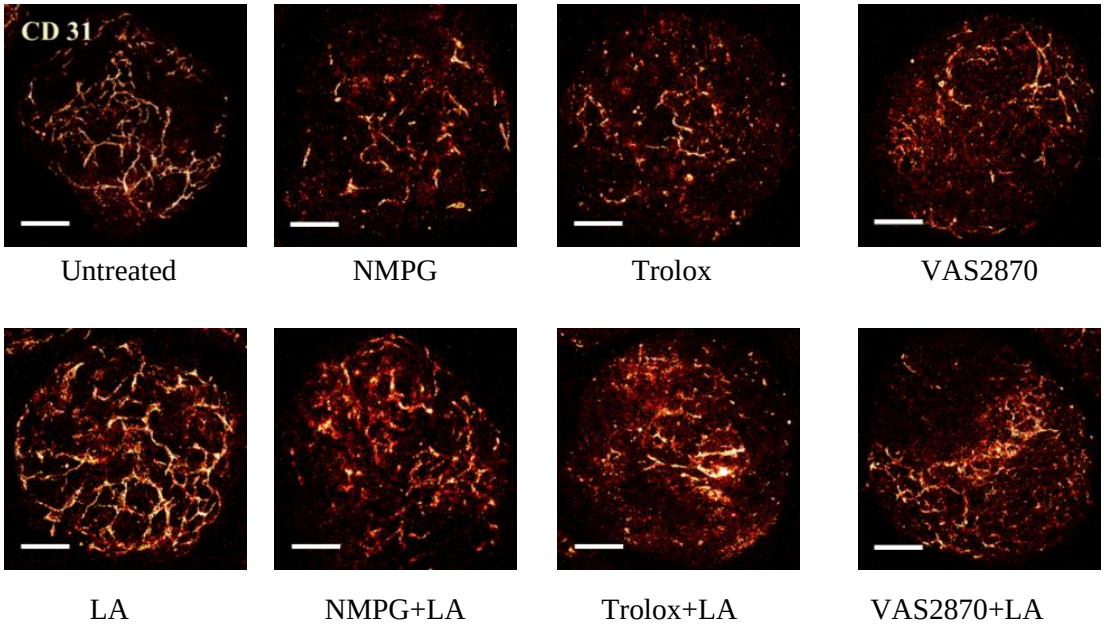
CD 31
Untreated
NMPG
Trolox
VAS2870
LA
NMPG+LA
Trolox+LA
VAS2870+LA

(E)

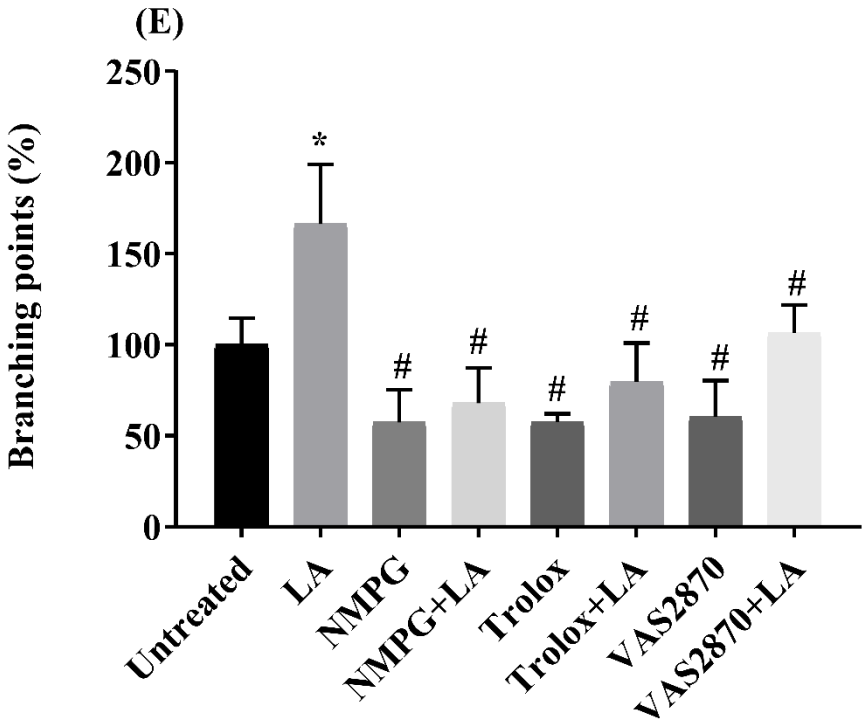
Branching points (%)
250
200
150
100
50
0
*
#
#
#
#
#
Untreated
LA
NMPG
NMPG+LA
Trolox
Trolox+LA
VAS2870
VAS2870+LA

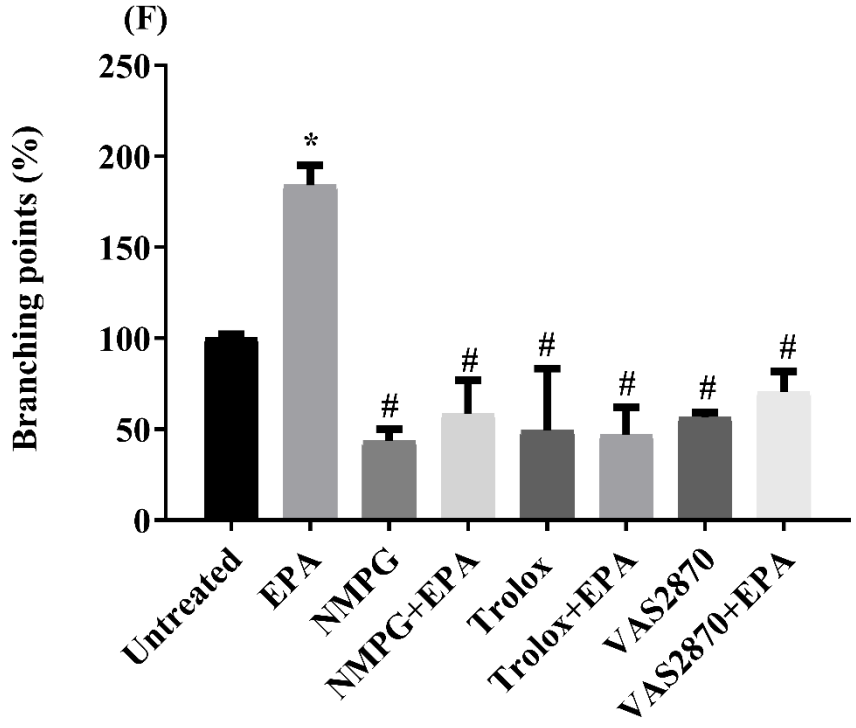

Figure 3.2: Generation of ROS in EPA as well as LA treated differentiating ES cells and effects of free radical scavengers and NADPH oxidase inhibition on vasculogenesis. (A and B) EBs (4-day-old) were treated with either 10 or 50µM LA (A) or EPA (B) or vehicle (DMSO), and ROS generation was assessed 24h thereafter using H_2DCF as fluorescent ROS indicator (n = 3). Shown are representative DCF-labeled EBs. The bar represents 200µm. (C) Time course of ROS generation after different min of LA (50µM) incubation (n = 3). (D–F) Effect of the free radical scavengers NMPG (100µM) and Trolox (100µM) or the NADPH oxidase inhibitor VAS2870 (50µM) on vascular branch formation. (D) Representative EBs stained with an antibody against CD31. The bar represents 200µm. (E and F) Quantitative analysis of vascular branching points (%) following treatment with (E) LA (50µM; n=3) or (F) EPA (n=3). *p ≤ .05, significantly different to the untreated control, #p ≤ .05, significantly different to the PUFA treated sample.

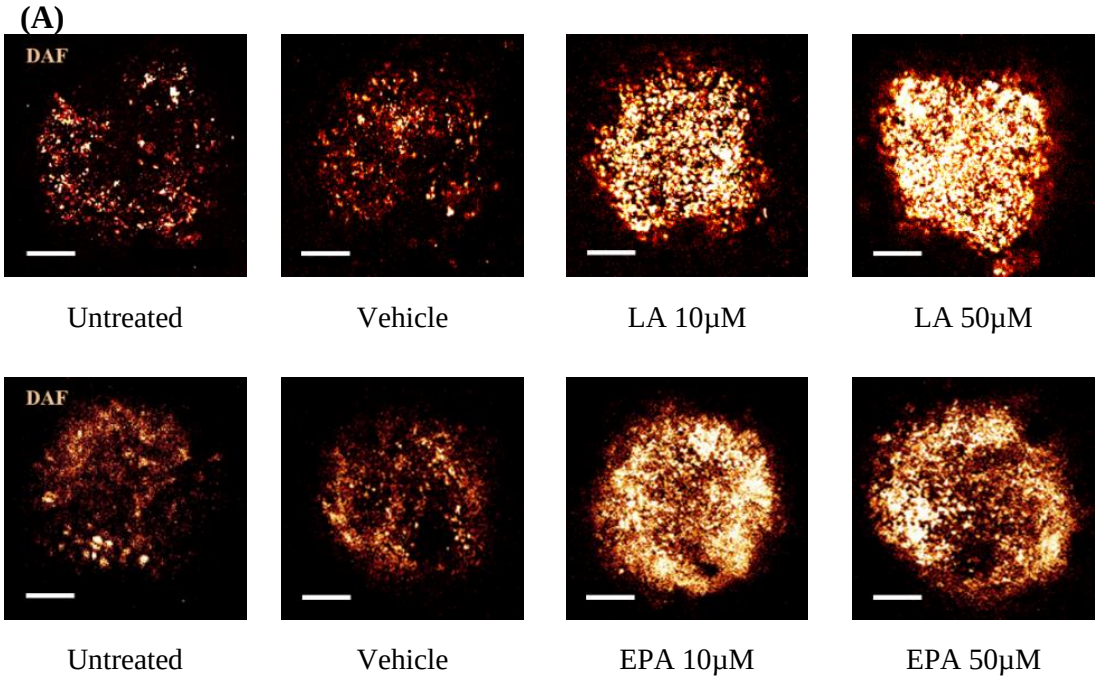
(A)
DAF
DAF
Untreated
Vehicle
LA 10μM
LA 50μM
Untreated
Vehicle
EPA 10μM
EPA 50μM

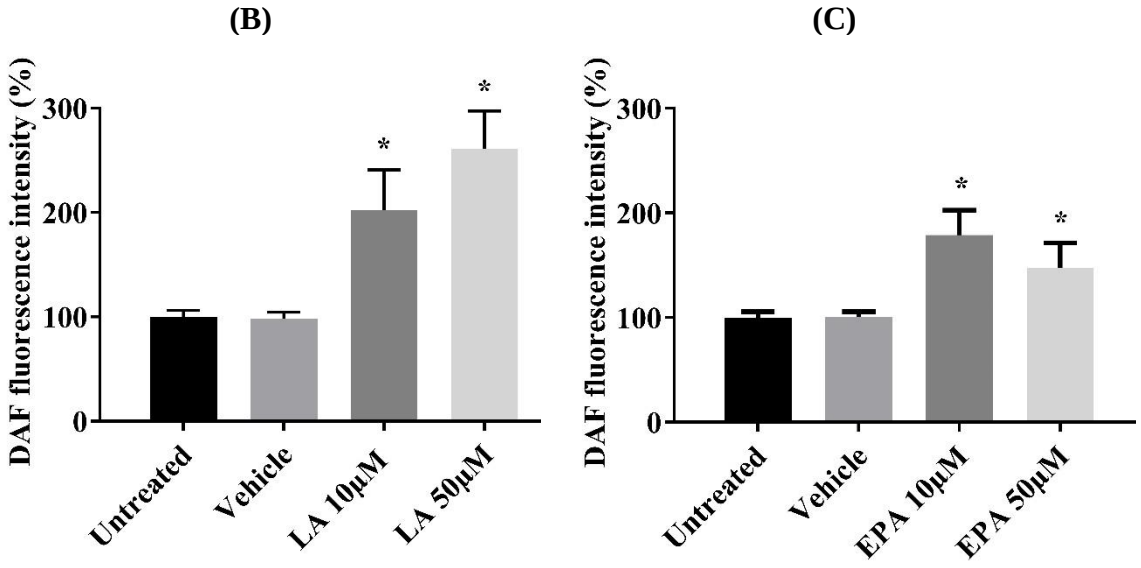
(B)
DAF fluorescence intensity (%)
300
200
100
0
*
*
Untreated
Vehicle
LA 10μM
LA 50μM

(C)
DAF fluorescence intensity (%)
300
200
100
0
*
*
Untreated
Vehicle
EPA 10μM
EPA 50μM

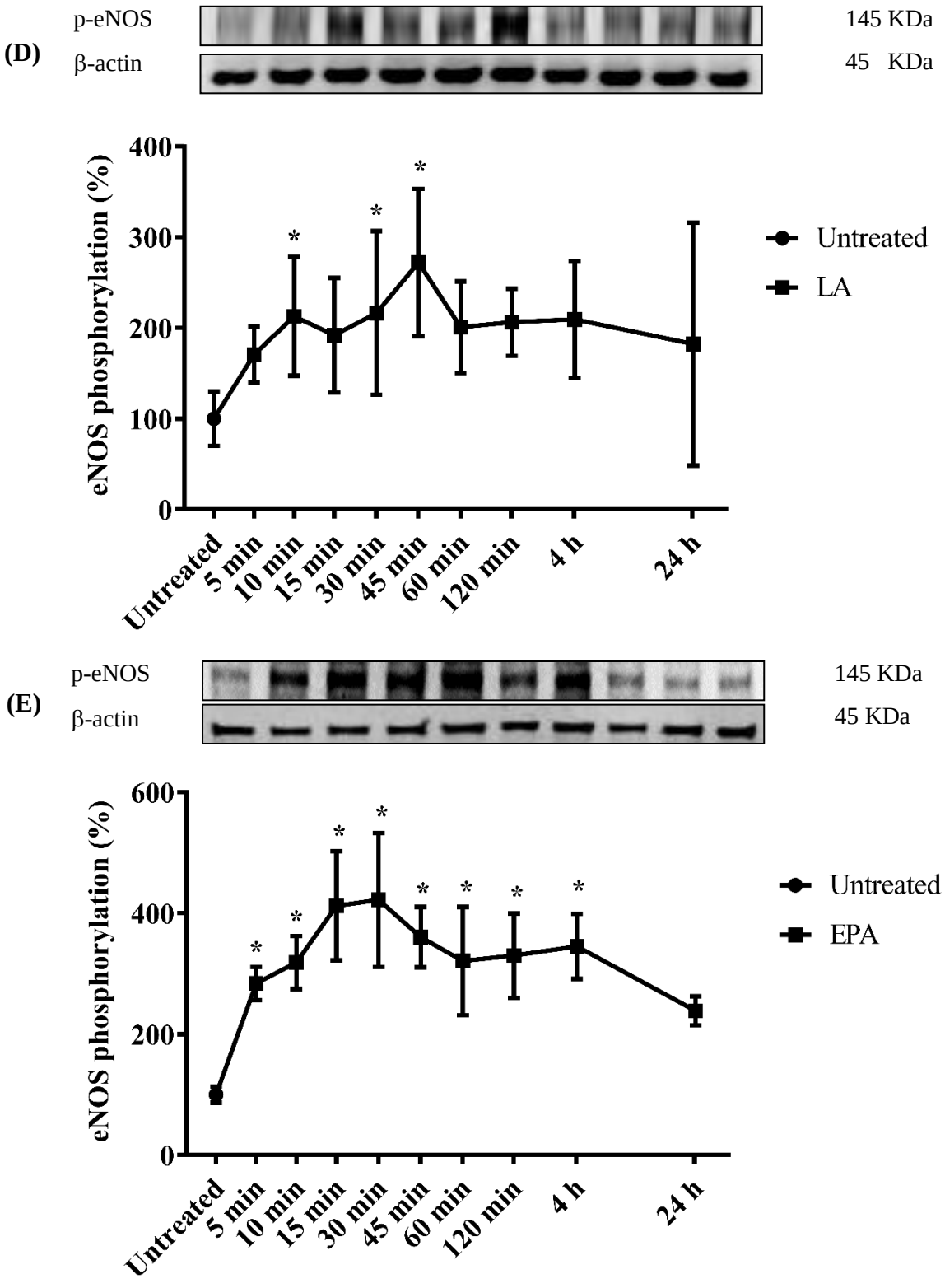
(D)
p-eNOS
β-actin
145 KDa
45 KDa
eNOS phosphorylation (%)
400
300
200
100
0
Untreated
LA
Untreated
5 min
10 min
15 min
30 min
45 min
60 min
120 min
4 h
24 h
(E)
p-eNOS
β-actin
145 KDa
45 KDa
eNOS phosphorylation (%)
600
400
200
0
Untreated
EPA
Untreated
5 min
10 min
15 min
30 min
45 min
60 min
120 min
4 h
24 h

(F)

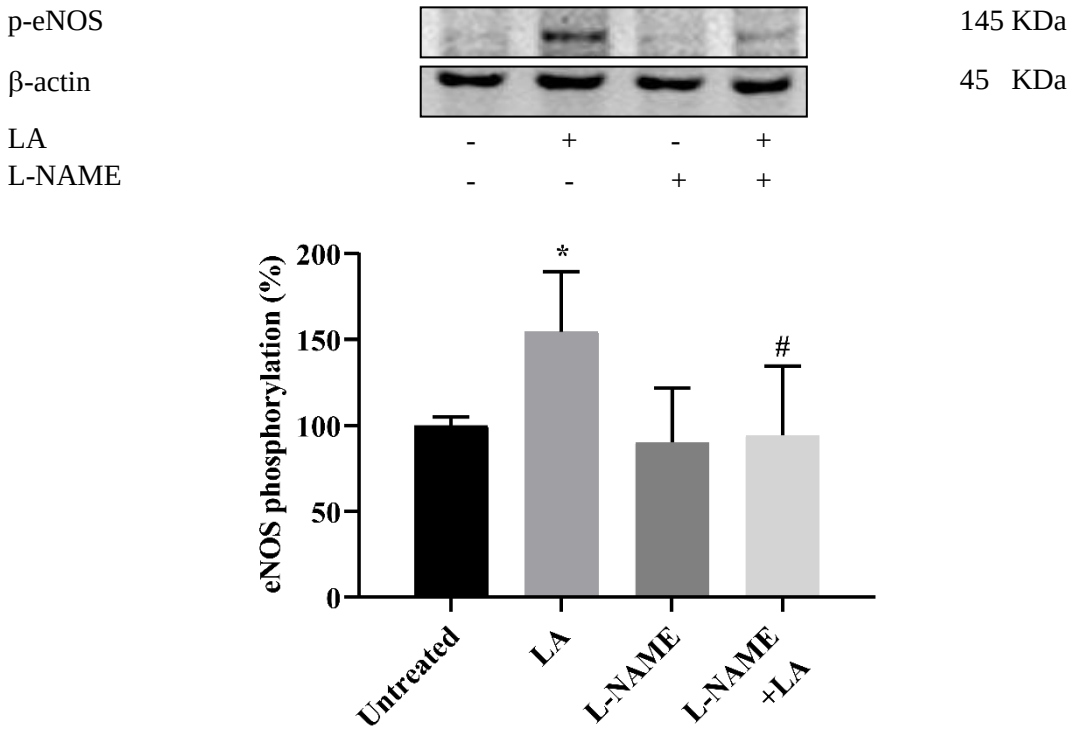
p-eNOS
β-actin
145 KDa
45 KDa
LA
L-NAME
- + - +
- - + +
eNOS phosphorylation (%)
200
150
100
50
0
*
#
Untreated
LA
L-NAME
L-NAME +LA

(G)

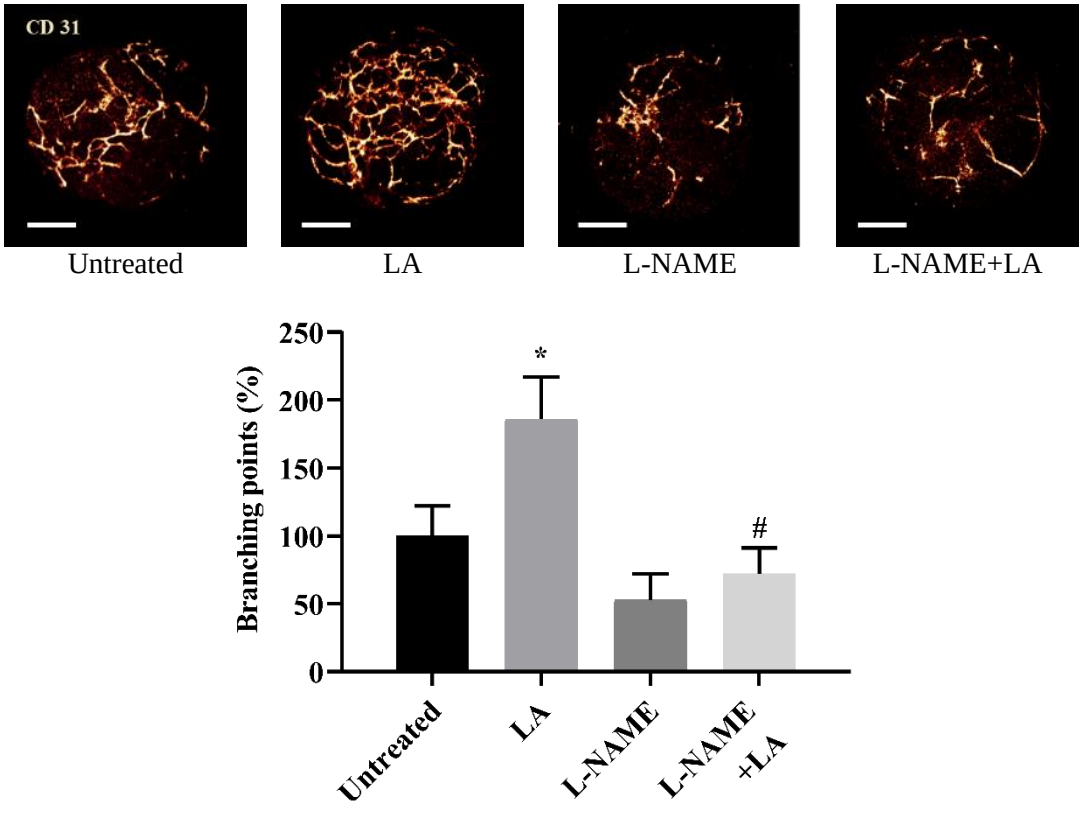
CD 31
Untreated
LA
L-NAME
L-NAME+LA
Branching points (%)
250
200
150
100
50
0
*
#
Untreated
LA
L-NAME
L-NAME +LA

Figure 3.3: Generation of NO in EPA as well as LA treated differentiating ES cells and effect of the NOS inhibitor L-NAME on vasculogenesis. (A–C) EBs (4-day-old) were treated with either (A and B) 10 or 50μM LA or (A and C) EPA or vehicle (DMSO), and NO generation was assessed 24h thereafter using DAF-FM as fluorescent NO indicator. In (A) representative EBs labeled with DAF-FM are shown which were treated with either 10 or 50μM LA and EPA, respectively. The bar represents 200μm. (B and C) Quantification of DAF fluorescence (%) following treatment with (B) LA (n=3) and (C) EPA (n = 4). (D and E) Western blot analysis of eNOS phosphorylation at different time points of (D) LA (50μM; n=6) and (E) EPA (50μM; n=3) application. (F) Effect of the NOS inhibitor L-NAME on eNOS phosphorylation following treatment of EBs with LA (50μM) as evaluated by western blot analysis (n=6). (G) Effect of L-NAME on vasculogenesis (PECAM-1 staining) elicited upon treatment of differentiating ES cells with LA (50μM; n=3). *P ≤ 05, significantly different to the untreated control, #P ≤ .05, significantly different to the PUFA treated sample.

3.1.2.2 Release of intracellular calcium upon PUFA treatment

Ω-3 as well as ω-6 PUFAs have been previously shown to raise intracellular calcium in different cells (Carrillo et al., 2011; Kim et al., 2015; Min Hee Kim et al., 2009; Mobraten et al., 2013). To investigate whether changes in intracellular calcium concentrations relay PUFA treatment to the cellular messengers ROS and NO as well as to vasculogenesis of ES cells, intracellular calcium changes were assessed by Fluo-4 microfluorometry. It was evidenced that both EPA and LA (50μM) treatment transiently raised intracellular calcium concentrations (figures 3. 4A, III, IV). In contrast, there was no noticeable change in the intracellular Ca^{2+} level in the untreated group as well as the vehicle (DMSO) control (figures 3.4A, I, II). Pretreatment for 30 min with the intracellular calcium chelator BAPTA-AM (10μM) completely abolished the calcium response observed with PUFAs, indicating that calcium was released from intracellular stores (figures 3.4A, VII, VIII). CD36 imports fatty acids inside cells and is a member of the class B scavenger receptor family of cell surface proteins (Glatz & Luiken, 2018). Since PUFA entry via CD36 may initiate the intracellular calcium response, it was investigated whether the CD36 inhibitor (SSO; 200μM) would affect PUFA-induced calcium transients. Indeed, the increase in intracellular calcium was associated to PUFA entry into the cell via CD36 since the calcium response was significantly reduced by SSO (figures 3.4A, V, VI). When cells were pre-incubated for 24h with a blocking antibody against CD36, the calcium response was decreased in amplitude at an antibody concentration of 2μg/ml (figures 3.4A, IX, X) and

totally abolished at 3µg/ml (figures 3.4A, XI, XII). Furthermore, to find out, whether ROS generation required intracellular Ca^{2+}, ROS generation upon PUFAs treatment was assessed under conditions of intracellular Ca^{2+} chelation. 5-day-old EBs were pre-treated for 2h with 10µM of the intracellular calcium chelator BAPTA-AM, and in parallel loaded either in the absence or in the presence (50µM) of PUFAs with the ROS indicator (H_2DCF-DA). The data show that the chelator BAPTA-AM (10µM) significantly blocked ROS generation stimulated by PUFAs. In other words, the enhancement of ROS generation by PUFAs requires Ca^{2+} release from intracellular stores (figures 3.4B, C). Moreover, the intracellular calcium response upon PUFA treatment was necessary for the vasculogenesis process since pre-incubation with BAPTA-AM significantly inhibited vascular structure formation following treatment of differentiating ES cells with either EPA (50µM) or LA (50µM; figure 3.4D, E).

(A)

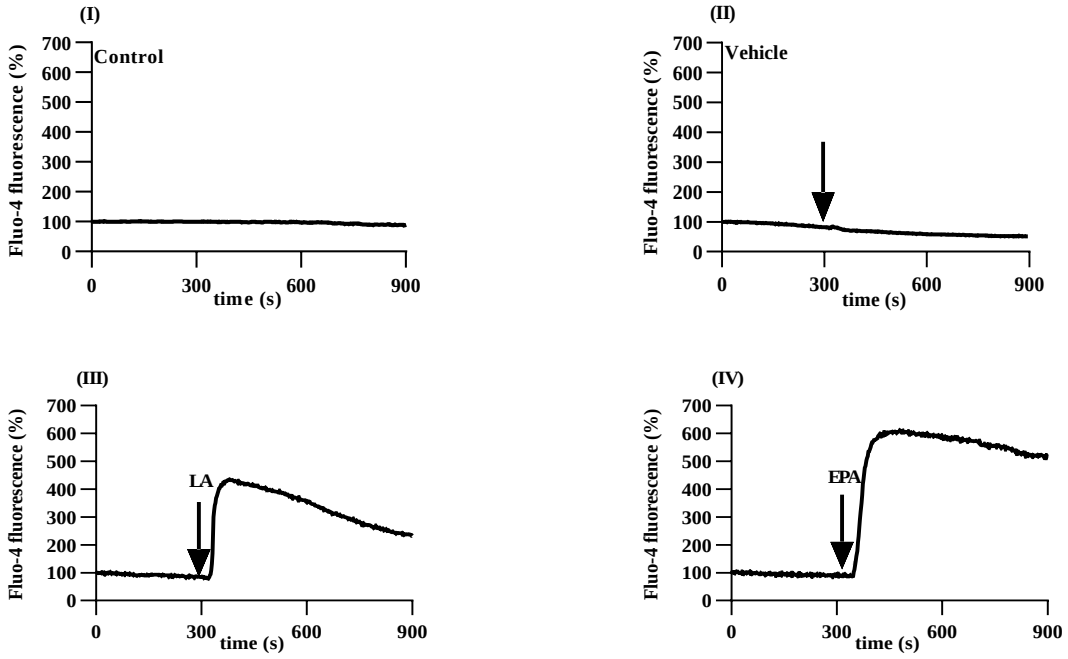

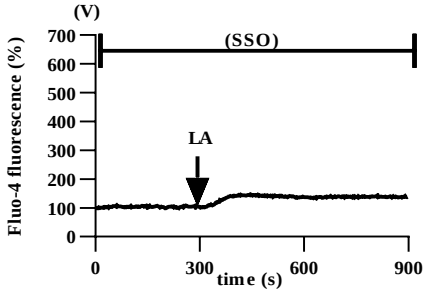
(V)
(SSO)
LA
Fluo-4 fluorescence (%)
time (s)

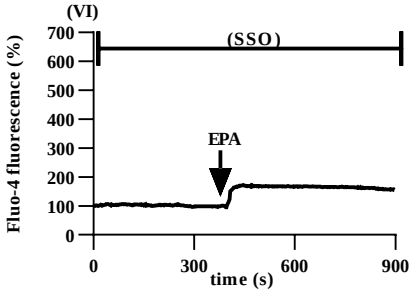
(VI)
(SSO)
EPA
Fluo-4 fluorescence (%)
time (s)

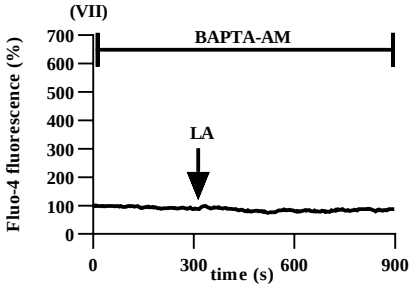
(VII)
BAPTA-AM
LA
Fluo-4 fluorescence (%)
time (s)

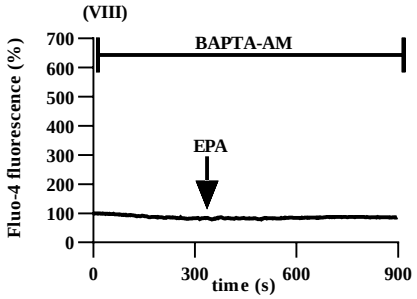
(VIII)
BAPTA-AM
EPA
Fluo-4 fluorescence (%)
time (s)

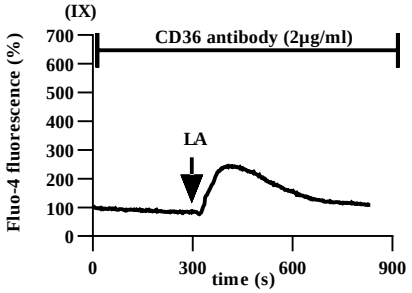
(IX)
CD36 antibody (2µg/ml)
LA
Fluo-4 fluorescence (%)
time (s)

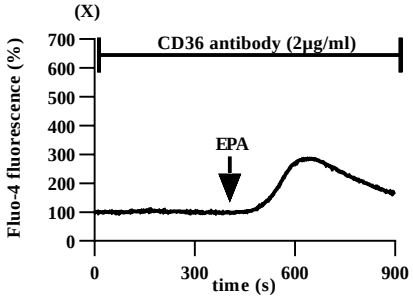
(X)
CD36 antibody (2µg/ml)
EPA
Fluo-4 fluorescence (%)
time (s)

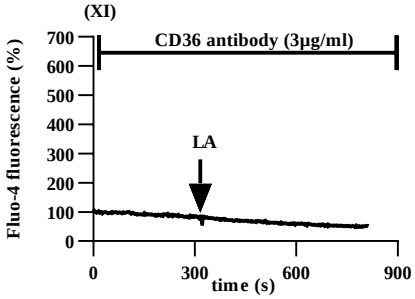
(XI)
CD36 antibody (3µg/ml)
LA
Fluo-4 fluorescence (%)
time (s)

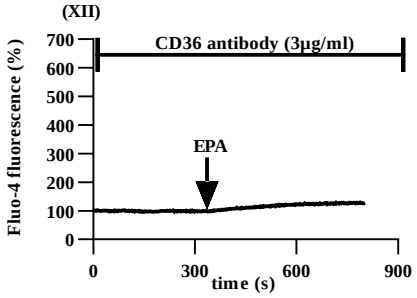
(XII)
CD36 antibody (3µg/ml)
EPA
Fluo-4 fluorescence (%)
time (s)

(B)

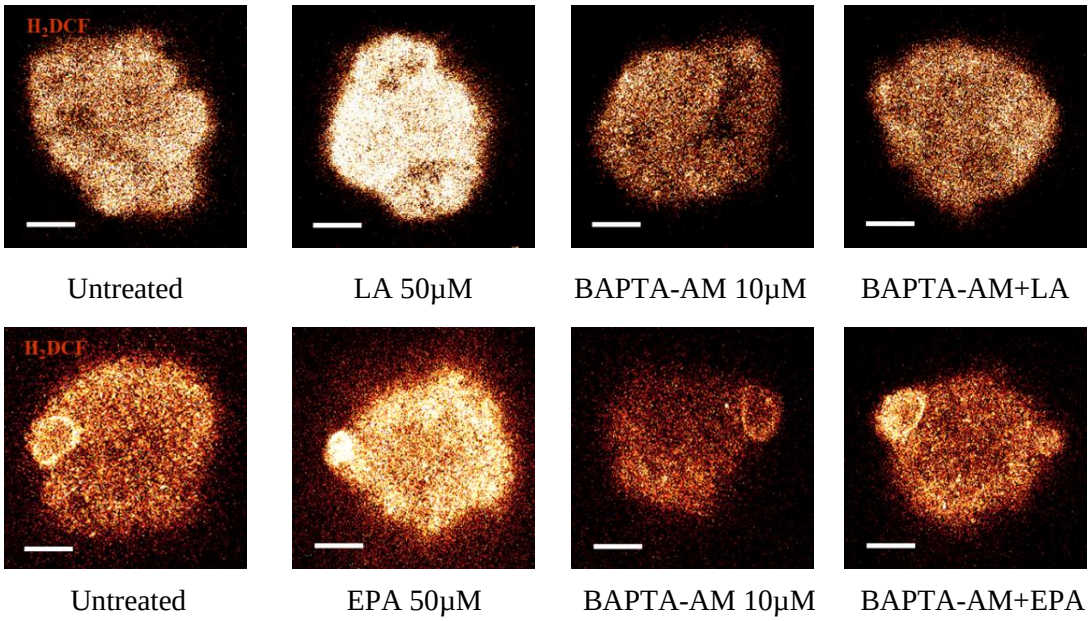
H2DCF
Untreated
LA 50μM
BAPTA-AM 10μM
BAPTA-AM+LA
H2DCF
Untreated
EPA 50μM
BAPTA-AM 10μM
BAPTA-AM+EPA

(C)

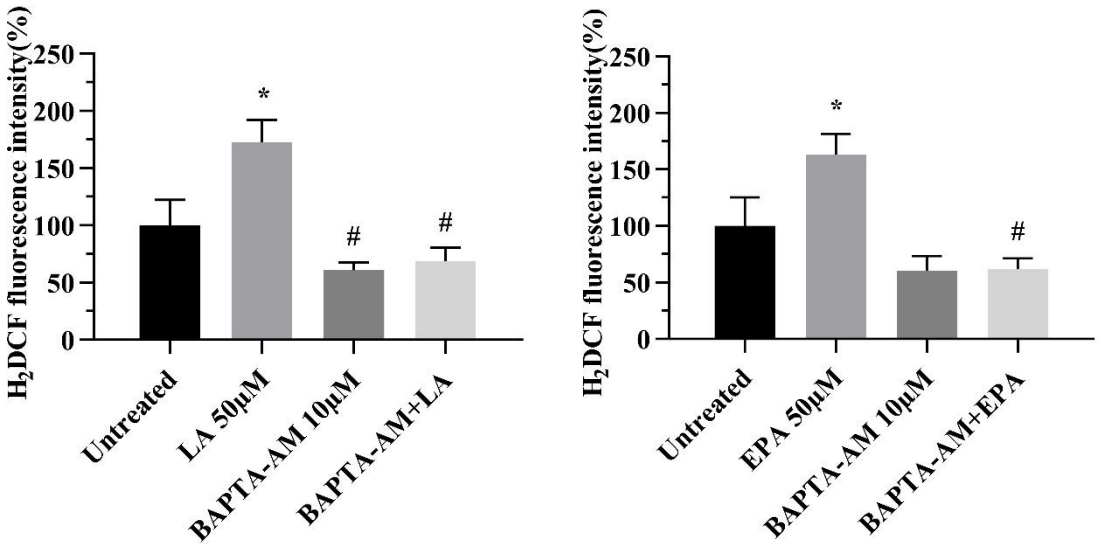
H2DCF fluorescence intensity(%)
250
200
150
100
50
0
*
#
#
Untreated
LA 50μM
BAPTA-AM 10μM
BAPTA-AM+LA
H2DCF fluorescence intensity(%)
250
200
150
100
50
0
*
#
Untreated
EPA 50μM
BAPTA-AM 10μM
BAPTA-AM+EPA

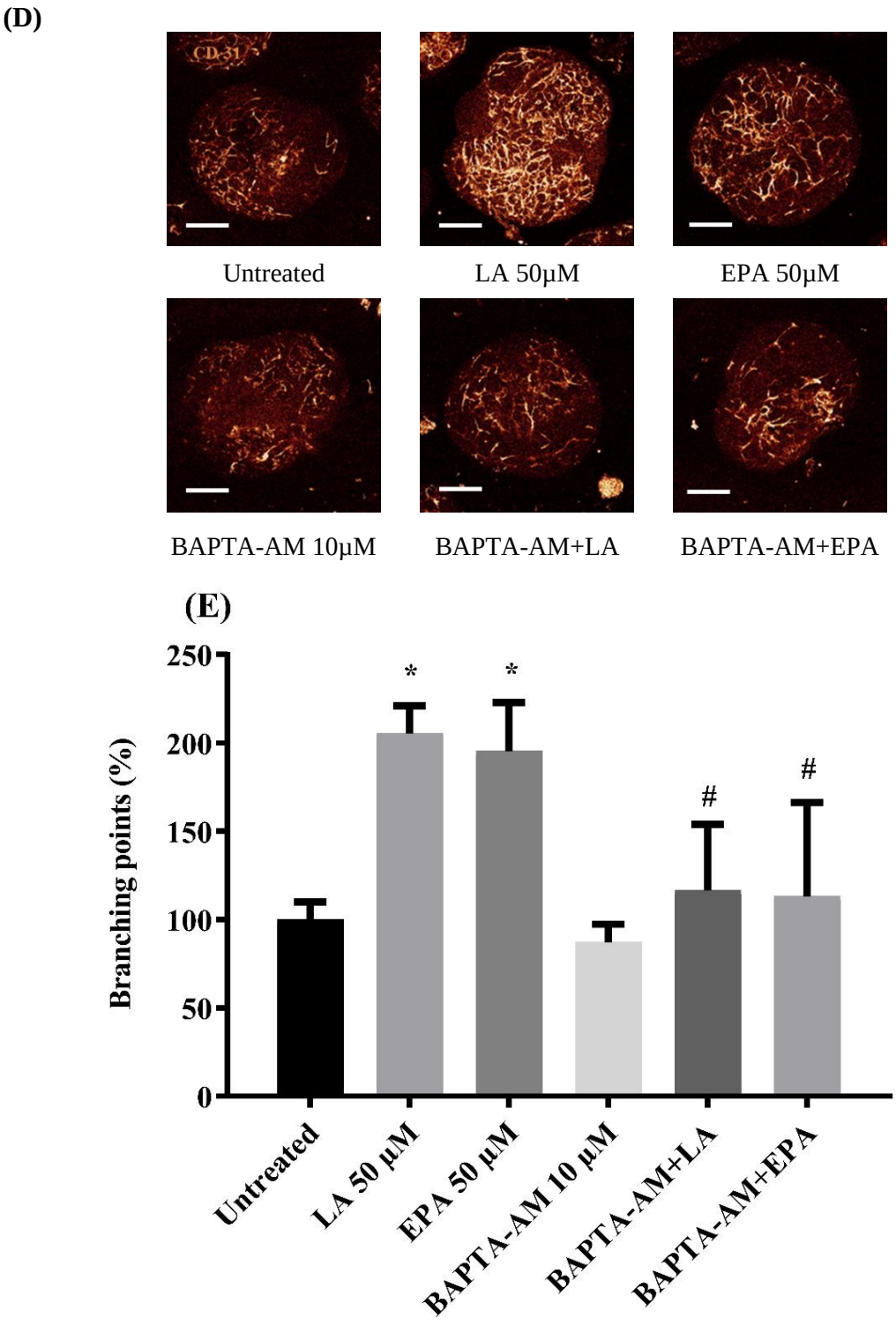

Figure 3.4: Release of intracellular calcium upon treatment of differentiating ES cells with EPA and LA. Intracellular calcium was monitored by Fluo-4 microfluorometry in single cells enzymatically dissociated from 3-day-old EBs. (AI) control (n = 4), (AII) vehicle (DMSO; n = 3), (AIII) LA (50µM; n = 3), (AIV) EPA (50µM; n = 3), (AV) LA

(50µM) in presence of SSO (200µM; n = 3), (AVI) EPA (50µM) in presence of SSO (200µM; n = 3), (AVII) LA (50µM) in presence of BAPTA-AM (10µM; n = 3), (AVIII) EPA (50µM) in presence of BAPTA-AM (10µM; n = 3), (AIX) LA (50µM), (AX) EPA (50µM) in presence of CD36 antibody (2µg/ml; n = 3), (AXI) LA (50µM), (AXII) EPA (50µM) in the presence of CD36 antibody (3µg/ml; n = 3). (B and C) Inhibition of PUFA-induced ROS generation by intracellular calcium chelation. (B) Representative images of the ROS indicator H_2DCF-DA, DCF fluorescence intensity was recorded by CLSM. Scale bars represent 200µm, (C) Bar charts show quantification of fluorescence intensity (%) of means ± SD of LA (n = 4) and EPA (n = 3) experiments. (D and E) Inhibition of PUFA-induced vasculogenesis by intracellular calcium chelation. EBs were treated from day 3 to 10 of differentiation with either EPA (50µM) or LA (50µM) either in absence of presence of BAPTA-AM (10µM). Vascular structures were visualized by PECAM-1 immunostaining. In (D) representative EBs labeled with an antibody against PECAM-1 are shown. The bar represents 200µm. The quantitative data on vascular branch formation (branching points (%)) (E) were assessed by computer-assisted image analysis of PECAM-1 positive vascular structures (n =3). *P ≤ .05, significantly different to the untreated control, #P ≤ .05, significantly different to the PUFA treated sample.

3.1.2.3 Activation of AMPK-α and PPAR-α upon PUFA treatment of ES cells

PUFAs regulate energy metabolism as ligands of PPARs. The transcription factor PPAR-α is essential for metabolic adaptation to starvation by inducing genes for β-oxidation and ketogenesis (Nakamura et al., 2014). In cooperation with AMPK, PPAR-α activates fatty acid oxidation in order to switch the cellular energy supply from glycolysis to fatty acid utilization (Grabacka et al., 2013). To investigate, whether LA and EPA activate PPAR-α and AMPK-α, phospho-specific antibodies were applied. Indeed, both LA (50µM) and EPA (50µM) increased phosphorylation of AMPK-α at residue Thr172, starting already 5 min after PUFA application (figures 3.5A, B), whereas total of protein expression remained unchanged (data not shown). Moreover, activation of PPAR-α at residue S12 was observed with comparable time kinetics (figure 3.5C, D). To identify the location of activated PPAR-α, cells enzymatically dissociated from 4-day-old EBs and plated on coverslips were incubated for 60 min with either EPA (50µM) or LA (50µM), and stained with a phospho-specific anti-PPAR-α antibody. The data clearly showed that phospho-PPAR-α exclusively localized to cell nuclei of all cells under inspection. This effect could be abolished upon pre-incubation (2h) with the PPAR-α inhibitor GW6471 (5µM), which drives the displacement of coactivators from PPAR-α and promotes the recruitment of co-repressor proteins like nuclear co-repressor (H Eric Xu et al., 2002) (figure 3.5E, F).

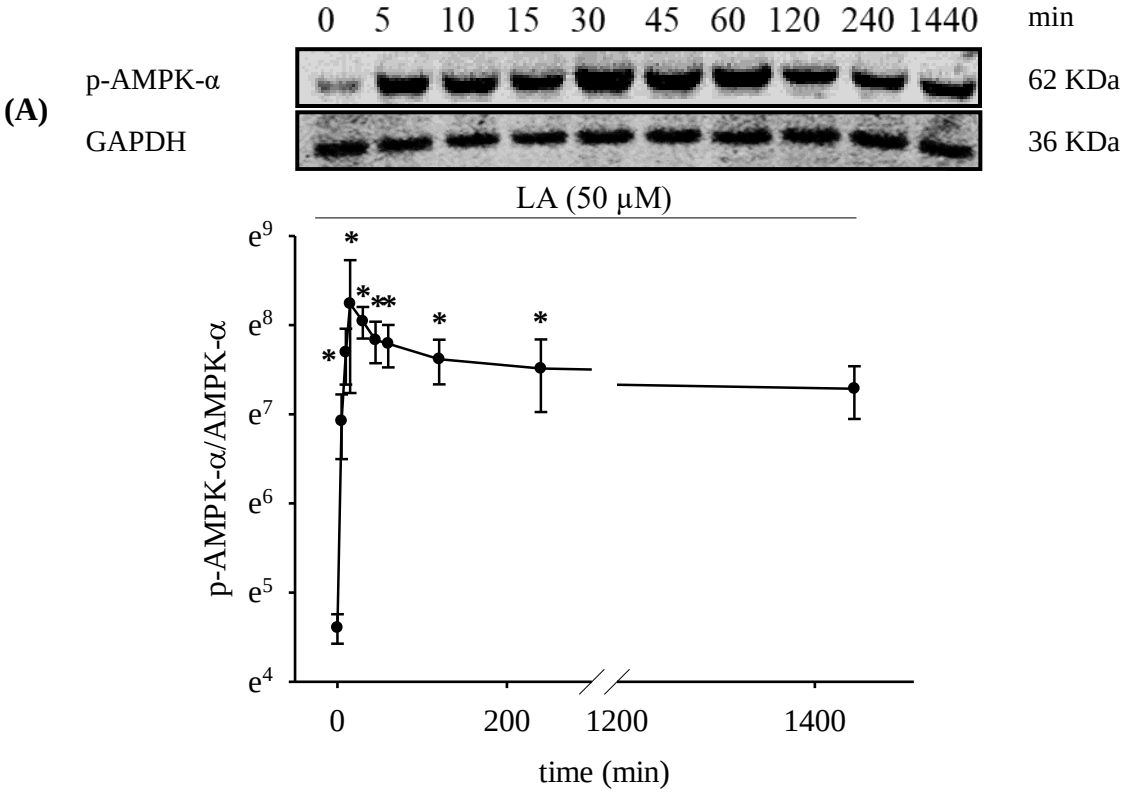
(A)
0 5 10 15 30 45 60 120 240 1440
min
p-AMPK-α
62 KDa
GAPDH
36 KDa
LA (50 μM)
p-AMPK-α/AMPK-α
e9
e8
e7
e6
e5
e4
0
200
1200
1400
time (min)

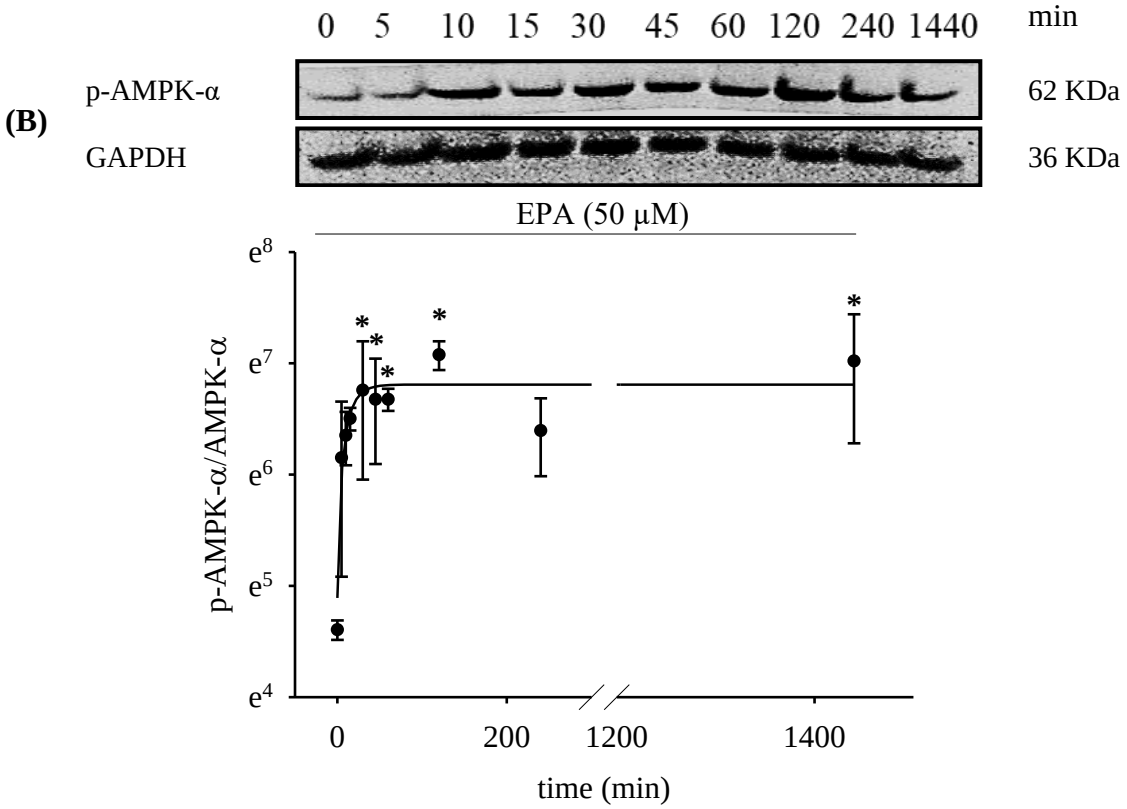
(B)
0 5 10 15 30 45 60 120 240 1440
min
p-AMPK-α
62 KDa
GAPDH
36 KDa
EPA (50 μM)
p-AMPK-α/AMPK-α
e8
e7
e6
e5
e4
0
200
1200
1400
time (min)

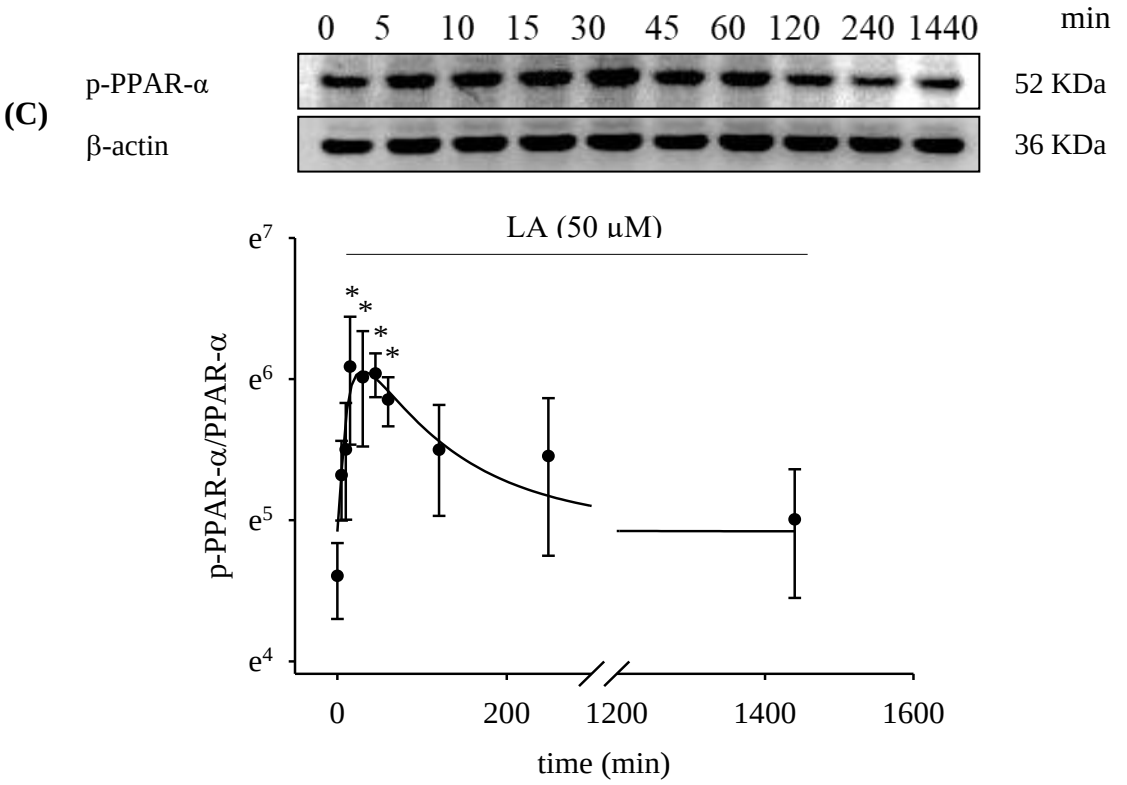
(C)
0 5 10 15 30 45 60 120 240 1440
min
p-PPAR-α
52 KDa
β-actin
36 KDa
LA (50 μM)
p-PPAR-α/PPAR-α
e7
e6
e5
e4
0 200 1200 1400 1600
time (min)

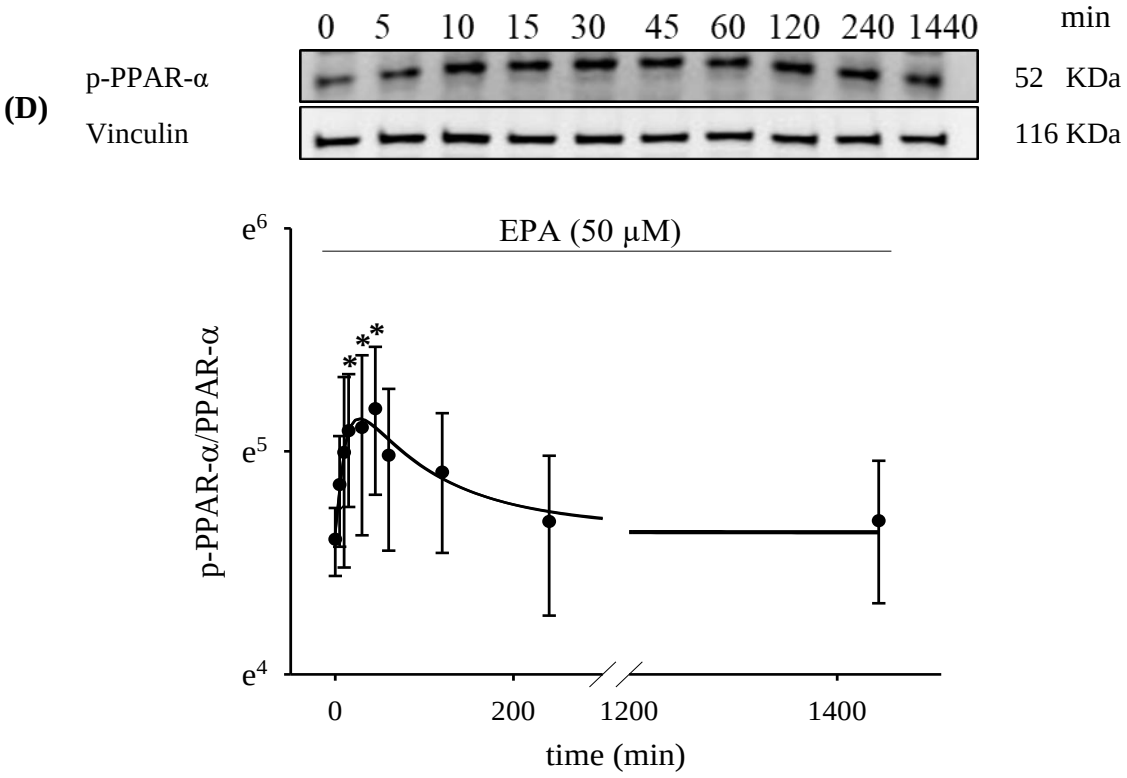
(D)
0 5 10 15 30 45 60 120 240 1440
min
p-PPAR-α
52 KDa
Vinculin
116 KDa
EPA (50 μM)
p-PPAR-α/PPAR-α
e6
e5
e4
0 200 1200 1400
time (min)

(E)

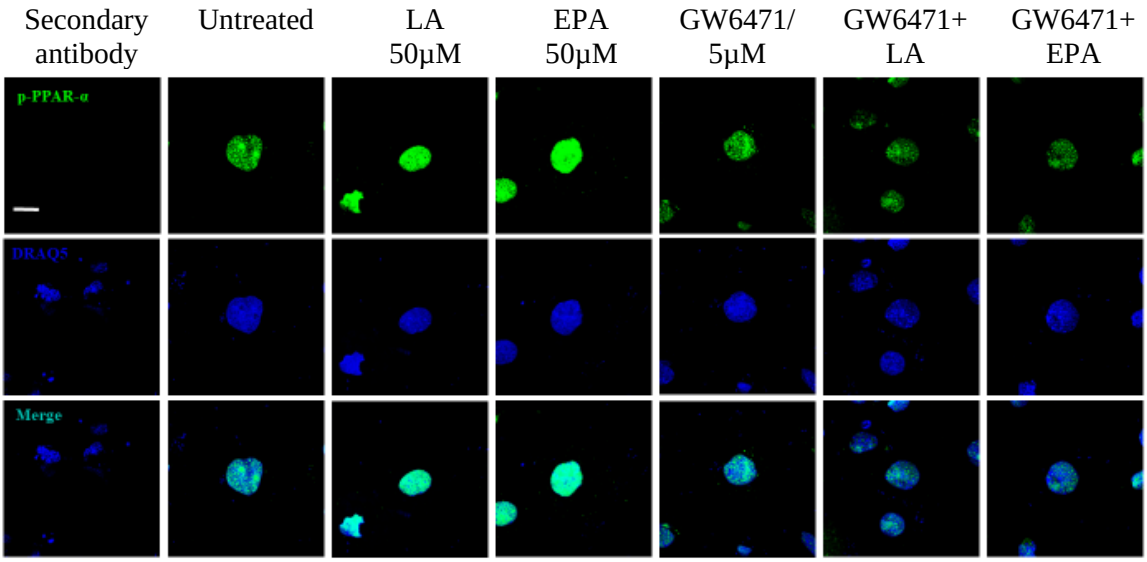
Secondary antibody
Untreated
LA 50µM
EPA 50µM
GW6471/ 5µM
GW6471+ LA
GW6471+ EPA
p-PPAR-α
DRAQ5
Merge

(F)

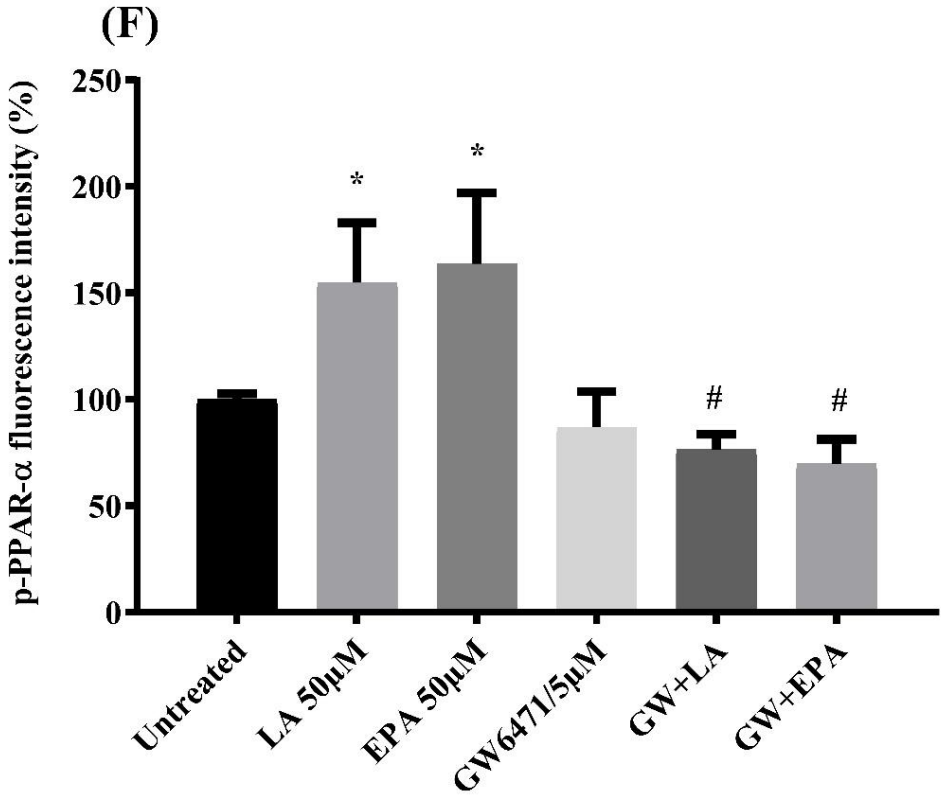
p-PPAR-α fluorescence intensity (%)
250
200
150
100
50
0
*
*
#
#
Untreated
LA 50µM
EPA 50µM
GW6471/5µM
GW+LA
GW+EPA

Figure 3.5: Time course of AMPK - α and PPAR - α activation upon treatment of differentiating ES cells with PUFAs. Five-day-old EBs were treated with 50µM of either LA or EPA, and protein was collected at different time points and subjected to western blot analysis. (A and B) AMPK-α phosphorylation following treatment with either (A) LA or (B) EPA. The upper panels show representative western blots stained with a phospho-specific antibody against AMPK-α. The lower panels show the means ± SD of (n = 4) experiments for LA and EPA, respectively, corrected for total AMPK-α protein expression (p-AMPK-α/AMPK-α). (C and D) PPAR-α phosphorylation following treatment with either LA (C) or EPA (D). The upper panels show representative western blots stained with a phospho-specific antibody against PPAR-α. The lower panels show the means ± SD of (n = 8) experiments for LA and (n = 10) for EPA, respectively, corrected for total PPAR-α protein expression (p-PPAR-α/PPAR-α). *P ≤ .05, significantly different to time 0 min. (E and F) Nuclear PPAR-α activation in single cells enzymatically dissociated from 3-day-old EBs upon treatment for 1h with either LA (50µM) or EPA (50µM) or pretreatment (2h) with GW6471 (5µM). (E) Representative cells which were labeled with a phospho-specific antibody against PPAR-α (upper row) or only secondary antibody, co-stained with the nuclear cell marker DRAQ5 (middle row) and merged (lower row). The bar represents 15µm. (F) Bar chart showing the means ± SD of nuclear p-PPAR-α expression upon PUFA treatment in absence and presence of GW6471 (5µM) (n =3) *P ≤ .05, significantly different to the untreated control and #P ≤ .05, significantly different to the PUFA treated sample.

3.1.2.4 Effect of calcium chelation as well as NADPH oxidase and eNOS inhibition on AMPK-α activation upon PUFA treatment of ES cells

The data of the present study demonstrate that treatment of differentiating ES cell with ω-3 and ω-6 PUFAs raised intracellular calcium, ROS and NO. To investigate whether the observed activation of AMPK-α is related to these intracellular messengers, experiments were carried out, where NADPH oxidase was inhibited with VAS2870 (50µM), intracellular calcium was chelated with BAPTA-AM (10µM), and eNOS was inhibited with L-NAME (100µM). The data demonstrate that inhibition of NADPH oxidase by VAS2870 totally abolished AMPK-α activation by LA (50µM) (figure 3.6A). Moreover, AMPK-α activation by LA (50µM) and EPA (50µM) was inhibited upon pre-incubation with L-NAME (figures 3.6D, E) as well as with BAPTA (figures 3.6B, C).

3.1.2.5 Abrogation of PUFA-mediated vasculogenesis upon inhibition of PPAR-α

If PUFAs are stimulating vasculogenesis of ES cells via AMPK-α and downstream of PPAR-α, inhibition of the latter should abolish this effect. To validate our assumption we performed experiments, where differentiating ES cells were co-incubated with the PPAR-α inhibitor GW6471. Our data demonstrate that upon co-incubation of EPA (50µM) and LA (50µM) with GW6471 (5µM) the stimulation of vasculogenesis, as evaluated by assessment of vascular branching points, was completely abolished (figure 3.6F, G). This finding clearly underscores the impact of PPAR-α for PUFA-induced vasculogenesis of ES cells (see figure 4.1).

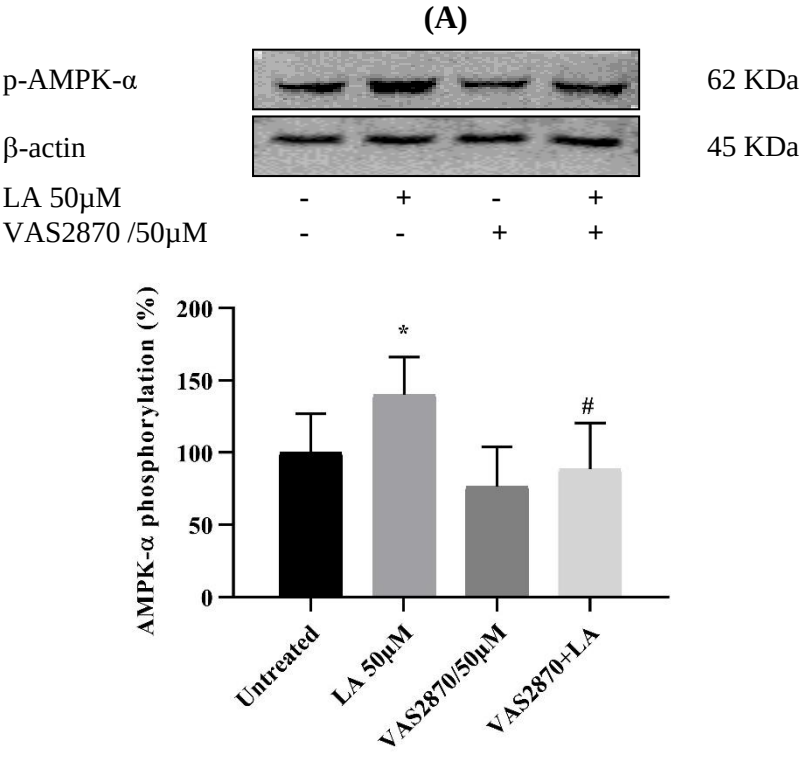

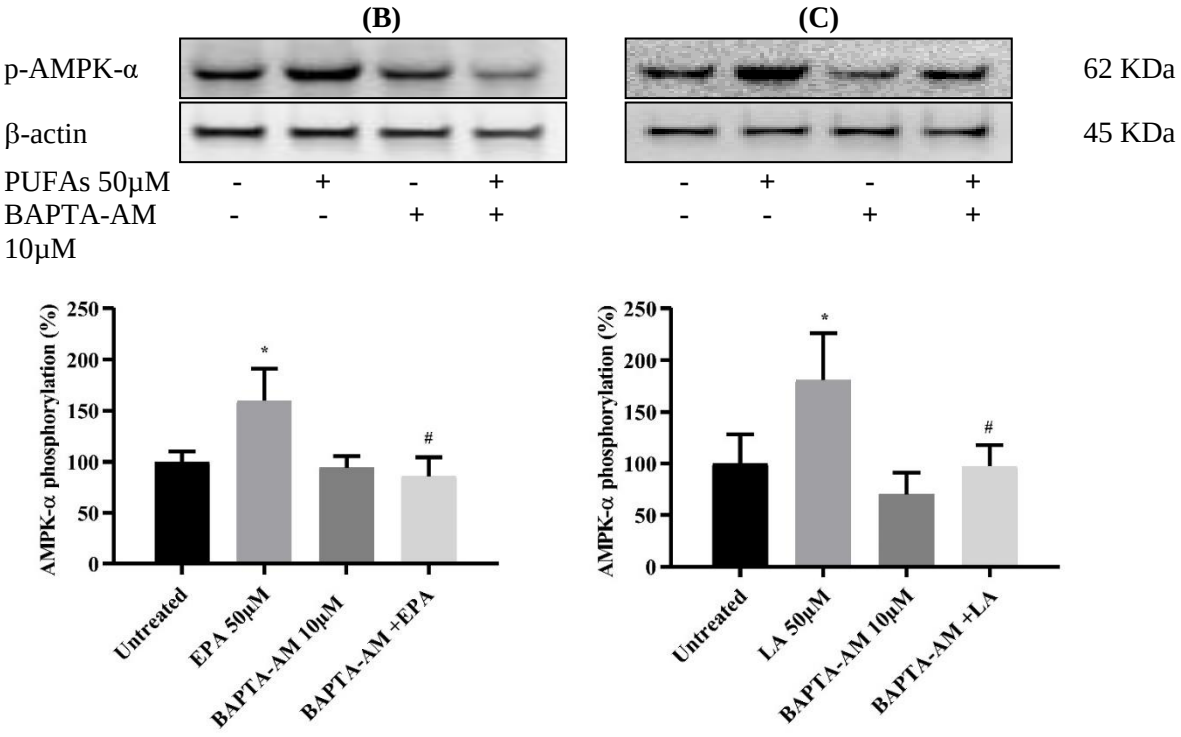
(B)
(C)
p-AMPK-α
β-actin
62 KDa
45 KDa
PUFAs 50μM - + - + - + - +
BAPTA-AM 10μM - - + + - - + +
AMPK-α phosphorylation (%)
250
200
150
100
50
0
*
#
Untreated
EPA 50μM
BAPTA-AM 10μM
BAPTA-AM+EPA
LA 50μM
BAPTA-AM+LA

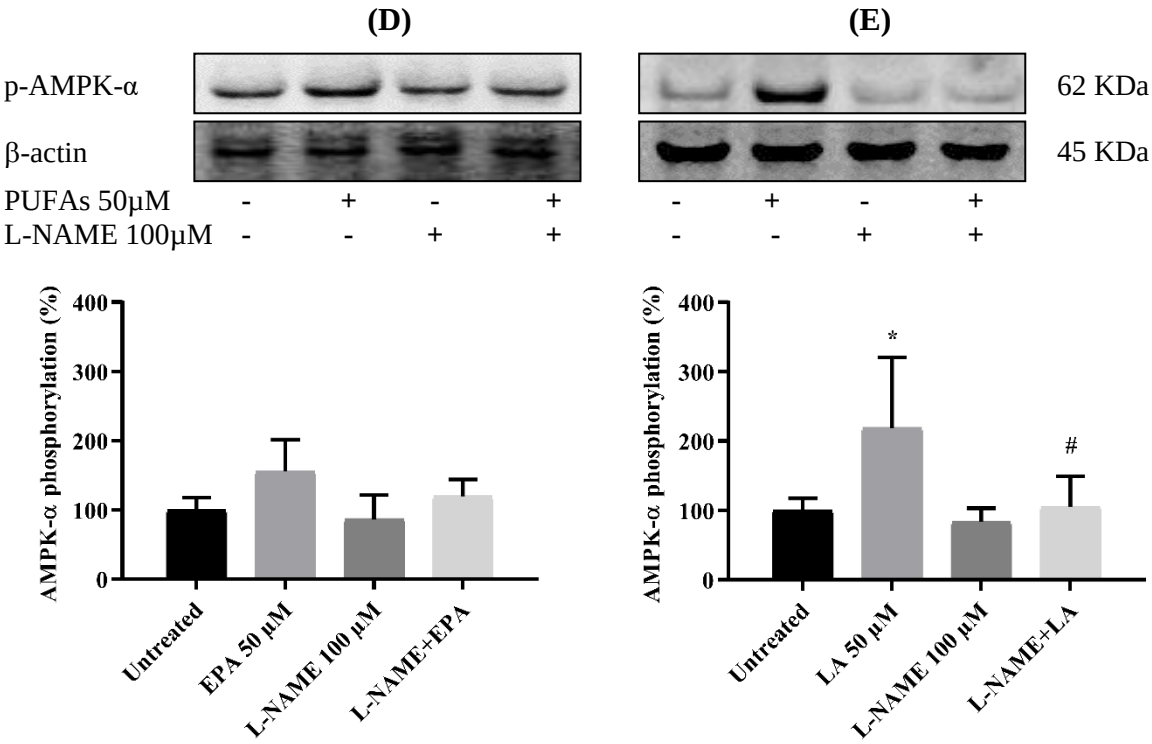
(D)
(E)
p-AMPK-α
β-actin
62 KDa
45 KDa
PUFAs 50μM - + - + - + - +
L-NAME 100μM - - + + - - + +
AMPK-α phosphorylation (%)
400
300
200
100
0
*
#
Untreated
EPA 50 μM
L-NAME 100 μM
L-NAME+EPA
LA 50 μM
L-NAME+LA

(F)

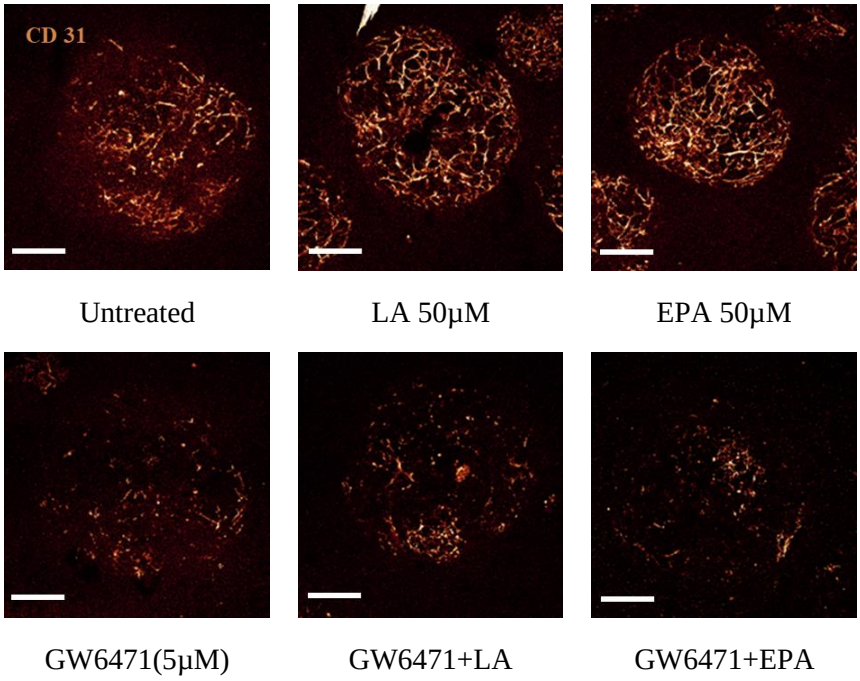
CD 31
Untreated
LA 50µM
EPA 50µM
GW6471(5µM)
GW6471+LA
GW6471+EPA

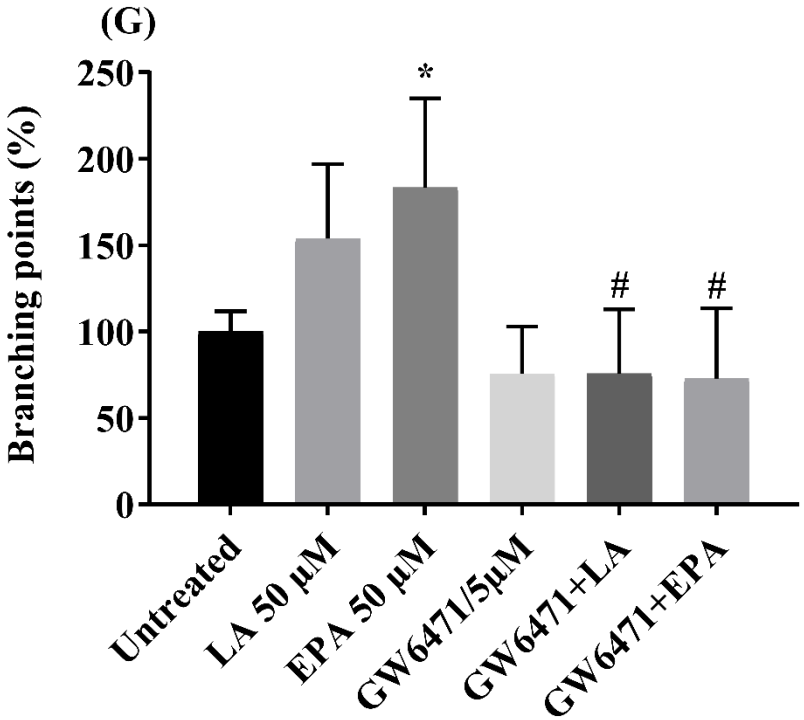
(G)
Branching points (%)
250
200
150
100
50
0
*
#
#
Untreated
LA 50 µM
EPA 50 µM
GW6471/5µM
GW6471+LA
GW6471+EPA

Figure 3.6: Inhibition of PUFA-induced AMPK-α activation by interference with calcium, ROS and NO signaling. Five-day-old EBs were treated with 50µM of either EPA or LA and protein was collected 30 min thereafter and subjected to western blot analysis. Pretreatment with VAS2870 (50µM), BAPTA-AM (10µM), L-NAME (100µM), and GW6471 (5µM) was done 2 h before addition of PUFAs. (A) LA-induced AMPK-α activation was abolished by the NADPH oxidase inhibitor VAS2870 (n = 7). (B and D) EPA, and (C and E) LA-induced AMPK-α activation was abolished by the NOS inhibitor L-NAME (n = 3 for EPA and n = 5 for LA), and the calcium chelator BAPTA-AM (n = 4 for EPA and LA, respectively). Shown are representative western blots as well as bar charts showing the means ± SD of the indicated number of experiments. (F and G) Inhibition of PUFA-induced vasculogenesis by the PPAR-α inhibitor GW6471. The images in (F) show representative EBs treated from day 3 to 10 of differentiation with PUFAs, either in absence or presence of GW6471 (the bar represents 200µm). The bar chart in (G) shows the means ± SD of n = 6 experiments. *$P \leq .05$, significantly different to the untreated control, #$P \leq .05$, significantly different to the PUFA treated sample.

3.2 Effect of PUFAs on cardiomyogenesis and cardiac cell function of ES cell-derived EBs

Under normal physiological states, fatty acid oxidation is fundamental for adult cardiomyocytes and prevails over the oxidation of other nutrients (Gaspar et al., 2014). Comparably to adult cardiac cells, cardiomyocytes derived from mESCs display a gene expression signature, which correlates with fatty acid metabolism and glycolysis (Sander et al., 2013). To investigate optimal concentrations of PUFAs to induce cardiomyogenesis in ES cells, 3-day-old EBs either outgrown on coverslips or in suspension culture were treated with different concentrations of LA and EPA versus untreated and vehicle groups (DMSO).

3.2.1 Effect of PUFAs on the beating function of cardiac cells

Spontaneous contractions are one of the fundamental functions of cardiomyocytes. To investigate, whether PUFAs accelerated the beating frequency of cardiomyocytes derived from ES cells or increase the number of contracting EBs, they were incubated with different concentrations of PUFAs (1, 5, 10, 50, and 100µM) from day 3 till day 10. In absence of PUFAs, spontaneous beating of cardiac cells clusters started on day 6 or 7. Therefore, beating frequency was evaluated by visual inspection on day 7 for each PUFA concentration in comparison with untreated and vehicle groups until day 10 of cell culture. The results showed that LA and EPA accelerated the beating frequency per min for cardiac contracting areas (foci), which was, however, non-significant in time and dose-dependent manner (figures 3.7A, B). In further experiments the number of contracting EBs was counted by microscopic inspection on day 10 of differentiation time upon PUFA treatment versus the control and vehicle group. The results showed that LA and EPA significantly increased the number of contracting EBs in dose-dependent manner (figures 3.8A, B), indicating stimulation of cardiomyogenesis upon PUFA treatment.

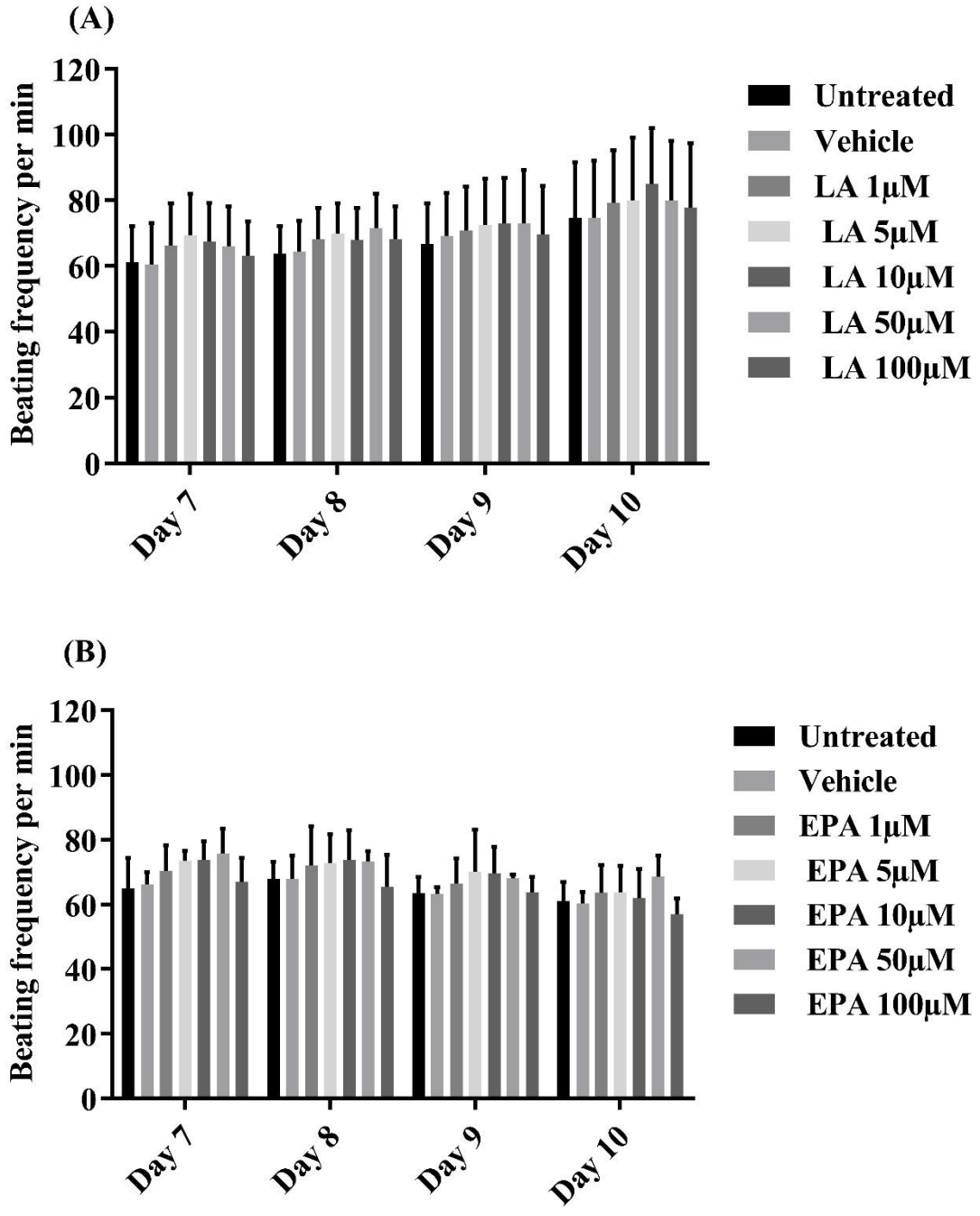

Figure 3.7: Effect of PUFAs on beating frequency of EBs differentiated from mES cells. (A, B) Beating frequency of cardiac cells clusters; 3-days-old EBs were incubated for 7 days with either LA (A) (n = 6) or EPA (B) (n = 3), and beating frequency per min was counted from day 7 to day 10 of cell culture. Shown are the means ± SD.

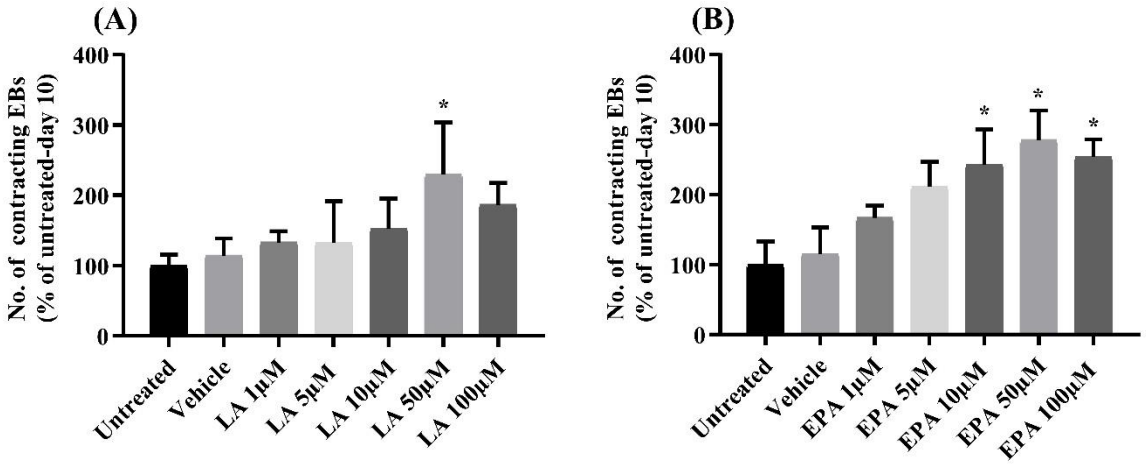

Figure 3.8: Effect of different concentrations of PUFAs on the number of spontaneously contracting EBs. (A, B) Bar charts show numbers (%) of spontaneously beating EBs (10-day-old) derived from ES cells. EBs were grown in presence of a series of concentrations of either LA (A) or EPA (B). Shown are the means ± SD of (A) (n = 3; LA) and (B) (n = 3; EPA). *P ≤ 0.05, statistically significant as compared with the untreated group.

3.2.2 Effect of PUFAs on the size of spontaneously contracting cardiac areas

To further investigate stimulation of cardiomyogenesis by PUFAs, the size of beating cardiac clusters following PUFA exposure was assessed. To achieve this aim EBs were labeled with a monoclonal mouse anti-sarcomeric α-actinin antibody. The α-actinin (actin-binding protein) is associated with the Z-lines in cardiomyocytes (Djinovic-Carugo et al., 1999) (figure 3.9A). Our data demonstrated that PUFAs significantly increased the size of α-actinin-positive cardiac cell clusters in a dose-dependent manner, suggesting that PUFAs increased the number of cardiomyocytes differentiated from ES cells (figures 3.9B, C).

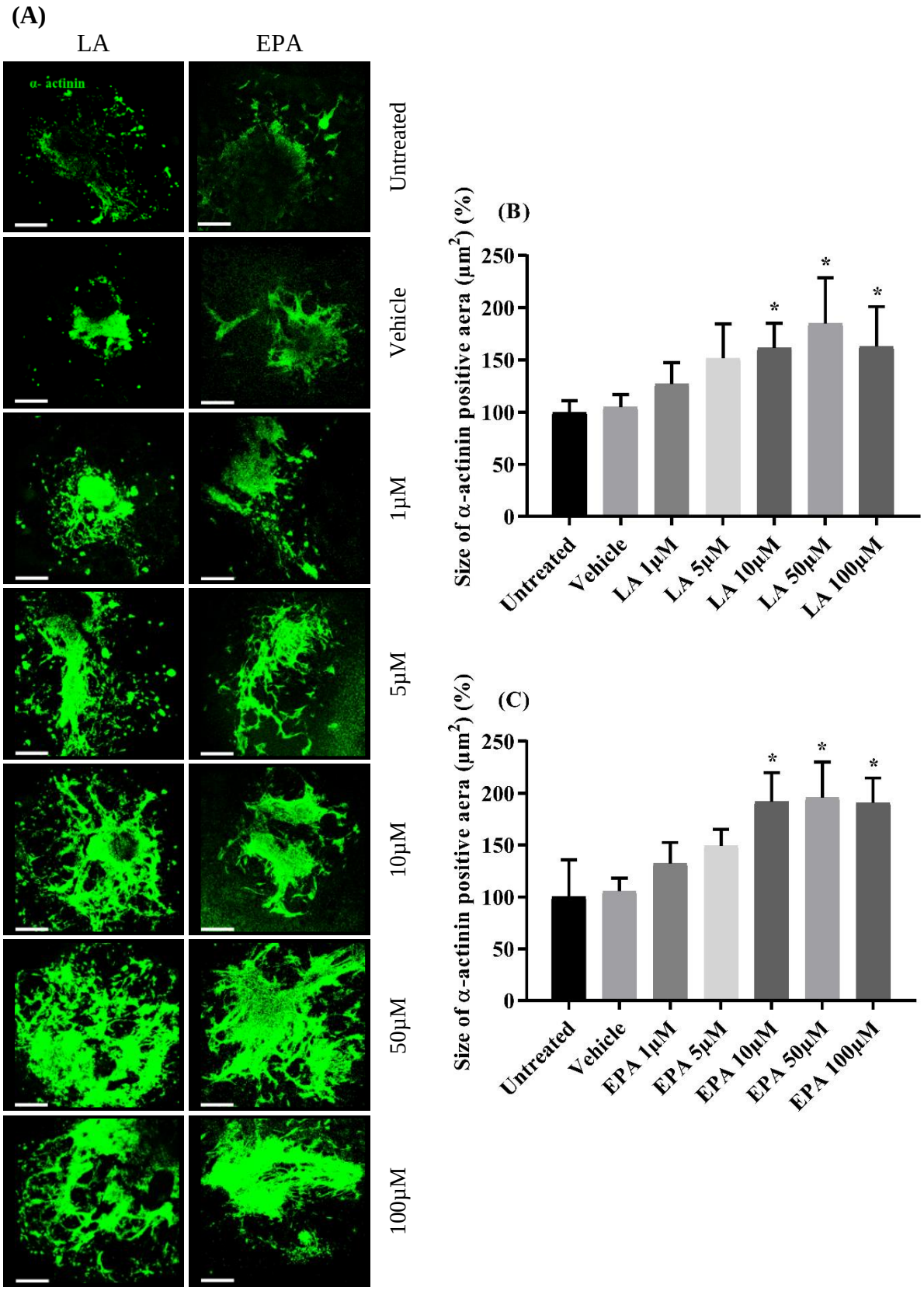
(A)
LA
EPA
α- actinin
Untreated
Vehicle
1μM
5μM
10μM
50μM
100μM
(B)
Size of α-actinin positive aera (μm²) (%)
250
200
150
100
50
0
Untreated
Vehicle
LA 1μM
LA 5μM
LA 10μM
LA 50μM
LA 100μM
(C)
Size of α-actinin positive aera (μm²) (%)
250
200
150
100
50
0
Untreated
Vehicle
EPA 1μM
EPA 5μM
EPA 10μM
EPA 50μM
EPA 100μM

Figure 3.9: Effect of PUFAs on the size of α-actinin-positive cardiac cells clusters differentiated from ES cells. (A, B) LA, (A, C) EPA. Shown are representative images of cardiac areas, which were stained with an antibody against α-actinin (green) after 10 days of cell culture. The scale bars represent 200µm. (B, C) Bar charts show quantification of the size of α-actinin-positive cardiac cell areas (μm^2). Shown are the means ± SD for LA (n = 4) and EPA (n = 3). *P ≤ 0.05, statistically significant as compared with the untreated group.

3.2.3 Cardiac structural protein expression upon PUFA treatment

To analyse the effects of PUFAs on cardiomyogenesis in more details, Western blot analysis was performed to investigate cardiac-structural protein expression under PUFA treatment conditions, i.e., α-actinin (figure 3.10A) and MLC2a (figure 3.10B). As shown in figure 3.10, PUFAs upregulated α-actinin (A) and MLC2a (B) protein expression in a dose-dependent manner. The optimal PUFA concentration was 50µM versus the untreated and vehicle (DMSO) group, while 100µM exerted slightly adverse effects.

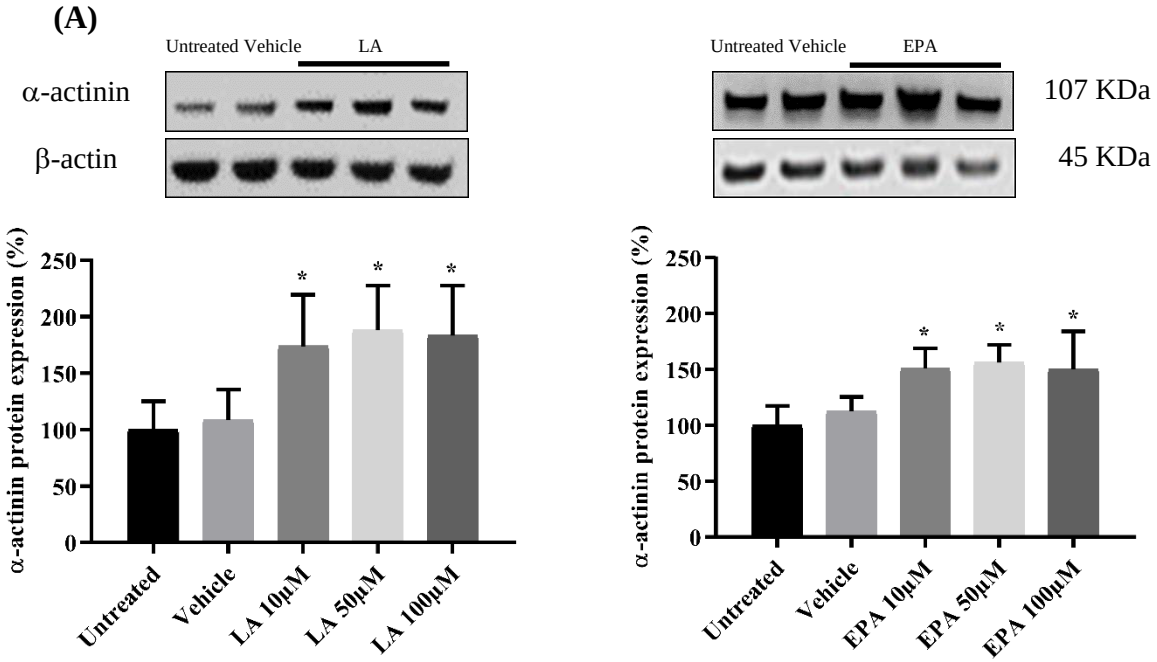

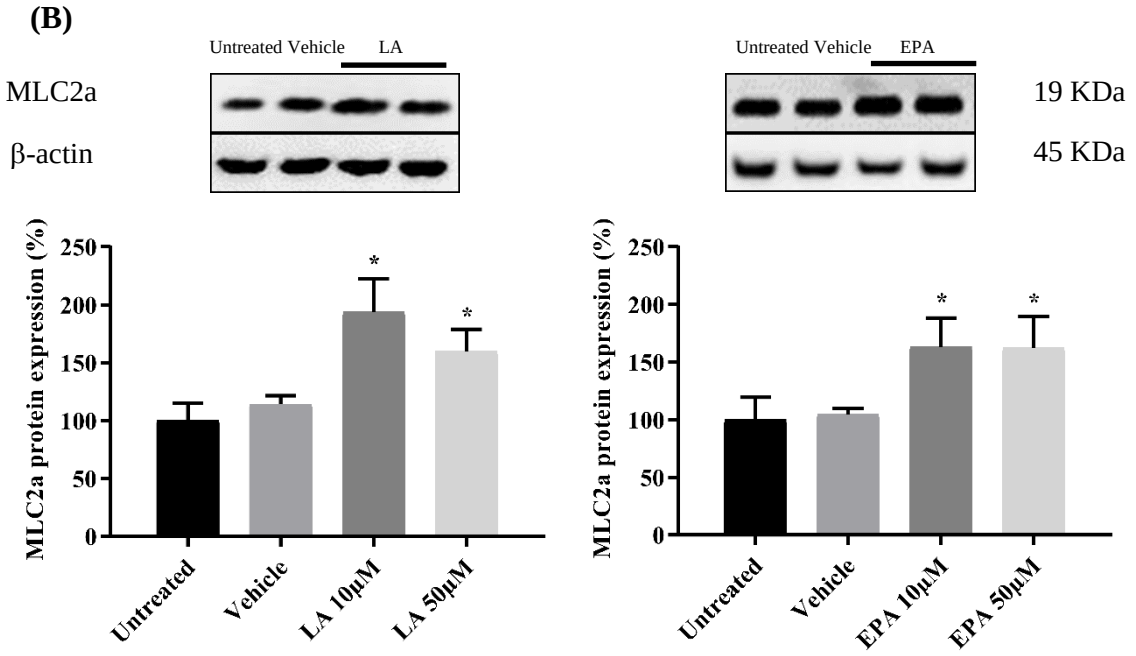

Figure 3.10: Effect of PUFAs on cardiac structural protein expression. (A, B) Upper panels, western blot analysis of α-actinin (A) and MLC2a (B) protein expression upon PUFA treatment. β-actin was used as internal loading control. (A, B) The bar charts show quantitative data of cardiac protein expression upon PUFA treatment in different concentrations conditions. Shown are the means ± SD of 4-independent experiments for (A) (LA) and (EPA) as well as (B) (LA) and (EPA). *P ≤ 0.05, statistically significant as compared with the untreated group.

3.2.4 Involvement of NADPH oxidase and PPAR-α in PUFA-induced cardiomyogenesis of ES cells

To investigate the hypothesis that PUFAs stimulate cardiomyogenesis from ES cells via NADPH oxidase and PPAR-α, EBs were pre-incubated from day 3 to 10 of cell culture either with the NADPH oxidase inhibitor VAS2870 (50µM) or with the PPAR-α antagonist GW6471 (5µM) in presence or absence of either LA (50µM) or EPA (50µM). Then, the size of cardiac areas (α-actinin-positive area) and beating frequency were evaluated. The results show that the NADPH oxidase inhibitor VAS2870 or PPAR-α antagonist GW6471 significantly reduced the PUFAs-induced differentiation of cardiac cells from ES cells as well as the increase in beating frequency observed upon PUFA treatment (figure 3.11A-E).

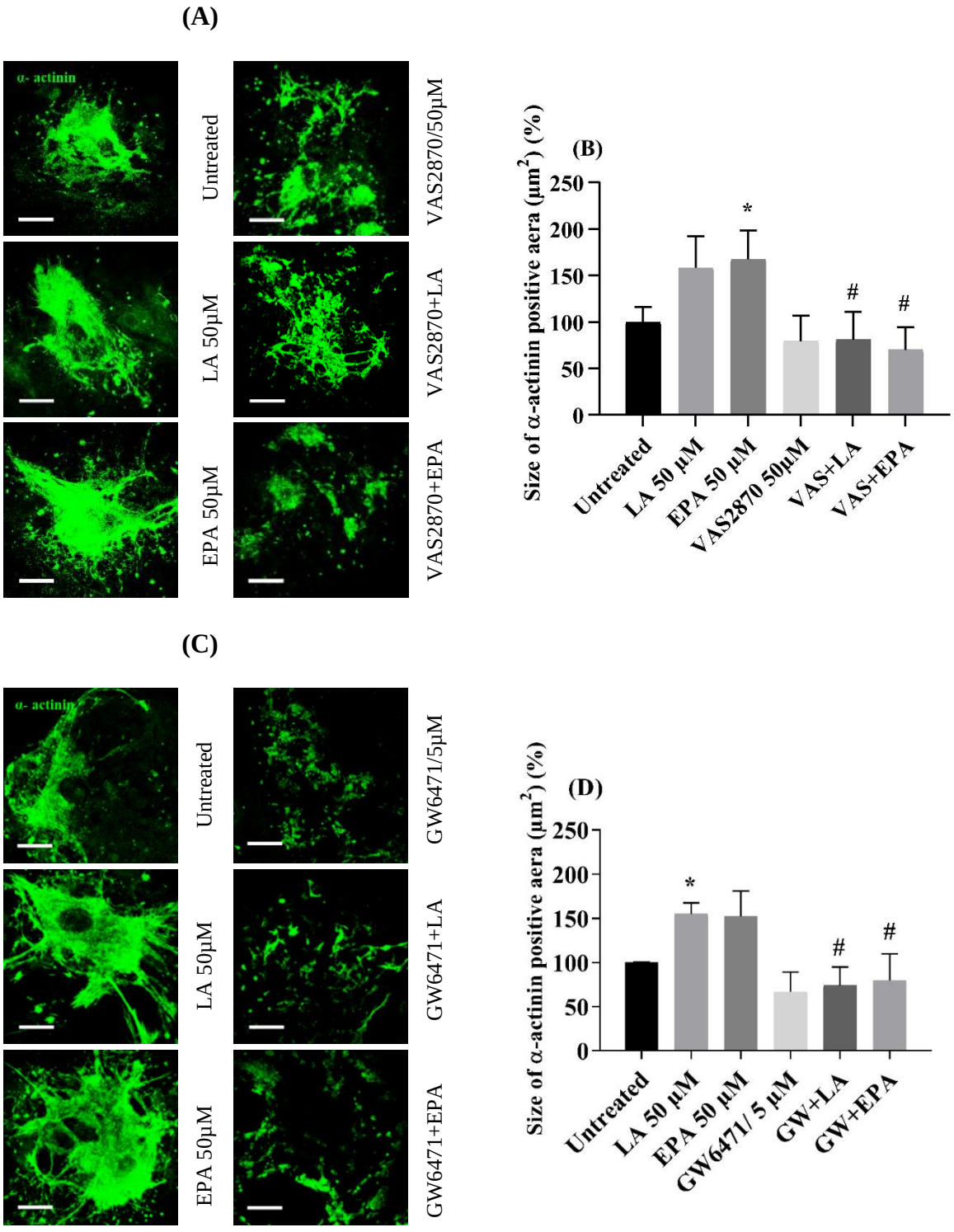
(A)
α- actinin
Untreated
LA 50µM
EPA 50µM
VAS2870/50µM
VAS2870+LA
VAS2870+EPA
(B)
Size of α-actinin positive aera (µm²) (%)
250
200
150
100
50
0
*
#
#
Untreated
LA 50 µM
EPA 50 µM
VAS2870 50µM
VAS+LA
VAS+EPA
(C)
α- actinin
Untreated
LA 50µM
EPA 50µM
GW6471/5µM
GW6471+LA
GW6471+EPA
(D)
Size of α-actinin positive aera (µm²) (%)
250
200
150
100
50
0
*
#
#
Untreated
LA 50 µM
EPA 50 µM
GW6471/ 5 µM
GW+LA
GW+EPA

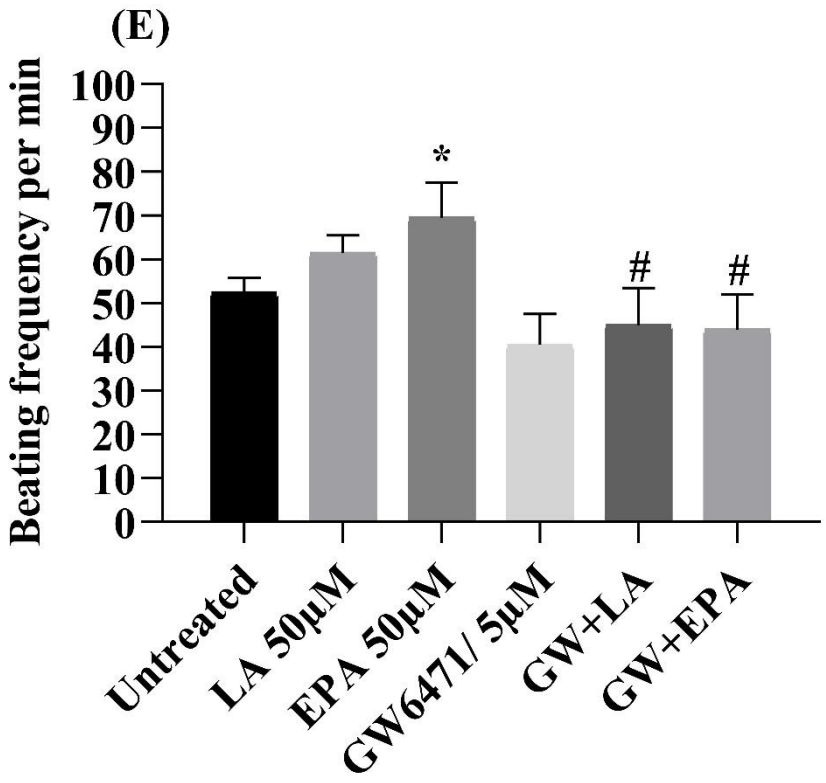

Figure 3.11: Effect of NADPH oxidase inhibition by VAS2870 and PPAR-α inhibition by GW6471 on PUFA-induced cardiomyogenesis. EBs were incubated from day 3 to 10 of differentiation with PUFAs, either in absence or presence of VAS2870 (50µM) or GW6471 (5µM). (A and C) Representative images of EBs cultivated on coverslips and labeled with an antibody against α-actinin (green) after 10 days of cell culture. The scale bars represent 200µm. (B and D) show bar charts representing the means ± SD of independent experiments for VAS2870 (50µM; n=3) and GW6471 (5µM; n=3). (E) The beating frequency per min was counted on day 10 of cell culture in absence or presence of GW6471 (5µM) condition (n=6). *P ≤ 0.05, statistically significant as compared with the untreated group. #P ≤ .05, significantly different to the PUFA treated sample.

4. Discussion

Objective of the present study was to investigate vasculogenesis and cardiomyogenesis of mES cells exposed to either EPA as ω-3 PUFA, LA as ω-6 PUFA or PA as a saturated fatty acid. Most previous studies have focused on small chemical molecules to stimulate stem cell differentiation. Only a few studies have examined the impact of the endogenous metabolism on cardiovascular differentiation (Yanes et al., 2010), although a number of studies have demonstrated that PUFAs exert distinct effects on the proliferation and differentiation of stem cells originating from different sources (see table 12).

Recently an *American Heart Association* presidential advisory on dietary fats and cardiovascular disease (CVD) discussed and suggested that lower intake of saturated fat and higher intake of polyunsaturated and monounsaturated fat is associated with lower rates of CVD and cardiovascular mortality (Rimm et al., 2018). In contrast, a recent analysis of published clinical trials suggested that increasing EPA and DHA has little or no effect on mortality or cardiovascular health (Abdelhamid et al., 2018). The main beneficial health effects have been mainly attributed to PUFAs. ALA is found in plant oils, EPA, and DHA are originating in marine algae and phytoplankton as well as in the ascending food chain in marine crustaceans and marine fish. The lead substance for ω-6 PUFAs is LA, which is produced in many nuts and seeds and is a precursor of AA (Sokoła-Wysoczańska et al., 2018). Mammals are unable to produce ω-3 fatty acids, but can ingest the shorter-chain ω-3 fatty acid ALA through diet and use it to synthetize the essential ω-3 PUFAs EPA and DHA. After uptake into cells, PUFAs are metabolized by COXs, LOXs, and CYP to generate bioactive eicosanoids, including prostanoids, LTs, HETEs, and EETs (Hu et al., 2018). CYP enzymes are membrane-bound, heme-containing terminal oxidases that are part of a multi-enzyme complex, which also includes a FAD/FMN-containing NADPH CYP reductase and cytochrome b5 (Hu et al., 2018).

4.1 Stimulation of vasculogenesis by PUFAs treatment

In the present study, the effects of EPA as a lead substance for ω-3 and LA for ω-6 PUFAs were investigated. It was demonstrated that EPA as well as LA stimulated vasculogenesis

in a comparable concentration range, that is, between 1 and 100μM and maximum effects at 10 and 50μM. Previously reported range of physiological concentrations of EPA and LA in human serum amount to 14–100μM and 2,270–3,850μM, respectively (Dumancas et al., 2010). Interestingly the saturated fatty acid PA did not show any effect on vasculogenesis of ES cells, suggesting that the unsaturated double bond chemical structure of fatty acids may be a decisive determinant for their biological function. Moreover, this finding supports the notion, that dietary intake of PUFAs may support vasculogenesis and vascular health in comparison to saturated fatty acids like PA.

EPA and LA treatment increased ROS as well as NO generation (see figure 4.1), which was abolished in presence of the NADPH oxidase inhibitor VAS2870 and the NOS inhibitor L-NAME. Moreover, PUFA-stimulated vasculogenesis was blunted upon inhibition of ROS and NO generation by using pharmacologic NADPH oxidase and eNOS inhibitors. These data corroborate previous studies of us showing that the stimulation of vasculogenesis in ES cells by AA was dependent on ROS generation (Huang et al., 2016). It is well reported that upon chemical reaction of ROS with NO, peroxynitrite is formed which-in high concentrations is generally regarded as very reactive and toxic substance and causes endothelial dysfunction (Kanaan & Harper, 2017). In low, physiologic concentrations, ROS/reactive nitrogen species (ROS/RNS) species including hydrogen peroxide, superoxide, and peroxynitrite are second messenger molecules, which involve in functional oxidative and nitrosative modification of proteins (Hansen et al., 2016; Sauer et al., 2001). In this respect, previous studies have demonstrated that ROS and NO are critical determinants in cardiovascular differentiation of stem cells (Bekhite et al., 2016; Gentile et al., 2013; Huang et al., 2010; Mazrouei et al., 2015; Sharifpanah et al., 2016).

Notably, peroxynitrite in low physiologic concentrations may be proangiogenic and act as intracellular messenger. This has been evidenced in studies, where peroxynitrite increased vascular endothelial growth factor (VEGF) expression in vascular endothelial cells (Platt et al., 2005), mediated VEGF-dependent angiogenic function in brain microvascular endothelial cells by c-src and MT1-matrix metalloproteinase activation (Prakash et al., 2012), and stimulated cell endothelial cell migration by focal adhesion kinase activation as well as low molecular weight protein tyrosine phosphatase S-glutathionylation (Abdelsaid

& El-Remessy, 2012). It is well known that ω-3 and ω-6 PUFAs are metabolized in distinct intracellular pathways. AA is the substrate for the series 2 PGs, prostacyclins, TXs, and LTs (LTB4, series B4 LT); EPA is the substrate for the series 3 prostanoids and LTB5 (series B5 LT) (Benatti et al., 2004). The redox biology of PUFAs is complex and not sufficiently investigated. Generally, it is assumed that ω-3 PUFAs are anti-oxidative and anti-inflammatory, whereas ω-6 PUFAs exert pro-oxidative and pro-inflammatory effects (Sokoła-Wysoczańska et al., 2018). However, this notion was recently challenged since a number of studies reported that also ω-3 PUFAs moderately raise ROS in several cell types like endothelial cells (Okada et al., 2017), vascular smooth muscle (Crnkovic et al., 2012) and skeletal muscle cells (da Silva et al., 2016). Interestingly, ROS arising from PUFAs have been frequently noticed in tumour cells, for example, colon cancer cells (Pettersen et al., 2016) as well as lung and melanoma cancer cells (Zajdel et al., 2013; Zajdel et al., 2015). This is of importance since aggressive cancer cells mimic early-development stem cells, and properties of ES cells are retained in cancer cells (Ratajczak et al., 2018).

The intracellular signaling cascade resulting in ROS/RNS generation is not sufficiently investigated. The initial step should be the uptake of PUFAs into the cell. The cellular import of PUFAs is accomplished by CD36, which is a member of the class B scavenger receptor family of cell surface proteins. Inside the cell, PUFAs may elicit intracellular calcium responses. This has been shown for LA in pancreatic β cells (Zhao et al., 2013), bovine neutrophils (Mena et al., 2013), HeLa cells (Figueroa et al., 2013) and mES cells (Min Hee Kim et al., 2009). EPA raised intracellular calcium in several cell types including endothelial cells (Kim et al., 2015; Okuda et al., 1994; Omura et al., 2001; Wu et al., 2018), human colon epithelial cells (Kim et al., 2015) and vascular smooth muscle cells (Engler et al., 1999). Intracellular calcium responses elicited by EPA in endothelial cells and SMCs were independent of NO generation (Okuda et al., 1997), which may indicate that the calcium response is upstream of NO generation. Calcium dependence of eNOS is well documented in the scientific literature (Vanhoutte et al., 2016). In the present study EPA as well as LA transiently raised intracellular calcium (see figure 4.1) which was totally inhibited upon pre-incubation with the calcium chelator BAPTA-AM and significantly reduced by the CD36 inhibitor SSO as well as by a blocking antibody against

CD36, suggesting that PUFAs enter cells via CD36 and release calcium from intracellular stores. The intracellular calcium response is apparently a prerequisite for ROS generation since BAPTA-AM abolished the effect. Moreover, ROS/NO are necessary for the vasculogenic effects of PUFAs since the NADPH oxidase inhibitor VAS2870 as well as the NOS inhibitor L-NAME abolished the differentiation of blood vessel-like structures upon PUFA treatment.

PUFAs have been previously shown to activate the metabolic sensor AMPK, which senses ATP deficiency and blocks anabolic processes (Shackelford & Shaw, 2009). Upon activation, AMPK inhibits glycolysis by phosphorylation of multiple forms of phosphofructo-2-kinase and by mammalian target of rapamycin inhibition, and in parallel initiates energy supply in form of fatty acid oxidation (Grabacka et al., 2013). The activity of AMPK is upstream of PPAR-α which is responsible for fat mobilization during fasting and activates mitochondrial and peroxisomal fatty acid β- and ω-oxidation and ketogenesis, simultaneously inhibiting glycolysis and fatty acid synthesis (Grabacka et al., 2013). The data of the present study show that EPA as well as LA activated AMPK-α and PPAR-α. Previous studies have evidenced that ω-3 PUFAs increased fatty acid oxidation in AMPK-dependent manner to generate ATP, thereby inhibiting unnecessary pathways, such as fatty acid synthesis (Lyons & Roche, 2018). Our data show that AMPK-α activation was dependent on PUFA-induced intracellular calcium, ROS and NO changes, since activation was abolished upon calcium chelation as well as inhibition of NADPH oxidase and NOS. This is in line with previous studies of us, demonstrating that PPAR-α agonists, such as WY14643, GW7647, and ciprofibrate stimulated cardiomyogenesis of ES cells by a mechanism involving ROS generation (Sharifpanah et al., 2008). Consequently, the PPAR-α inhibitor GW6471 inhibited vasculogenesis elicited by EPA and LA in the present study.

4.2 Effect of LA and EPA on cardiomyogenesis of ES cells and cardiac cell function

Several reports have shown that one of the significant causes of morbidity and mortality worldwide is CVD. It is responsible for 17 million cases of deaths every year that represent about 31% of all global deaths such as ischemic heart disease (IHD), heart failure (HF) and

myocardial infarction (MI). It is well known that the regenerative capacity of the heart is limited, which necessitates to differentiate and cultivate cardiac cells under cell culture conditions for cell therapy approaches of diseased hearts. The most promising source of cells for cardiomyoplasty are ES cells. Cardiomyocytes differentiated from pluripotent ES cells are currently used in the development of tools for in vitro generation of cardiac tissues for disease modelling, drug testing, and illustrating developmental processes (du Pré et al., 2013; Madonna et al., 2019; Park & Yoon, 2018; Shen et al., 2017; World Health Organization, 2014). Moreover, cardiac cell therapy holds the potential to enhance healing of ischemic heart, repopulate injured myocardium and recover cardiac function (Der Sarkissian et al., 2017). Reaching these aims requires the improvement of efficient protocols, which induce and direct cardiomyocyte differentiation from ES cells to achieve sufficient cardiac cell numbers for cell therapy. It is therefore necessary to perform studies, which focus on exogenous and endogenous signaling pathways to differentiate ES cells towards cardiovascular lineages. Previous studies have outlined the importance of PUFAs such as LA and EPA to improve coronary heart disease (CHD) as well as CVD. Farvid and his colleagues have demonstrated that higher dietary consumption of LA is correlated with a lower risk of (CHD). They therefore recommended to replace the use of saturated fatty acid by PUFAs in the diet (Farvid et al., 2014). Moreover, ω-3 and ω-6 PUFAs, and their metabolites are crucial elements of cell structure and function that could affect stem cell fate. The available evidence demonstrates that ω-6 and ω-3 PUFAs and their metabolites can perform through multiple mechanisms to contribute to the proliferation and differentiation of several stem cell types (Table. 12) (Kang et al., 2014). These and our own observations suggest that PUFAs could activate distinct signaling networks to advance the cardiomyocyte differentiation of ES cells.

Fatty acids include the major metabolites for energy supply in cardiomyocytes (Lopaschuk et al., 2010). They also contribute to the regulation of cardiac-specific gene expression as well as activity of ion channels that are taking charge of heart beating (S. S. Chan et al., 2009; Leifert et al., 1999; Xiao et al., 2001). Energy metabolism is a fundamental aspect of cardiomyocyte biology. The heart is a metabolic omnivore, and the adult heart picks the substrate best suited for each condition. Fatty acid oxidation is considered the most

important source of ATP production, and is preferred in order to achieve the high energy requirement of the contracting myocardium (Malandraki-Miller et al., 2018; Ulmer et al., 2018).

The data of the present study demonstrated that LA and EPA stimulated cardiomyocyte differentiation from ES cells. The beating frequency of cardiomyocytes-derived from ES cells under LA and EPA conditions was accelerated, indicating improvement of cardiac cell function. Recently it has been demonstrated that PUFA analogues vary in their selectivity for human voltage-gated ion channels involved in the ventricular action potential (Bohannon et al., 2020). Selectivity for a specific ion channel to broadly modulating cardiac ion channels was evidenced for all three ion channel families, i.e. voltage-gated sodium channel (Na_V), voltage-gated calcium channel (Ca_V), and voltage-gated potassium channel (K_V), which generate the cardiac action potential. Other authors showed that PUFAs induced activation $K_V7.1$ and $K_V7.1$-KCNE1 channels in cardiac cells. Kv7.1-KCNE1 channels produce the slow-delayed rectifying K^+ current, I_{Ks}, which is important during the repolarization phase of the cardiac action potential (Liin et al., 2018; Thompson et al., 2021). These data support the notion that PUFAs exert anti-arrhythmic properties which may be related to improvement of gap-junctional coupling via connexin 43 (Cx43) (Benova et al., 2019). The anti-arrhythmic properties of PUFAs were confirmed in a recent clinical study which showed that ω-3 PUFA supplementation of the diet improved cardiac function in children with premature ventricular contractions (Oner et al., 2018). Another important finding of the present study was that PUFAs dose-dependent increased the number of contracting EBs in a specific time window of differentiation, i.e. day 7-10 of cell culture which indicates an increase in the number of differentiated cardiomyocytes from ES cells. Prior studies have reported the importance of this time window in cardiomyogenesis of ES cells (Bartsch et al., 2011; Boheler et al., 2002). PUFAs dose-dependent increased the α-actinin-positive area and enhanced cardiac protein expression such as α-actinin and MLC2a. In accordance with the present results, previous studies have demonstrated that a low dose (10μM) of EPA promoted ES cell differentiation toward cardiomyocytes, increased the cell area of contracting cardiomyocytes and the expression of cardiac markers such as Nkx2.5, MEF2C, MYH6,

TNNT2, and Cx43 in EBs derived from mES cells (Shabani et al., 2015). The same group reported that preincubation of ES cell-derived cardiac cells with ω-3 PUFAs and ascorbic acid improved the regenerative capacity and reduced fibrosis in a rat infarction model (Shabani et al., 2019).

Since data of the present study showed that stimulation of vascular differentiation by PUFAs was mediated by ROS, we investigated whether the same effect would underlie cardiomyogenesis. Our data demonstrated that PUFA-induced cardiomyogenesis was blunted in presence of the ROS inhibitor NADPH oxidase inhibitor VAS2870. This observation corroborates previous research from our group and others which demonstrated that intracellular ROS are implicated in cardiomyocyte differentiation from ES cells via different ROS-involving signaling cascades (Bartsch et al., 2011; Buggisch et al., 2007; Crespo et al., 2010; Murray et al., 2013; Sauer et al., 2004; Sauer et al., 2000; Schmelter et al., 2006; Wo et al., 2008).

4.3 Impact of PUFAs on cardiac cell maturation

Besides stimulating the differentiation, proliferation and function of cardiac cells, PUFAs may also regulate maturation of cardiomyocytes. Recently it has been outlined that the energy metabolism may be involved in the regulation of maturation of cardiomyocytes derived from pluripotent stem cells with unexpected effects on electrical and mechanical function, and it has been discussed that PUFAs may activate multiple signaling networks leading to improved maturation of cardiac progenitor cells from the fetal phenotype (Karbassi et al., 2020). Cardiomyocytes differentiated from pluripotent stem cells are significantly immature compared to adult cardiomyocytes and display a fetal-like phenotype (Feric & Radisic, 2016; Yang et al., 2014). The immature properties of cardiomyocyte limit their efficacy in disease modeling and therapeutic purposes. Although some progress has been performed to achieve more mature human pluripotent stem cell-derived cardiomyocytes (hPSC-CMs), there is enough space for improvement because of the marked postnatal cardiac metabolism changes associated to cardiac cell maturation (Makinde et al., 1998; Yang et al., 2019). Maturation refers to the end state of heart development and primes the organ for powerful, effective and persistent pumping during

lifespan. It is characterized by structural, gene expression, metabolic and functional specializations in terminally differentiated cardiomyocytes as the heart transits from fetal to adult states. Due to maturation defects in pluripotent stem cell–derived cardiomyocytes, their use in myocardial regeneration and their possible contribution to cardiac disease is so far limited. There are measurable parameters that distinguish cardiomyocyte maturation, such as myofibril maturation, changes in electrophysiology and Ca^{2+} metabolism, and others (Guo & Pu, 2020)**.** Yang and his colleagues have mentioned that metabolic substrate shift from glucose to fatty acids is an essential feature of postnatal cardiomyocyte maturation. They suggested that applying fatty acids would improve hPSC-CM maturation. They designed a cocktail based on breastfed human infant serum (Hardell & Walldius, 1980) and breast milk (Gibson & Kneebone, 1981). Their study evidenced that palmitate, oleate and linoleate could induce hPSC-CM hypertrophic growth, force generation, calcium dynamics, action potential upstroke velocity and oxidative capacity and that these molecules activate multiple signaling pathways (Yang et al., 2019). Knight et al., (2021) have exhibited a modified method to create further mature human induced pluripotent stem cell-derived cardiomyocytes (hiPSC-CMs) by seeding cells in a medium supplemented with fatty acids as an important energy source and plating these cells on micropatterned growth surfaces. They noted that cells displayed elongation, enhanced sarcomeric maturity, metabolic gene expression, mitochondrial fatty acid uptake and cardiolipin maturation under these conditions. The isolated myofibrils from these cells showed that mechanical performance more similarly resembled those from adult human ventricular tissue, particularly in terms of force generation. These mature hiPSC-CMs also respond well to hypertrophic stimulation, producing an adult-like hypertrophic response and alterations in myofibril relaxation similar to human hypertrophic cardiomyopathy (HCM) tissue (Knight et al., 2021) . In addition, Zhang and his colleagues have demonstrated that hPSC-CM are dependent upon exogenous sources of lipids for metabolic maturation (Zhang et al., 2020).
The mechanism of PUFAs to enhance cardiomyocyte maturation is not sufficiently investigated. In mature cardiomyocytes, CD36 and fatty acid transport proteins (FATPs) facilitate fatty acid uptake to produce ATP by mitochondrial oxidative phosphorylation utilized to drive cardiac contraction (Steinbusch et al., 2011). Moreover, the expression of

many key genes such as fatty acid oxidation and CD36 increased upon maturation treatment in hiPSC-CMs (Gentillon et al., 2019). In the heart, CD36 not only facilitates long-chain fatty acid uptake, but also regulates other cellular activities such as intracellular Ca^{2+} signaling (Pietka et al., 2012) and AMPK activation (Samovski et al., 2015). Notably, the data of the present study demonstrated that intracellular Ca^{2+} elicited by PUFAs was inhibited by the pharmacological CD36 inhibitor SSO as well as by neutralizing antibodies against CD36, thus relating PUFA import with intracellular Ca^{2+} signaling cascades and presumably cardiac maturation processes.

A further major player in cardiac cell maturation is PPAR-α. PPARs (comprising of PPAR-α, ß and γ) are nuclear receptors that perform as ligand-dependent transcription factors, which are activated by different types of fatty acids. PPARs have important roles for various metabolic and cellular processes such as fatty acid β-oxidation and adipogenesis (lipid homeostasis). Moreover, PPARs perform an essential function during placental, embryonal, and fetal development and regulatory processes related to aging, comprising oxidative stress, inflammation, and neuroprotection (Echeverría et al., 2016). Recently, proteomic analysis of hES cell-derived, fetal and adult ventricular cardiomyocytes demonstrated that protein expression related to PPAR-α signalling cascades were differentially regulated in ES cell-derived and fetal cardiomyocytes as compared to adult cardiac cells. Stimulation of PPAR-α with WY-14643 resulted in increased fatty oxidative enzyme level, hyperpolarized mitochondrial membrane potential and induced a more organized morphology (Poon et al., 2015). Previous studies of us reported that agonists of PPAR-α increased cardiac differentiation from ES cells (Sharifpanah et al., 2008), which was related to elevation in the expression of cardiac-specific transcription factors and proteins. In the present study it was evidenced that EPA and LA activated PPAR-α in cell nuclei of differentiating cardiac cells which was inhibited in presence of the PPAR-α antagonist GW6471. This observation indicated that in addition to the activation of genes encoding contractile proteins, myofibrillogenesis is supported by enzymes involved in fatty acid metabolism (Kraft et al., 2006). In the experiments of the present study co-incubation of LA and EPA with the PPAR-α antagonist GW6471 abolished PUFA-induced cardiomyogenesis. Ding and colleagues (2007) who

demonstrated that activation of PPAR-α is a pre-requisite for cardiomyocyte differentiation of murine ES cells. PPAR-α activation is dependent on either pharmacological ligands like fibrates or natural ligands, e.g. fatty acids (Ding et al., 2007). Previous transcriptomic analyses performed in mice demonstrated that single oral dose of synthetic triglycerides composed of one single fatty acid stimulated expression of cardiac genes which were regulated in a PPARα-dependent manner, thus underscoring the importance of PPARα in mediating transcriptional regulation by fatty acids in the heart (Georgiadi et al., 2012). Recently, research was undertaken to promote hiPSC-CM maturation by combining hypoxia inducible factor 1-α (HIF-1α) inhibition with molecules that target key pathways involved in the energy metabolism. In this study hiPSC-CMs were treated with a HIF-1α inhibitor alone or in combination with the PPAR-α agonist WY-14643 and the postnatal factors triiodothyronine hormone T3, insulin-like growth factor-1 (IGF-1) and dexamethasone (Gentillon et al., 2019). The treatment resulted stimulated fatty acid oxidation, increased mitochondrial number and cardiac cell maturation thus supporting notion of the present study that stimulation of fatty acid oxidation by PUFAs supports cardiac cell maturation via signaling pathways, which involve the energy sensor AMPK-α and PPAR-α-mediated signaling cascades.

Stem cell pluripotency does not represent a single defined metabolic state. Metabolic signatures are highly characteristic for a cell and may contribute to the fate of the cell (Ellen Kreipke et al., 2016). Cellular metabolism is changing between naïve (early stage) and primed (late stage) ES cells, representing preimplantation and postimplantation embryos, respectively. The transition from naïve to primed ES cells has been shown to be accompanied by a distinct metabolic switch from bivalent (fatty acid oxidation/glycolytic) to highly glycolytic state which adopts the cells to the hypoxic condition of the early postimplantation embryo and protects the embryo from oxidative stress (Ellen Kreipke et al., 2016). During the following differentiation and maturation processes a second metabolic switch towards oxidative phosphorylation occurs. Then highly respiring mitochondria fulfill the dramatically augmenting energy needs during shaping of the cardiovascular system and organ formation. This physiological “metabolic inflammation”

requires ROS/RNS as well as PUFA-derived eicosanoids as intracellular messengers to initiate differentiation and maturation of progenitor cells in the cardiovascular system.

Table 12. The effects of PUFAs and their metabolic products on the proliferation and differentiation from various stem cell types. The table was modified and updated with permission of Kang and his colleagues (Kang et al., 2014).

Fatty acids/ Metabolites	Stem cell models	Effects	Potential pathways	References
LA	ES cells	Increase proliferation	Ca21/PKC, PI3K/Akt and MAPKs	(Min Hee Kim et al., 2009)
		Promote differentiation	Ca^{2+}, ROS, NO, AMPK-α and PPAR-α	(Taha et al., 2020)
AA	ES cells	Promote differentiation	LT signaling pathway and 5-LOX-activating protein (FLAP)	(Huang et al., 2016)
	C2C12 cells	By prolonging proliferation and preventing differentiation, PUFAs control the transition cells from proliferation to differentiation.	Wnt signaling pathway	(Huang et al., 2016; Risha et al., 2021)
	Mesenchymal stem cells	Promote differentiation	Unknown	(Kan et al., 2007)
ALA	Embryonic neural stem cells	Increase proliferation Promote differentiation	Notch1, hes1 and Ki-67	(Mahmoudi et al., 2019)
EPA	ES cells	Promote differentiation	Unknown	(Shabani et al., 2015)
			Ca^{2+}, ROS, NO, AMPK-α and PPAR-α	(Taha et al., 2020)
DHA	Neural stem cells	Promote differentiation, increase proliferation	RXR, PPAR, dendritic spine-related genes and basic helix–loop–helix	(He et al., 2009; Kan et al., 2007; Katakura et al., 2009; Sakamoto et al., 2007)
	Mesenchymal stem cells	Promote osteogenic differentiation	Enhanced Akt activation at the plasma membrane	(Levental et al., 2017)
		Promote neuronal differentiation	Unknown	(Kan et al., 2007)
	C2C12 cells	By prolonging proliferation and preventing differentiation, PUFAs control the transition cells from proliferation to differentiation.	Wnt signaling pathway	(Risha et al., 2021)
PGE1	Hematopoietic stem cells	Inhibit proliferation	Unknown	(Gidàli & Fehèr, 1977; Kurland et al., 1978; Motomura & Dexter, 1980)
PGE2	Hematopoietic stem cells	Increase proliferation, inhibit apoptosis, promote differentiation to dendritic cells	CXCR4, survivin, and Wnt	(Chen et al., 2007; Goessling et al., 2009; Pelus et al., 1979)

	ES cells	Increase proliferation, inhibit apoptosis	PI3K/Akt	(Hou et al., 2013; SP Yun et al., 2009)
	Human umbilical cord blood-derived mesenchymal stem cells	Increase proliferation	Epac1/Rap1/Akt, and α-arrestin-1/JNK	(Jang et al., 2012; Yun et al., 2011)
	Neural stem cells	Increase proliferation	Unknown	(Jung et al., 2006; Sasaki et al., 2003)
	Bone marrow-derived cells	Promote endothelial	AMPK	(Zhu et al., 2011)
	Tendon stem cells	Promote osteogenic differentiation	PI3K/Akt	(Liu et al., 2013)
Δ12,14-PGJ2	ES cells	inhibit proliferation	JAK-STAT	(Rajasingh & Bright, 2006)
	Neural stem cells	Biphasic regulation of proliferation	Unknown	(Katura et al., 2009, 2010)
LTB4	Neural stem cells	Biphasic regulation of proliferation, promote differentiation to neurons	Hedgehog	(Bijlsma et al., 2008; Wada et al., 2006)
	Hematopoietic stem cells	Increase proliferation, inhibit apoptosis	Unknown	(Chung et al., 2005)
LTD4	ES cells	Increase proliferation	STAT3, calcineurin, PI3K/Akt, and GSK 3b/b-catenin	(Kim et al., 2010)
LXA4	Neural stem cells	Directly regulates proliferation and differentiation to neurons	EGFR, cyclin E, p27, and caspase 8	(Wada et al., 2006)
NPD1	ES cells	Promote neuronal and cardiac differentiation	Unknown	(Yanes et al., 2010)
TXA2	Adipose tissue-derived mesenchymal stem cells	Increase proliferation, promote differentiation to smooth-muscle-like cells	ERK, p38 MAPK	(Mi Ra Kim et al., 2009; Doo Hee Yun et al., 2009)

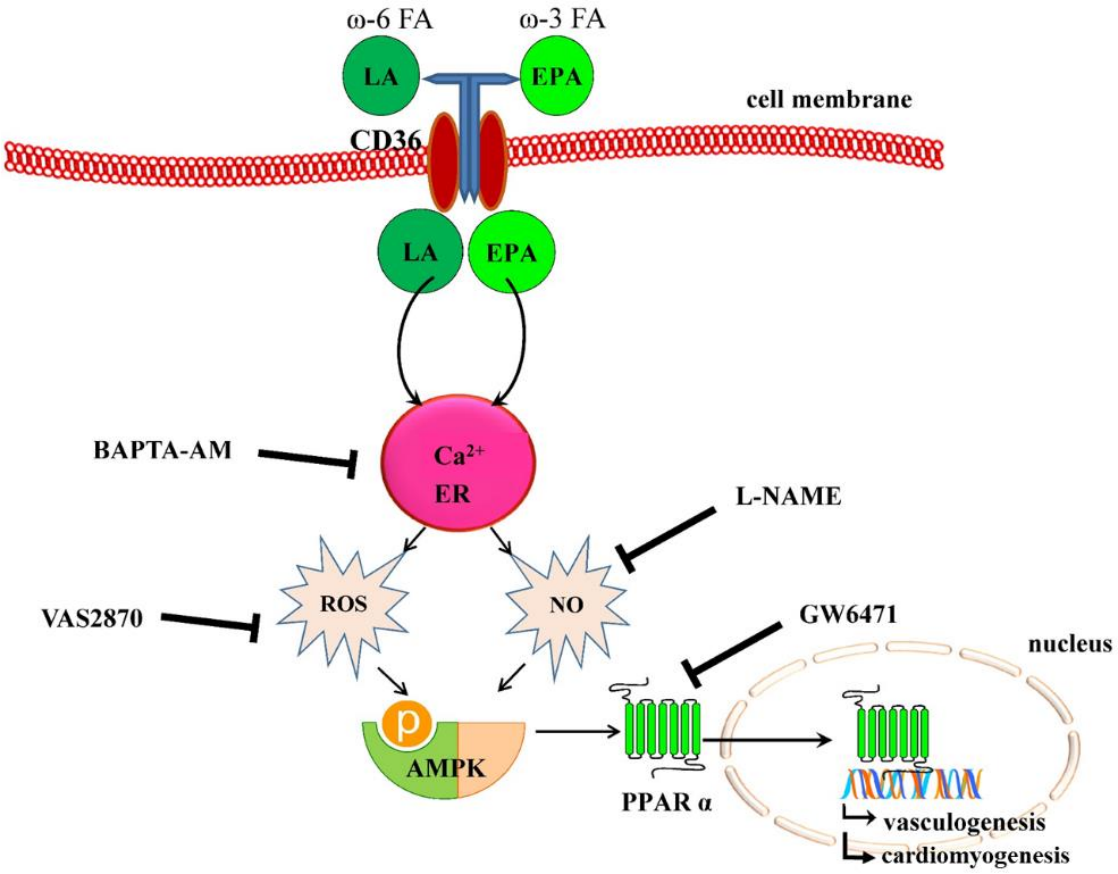

Figure 4.1: Schematic view of the stimulation of cardiomyogenesis and vasculogenesis in ES cells by PUFAs. LA and EPA are entering the cell through CD36 and release intracellular calcium from intracellular stores. Calcium stimulates ROS from NADPH oxidase and NO from eNOS, which in concert activate AMPK-α. Downstream of AMPK, PPAR-α is phosphorylated in the cell nucleus and initiates vasculogenic and cardiomyogenic genes. Figure adapted with permission from (Taha et al., 2020); copyright John Wiley and Sons.

5-Summary

PUFAs and their metabolites may influence differentiation processes of stem cells. The aim of the current study was to determine the effects of LA as ω-6-PUFA and EPA as ω-3-PUFA on vasculogenesis and cardiomyogenesis of ES cells.

LA and EPA increased vascular structure formation and protein expression of the endothelial-specific markers FLK-1, PECAM-1, and VE-Cadherin, whereas the saturated fatty acid PA was without effect. LA and EPA increased ROS and NO, activated eNOS and raised intracellular calcium. The calcium response was inhibited by the intracellular calcium chelator BAPTA-AM and SSO, which is an antagonist of CD36, the scavenger receptor for fatty acid uptake. Comparable effects were achieved with CD36-neutralizing antibodies.

In a dose-dependent manner, LA and EPA enhanced cardiomyocyte differentiation and function. LA and EPA accelerated beating frequency of cardiac cells cluster (foci), increased the percentage of contracting EBs, the area of α-actinin-positive cardiac cells (beating area), and protein expression of the cardiac-specific markers α-actinin and MLC2a.

Prevention of ROS generation by radical scavengers or the NADPH oxidase inhibitor VAS2870 blunted vasculogenesis and cardiomyogenesis of ES cells. Moreover, inhibition of eNOS by L-NAME abolished vasculogenesis of ES cells.

PUFAs stimulated AMPK-α as well as PPAR-α. AMPK-α activation was abolished by calcium chelation as well as inhibition of ROS and NO generation. Moreover, PUFA-induced vasculogenesis and cardiomyogenesis were blunted by the PPAR-α inhibitor GW6471.

In conclusion, the data demonstrated that, LA as well as EPA, enhance cardiomyogenesis and vasculogenesis by mechanisms involving ROS, NO and changes in intracellular calcium, which are locked to the energy sensors AMPK-α and PPAR-α.

6- Zusammenfassung

Mehrfach ungesättigten Fettsäuren (PUFAs) beeinflussen möglicherweise Differenzierungsprozesse von Stammzellen. In der vorliegenden Studie wurde die Bedeutung von Linolsäure (LA), als Beispiel einer ω-6-PUFA, und Eicosapentaensäure (EPA), als Beispiel einer ω-3-PUFA, für die Vaskulogenese und Kardiomyogenese embryonaler Stammzellen der Maus untersucht.

LA und EPA stimulierten die Bildung reaktiver Sauerstoffspezies (ROS) und Stickmonoxid (NO), aktivierten die endotheliale NO-Synthase (eNOS) und erhöhten das intrazelluläre Calcium. Die Calciumantwort wurde durch den intrazellulären Calciumchelator BAPTA-AM und Sulfo-N-Succinimidyl Oleat (SSO), einen Antagonisten von CD36, dem Scavenger-Rezeptor für die Aufnahme von Fettsäuren, inhibiert. Vergleichbare Effekte wurden durch einen neutralisierenden Antikörper gegen CD36 erzielt.

LA und EPA stimulierten Dosis-abhängig die Kardiomyozyten-Differenzierung und Funktion. LA and EPA beschleunigten die Kontraktionsfrequenz der kontraktilen kardialen Areale, erhöhten die Anzahl kontrahierender EBs, die Fläche der kardialen Zellareale sowie die Proteinexpression der kardialen Marker α-Actinin and MLC2a. LA und EPA erhöhten außerdem die Bildung vaskulärer Strukturen und die Protein-Expression der Endothel-spezifischen Marker FLK-1, PECAM-1 und VE-Cadherin. Im Gegensatz zu LA und EPA konnte keine Stimulation der Vaskulogenese durch die gesättigte Fettsäure PA festgestellt werden.

Unterdrückung der ROS-Erzeugung durch Radikalfänger oder den NADPH-Oxidase-Inhibitor VAS2870 inhibierte die PUFA-vermittelte Vaskulogenese und Kardiomyogenese von ES-Zellen. Darüber hinaus führte die Inhibition der eNOS durch N(ω)-Nitro-L-Argininmethylester (L-NAME) zur Hemmung der Vaskulogenese von ES-Zellen.

PUFAs stimulierten die AMP-aktivierte Proteinkinase (AMPK-α) sowie den Peroxisom-Proliferator-aktivierten Rezeptor-α (PPAR-α). Die PUFA-vermittelte AMPK-α-Aktivierung wurde durch Chelation von Calcium sowie die Hemmung der ROS und NO

inhibiert. Weiterhin wurde die PUFA-induzierte Kardiomyogenese und Vaskulogenese der Stammzellen durch den PPAR-α-Inhibitor GW6471 verhindert.

Zusammenfassend zeigen die Daten der vorliegenden Studie, dass die PUFAs LA und EPA die Kardiomyogenese und Vaskulogenese embryonaler Stammzellen durch Signalkaskaden stimulieren, die von einer Erhöhung der Signalmoleküle Calcium, ROS und NO begleitet, und mit einer Aktivierung der Energiesensoren AMPK-α und PPAR-α verknüpft sind.

7. List of abbreviations

°C	Degrees Celsius
µl	Microliter
µs	Microsecond
8-EETs	8-epoxyeicosatrienoic acids
AA	Arachidonic acid
ADP	adenosine diphosphate
AICAR	5-aminoimidazole-4-carboxamide riboside
AKT	Protein kinase B
ALA	α-linolenic acid
AMP	adenosine monophosphate
AMPK	5' adenosine monophosphate-activated protein kinase
ANOVA	Analysis of variance
ATP	Adenosine triphosphate
BMP	Bone morphogenetic protein
BSA	Bovine serum albumins
Cat. No.	Catalog number
Cav	Voltage-gated calcium channel
CC BY 2.0	Creative Commons Attribution 2.0 Generic
CC BY 4.0	Creative Commons Attribution 4.0 International
CC-BY-NC-ND	Creative Commons Attribution Non-Commercial No Derivatives
CD31	Cluster of differentiation 31
cGMP	Cyclic guanosine monophosphate
CHD	Coronary heart disease
CLSM	Confocal laser scanning microscope
COX	Cyclooxygenases
CPN	Core pluripotency network
CVD	Cardiovascular disease
Cx43	Connexin 43
CYP	Cytochrome P450
D5D	Delta-5 desaturase
D6D	Delta-6 desaturase
DAF-FM DA	4-amino-5-methylamino-2',7'-difluorofluorescein diacetate
DGLA	Dihomo-gamma-linolenic acid
DHA	Docosahexaenoic acid
DMEM	Dulbecco’s modified Eagle medium
DMSO	Dimethyl sulfoxide
DNA	Ddeoxyribonucleic acid
DPA	Docosapentaenoic acid
DRAQ5	1,5-bis(2-(di-methylamino)ethylamino)-4,8-dihydroxyanthracene-9,10-dione
DUOX	Dual oxidase
DW	Distilled water
EB	Embryoid body
ECL	Enhanced chemiluminescence
EDTA	Ethylenediaminetetraacetic acid
EETs	Epoxyeicosatrienoic acids
EFAs	Essential fatty acids
EGFR	Epidermal growth factor receptor

List of abbreviations

ELOVLs	Elongation of very long-chain fatty acids
eNOS / NOS III	Endothelial nitric oxide synthase
EPA	Eicosapentaenoic acid
ER	Endoplasmic reticulum
ERK	Extracellular signal-regulated kinase
ES cells	Embryonic stem cells
Esrrb	Estrogen-related receptor beta
ETA	Eicosatetraenoic acid
ETC	Electron transport chain
FADS	Fatty acid desaturase
FATPs	Ffatty acid transport proteins
FCS	Fetal calf serum
FGF	Fibroblast growth factor
FLAP	5-LOX-activating protein
Flk-1	Fetal liver kinase-1
Fluo-4-AM	4-(6-Acetoxymethoxy-2,7-difluoro-3-oxo-9-xanthenyl)-4´-methyl-2,2´-(ethylenedioxy)dianiline-N,N,N´,N´-tetraacetic acid tetrakis (acetoxymethyl) ester
g	Gram
g	Gravity 1g = 9,81m/s²
GAPDH	Glyceraldehyde-3-phosphate dehydrogenase
GLA	Gamma-linolenic acid
h	Hour
H_2DCF-DA	2´7´-dichlorodihydrofluorescein diacetate
HCl	Hydrochloric acid
HCM	Hypertrophic cardiomyopathy
HDL	High-density lipoprotein
hESCs	Human embryonic stem cells
HETEs	5-hydroxyeicosatetraenoic acids
HF	Heart failure
HIF-1α	Hypoxia inducible factor 1-α
hiPSC-CMs	Human induced pluripotent stem cell-derived cardiomyocytes
hPSC-CMs	Human pluripotent stem cell-derived cardiomyocytes
HRP	Horseradish peroxidase
ICM	Inner cells mass
IGF-1	Insulin-like growth factor-1
IgG	Immunoglobulin G
IHD	Ischemic heart disease
IL-6	Interleukin-6
iNOS/ NOS II	Inducible nitric oxide synthase
IP3	Inositol trisphosphate
iPSCs	Induced pluripotent stem cells
JNK	c-Jun N-terminal kinase
KDa	Kilodaltons
Klf4	Kkruppel-like factor 4
Kv	Voltage-gated potassium channel
LA	Linoleic acid
LDL	Low-density lipoprotein
LIF	Leukemia inhibitory factor

LIF-pLpro	LIF-Plasmocin-Prophylactic
LIMP2	Lysosomal integral membrane protein II
L-NAME	Nω-Nitro-L-arginine methyl ester
LOX	Lipoxygenases
LTs	Leukotrienes
mA	Milliampere
MAPK	Mitogen-activated protein kinase
MEF2C	Myocyte enhancer factor 2C
MEFs	Mouse embryonic fibroblasts
mES cells	Mmouse embryonic stem cells
mg	Milligram
MI	Myocardial infarction
min	Minute
ml	Milliliter
MLC2a	Myosin regulatory light chain 2, atrial isoform
mm	millimeter
mM	Millimolar
MUFAs	Monounsaturated fatty acids
mW	Milliwatts
NA	Numerical aperture
MW	Molecular weight
NADPH	Nicotinamide adenine dinucleotide phosphate
Nanog	Nanog homeobox protein
Nav	Voltage-gated sodium channel
NEAA	Non-essential amino acids
nm	Nanometers
NMPG	N-(2-mercaptopropionyl)-glycine
nNOS/ NOS I	Neuronal nitric oxide synthase
NO	Nitric oxide
NOS	Nitric oxide synthase
NPD1	Neuroprotectin D1
Oct4	Octamer-binding transcription factor 4
PA	Palmitic acid
p-AMPK-α	Phosphorylation of AMP-activated protein kinase- α-subunits
PBS	Phosphate buffered saline
PD1	protectins D1
PECAM-1	Platelet endothelial cell adhesion molecule-1
p-eNOS	Phosphorylation of Endothelial Nitric-oxide Synthase
PGRN	Pluripotency gene regulatory network
PGs	Prostaglandins
PI3K	Phosphatidylinositol-3-kinase
PKC	Protein kinase C
PKG-1	Protein kinase G
PPAR-α	Peroxisome proliferator-activated receptor alpha
p-PPAR-α	Phosphorylation of peroxisome proliferator-activated receptor αalpha
PUFAs	Polyunsaturated fatty acids
RIPA	Radioimmunoprecipitation assay
RNS	Reactive nitrogen species
ROS	Reactive oxygen species

RT	Room temperature
Rvs	Resolvins
RyRs	Ryanodine receptors
s	Second
SCARB3	Scavenger receptor class B member 3
SDA	Stearidonic acid
SDS	Sodium dodecyl sulfate
Ser	Serine
sGC	Soluble guanylate cyclase
SMCs	Smooth muscle cells
SOD	Superoxide dismutase
SOX2	Sex-determining region Y/Box 2
SR	Sarcoplasmic reticulum
SR-B1	Scavenger receptor-B1
SSO	Sulfo-N-succinimidyl oleate
STAT3	Signal transducer and activator of transcription 3
TBST	Tris-buffered saline with 0.1% Tween
Tbx3	T-box transcription factor 3
Thr	Threonine
TIFF	Tagged image file format
TXs	Thromboxanes
V	Voltage
v/v	volume/volume
VE-Cadherin	Vascular endothelial cadherin
VEGF	Vascular endothelial growth factor
VEGFRs	Vascular endothelial growth factor receptors
VLCFAs	Very long-chain fatty acids
w/v	Wweight/volume
XO	Xanthine oxidase
Δ12,14-PGJ2	15-Deoxy-delta(12,14)-prostaglandin J(2)
µm	Micrometer
µM	Micromolar
ω-3	Omega-3
ω-6	Omega-6

8. List of figures and tables

8.1 List of figures

8.2 List of tables

9. References

Abdelhamid, A. S., Brown, T. J., Brainard, J. S., Biswas, P., Thorpe, G. C., Moore, H. J., Deane, K. H., AlAbdulghafoor, F. K., Summerbell, C. D., Worthington, H. V., Song, F., & Hooper, L. (2018). Omega-3 fatty acids for the primary and secondary prevention of cardiovascular disease. *Cochrane Database of Systematic Reviews, 7*, Cd003177.

Abdelsaid, M. A., & El-Remessy, A. B. (2012). S-glutathionylation of LMW-PTP regulates VEGF-mediated FAK activation and endothelial cell migration. *Journal of Cell Science, 125*(20), 4751-4760.

Adams, R. H., & Alitalo, K. (2007). Molecular regulation of angiogenesis and lymphangiogenesis. *Nature Reviews Molecular Cell Biology, 8*(6), 464-478.

Agbaga, M.-P., Brush, R. S., Mandal, M. N. A., Henry, K., Elliott, M. H., & Anderson, R. E. (2008). Role of Stargardt-3 macular dystrophy protein (ELOVL4) in the biosynthesis of very long chain fatty acids. *Proceedings of the National Academy of Sciences, 105*(35), 12843-12848.

Aird, W. C. (2006). Mechanisms of endothelial cell heterogeneity in health and disease. *Circulation Research, 98*(2), 159-162.

Alderton, W. K., Cooper, C. E., & Knowles, R. G. (2001). Nitric oxide synthases: structure, function and inhibition. *Biochemical Journal, 357*(Pt 3), 593-615.

Ali, E., Sharifpanah, F., Wartenberg, M., & Sauer, H. (2018). Silibinin from Silybum marianum stimulates embryonic stem cell vascular differentiation via the STAT3/PI3-K/AKT axis and nitric oxide. *Planta Medica, 84*(11), 768-778.

Baker, C. L., & Pera, M. F. (2018). Capturing totipotent stem cells. *Cell Stem Cell, 22*(1), 25-34.

Balić, A., Vlašić, D., Žužul, K., Marinović, B., & Bukvić Mokos, Z. (2020). Omega-3 Versus Omega-6 Polyunsaturated Fatty Acids in the Prevention and Treatment of Inflammatory Skin Diseases. *International Journal of Molecular Sciences, 21*(3), 741.

Bartsch, C., Bekhite, M. M., Wolheim, A., Richter, M., Ruhe, C., Wissuwa, B., Marciniak, A., Müller, J., Heller, R., & Figulla, H.-R. (2011). NADPH oxidase and eNOS control cardiomyogenesis in mouse embryonic stem cells on ascorbic acid treatment. *Free Radical Biology and Medicine, 51*(2), 432-443.

Bass, D., Parce, J. W., Dechatelet, L. R., Szejda, P., Seeds, M., & Thomas, M. (1983). Flow cytometric studies of oxidative product formation by neutrophils: a graded response to membrane stimulation. *The Journal of Immunology, 130*(4), 1910-1917.

Bedard, K., & Krause, K.-H. (2007). The NOX family of ROS-generating NADPH oxidases: physiology and pathophysiology. *Physiological Reviews, 87*(1), 245-313.

Bekhite, M., Müller, V., Tröger, S., Müller, J., Figulla, H., Sauer, H., & Wartenberg, M. (2016). Involvement of phosphoinositide 3-kinase class IA (PI3K 110α) and NADPH oxidase 1 (NOX1) in regulation of vascular differentiation induced by vascular endothelial growth factor (VEGF) in mouse embryonic stem cells. *Cell and Tissue Research, 364*(1), 159-174.

BelAiba, R. S., Djordjevic, T., Petry, A., Diemer, K., Bonello, S., Banfi, B., Hess, J., Pogrebniak, A., Bickel, C., & Görlach, A. (2007). NOX5 variants are functionally active in endothelial cells. *Free Radical Biology and Medicine, 42*(4), 446-459.

Beltran-Povea, A., Caballano-Infantes, E., Salguero-Aranda, C., Martín, F., Soria, B., Bedoya, F. J., Tejedo, J. R., & Cahuana, G. M. (2015). Role of nitric oxide in the maintenance of pluripotency and regulation of the hypoxia response in stem cells. *World Journal of Stem Cells, 7*(3), 605-617.

Benatti, P., Peluso, G., Nicolai, R., & Calvani, M. (2004). Polyunsaturated fatty acids: biochemical, nutritional and epigenetic properties. *Journal of the American College of Nutrition, 23*(4), 281-302.

Benova, T. E., Viczenczova, C., Bacova, B. S., Knezl, V., Dosenko, V., Rauchova, H., Zeman, M., Reiter, R. J., & Tribulova, N. (2019). Obesity-associated alterations in cardiac connexin-43 and PKC signaling are attenuated by melatonin and omega-3 fatty acids in female rats. *Molecular and Cellular Biochemistry, 454*(1), 191-202.

Berridge, M., Lipp, P., & Bootman, M. (1999). Calcium signalling. *Current Biology, 9*(5), R157-R159.

Bigarella, C. L., Liang, R., & Ghaffari, S. (2014). Stem cells and the impact of ROS signaling. *Development, 141*(22), 4206-4218.

Bijlsma, M. F., Peppelenbosch, M. P., Spek, C. A., & Roelink, H. (2008). Leukotriene synthesis is required for hedgehog-dependent neurite projection in neuralized embryoid bodies but not for motor neuron differentiation. *Stem Cells, 26*(5), 1138-1145.

Blanpain, C., Horsley, V., & Fuchs, E. (2007). Epithelial stem cells: turning over new leaves. *Cell, 128*(3), 445-458.

Block, K., & Gorin, Y. (2012). Aiding and abetting roles of NOX oxidases in cellular transformation. *Nature Reviews Cancer, 12*(9), 627.

Bohannon, B. M., de la Cruz, A., Wu, X., Jowais, J. J., Perez, M. E., Dykxhoorn, D. M., Liin, S. I., & Larsson, H. P. (2020). Polyunsaturated fatty acid analogues differentially affect cardiac NaV, CaV, and KV channels through unique mechanisms. *Elife, 9*, e51453.

Boheler, K. R., Czyz, J., Tweedie, D., Yang, H.-T., Anisimov, S. V., & Wobus, A. M. (2002). Differentiation of pluripotent embryonic stem cells into cardiomyocytes. *Circulation Research, 91*(3), 189-201.

Bootman, M. D., Lipp, P., & Berridge, M. J. (2001). The organisation and functions of local Ca^{2+} signals. *Journal of Cell Science, 114*(12), 2213-2222.

Boyer, L. A., Lee, T. I., Cole, M. F., Johnstone, S. E., Levine, S. S., Zucker, J. P., Guenther, M. G., Kumar, R. M., Murray, H. L., & Jenner, R. G. (2005). Core transcriptional regulatory circuitry in human embryonic stem cells. *Cell, 122*(6), 947-956.

Breier, G., Breviario, F., Caveda, L., Berthier, R., Schnurch, H., Gotsch, U., Vestweber, D., Risau, W., & Dejana, E. (1996). Molecular cloning and expression of murine vascular endothelial-cadherin in early stage development of cardiovascular system. *Blood, 87*(2), 630-641.

Buggisch, M., Ateghang, B., Ruhe, C., Strobel, C., Lange, S., Wartenberg, M., & Sauer, H. (2007). Stimulation of ES-cell-derived cardiomyogenesis and neonatal cardiac cell

proliferation by reactive oxygen species and NADPH oxidase. *Journal of Cell Science, 120*(5), 885-894.

Caballano-Infantes, E., Terron-Bautista, J., Beltrán-Povea, A., Cahuana, G. M., Soria, B., Nabil, H., Bedoya, F. J., & Tejedo, J. R. (2017). Regulation of mitochondrial function and endoplasmic reticulum stress by nitric oxide in pluripotent stem cells. *World Journal of Stem Cells, 9*(2), 26-36.

Carrillo, C., a del Mar Cavia, M., & Alonso-Torre, S. R. (2011). Oleic acid versus linoleic and α-linolenic acid. Different effects on Ca^{2+} signaling in rat thymocytes. *Cellular Physiology and Biochemistry, 27*(3-4), 373-380.

Carta, G., Murru, E., Banni, S., & Manca, C. (2017). Palmitic acid: physiological role, metabolism and nutritional implications. *Frontiers in Physiology, 8*, 902.

Cencioni, C., Spallotta, F., Savoia, M., Kuenne, C., Guenther, S., Re, A., Wingert, S., Rehage, M., Sürün, D., & Siragusa, M. (2018). Zeb1-Hdac2-eNOS circuitry identifies early cardiovascular precursors in naive mouse embryonic stem cells. *Nature Communications, 9*(1), 1-15.

Chan, E. C., Jiang, F., Peshavariya, H. M., & Dusting, G. J. (2009). Regulation of cell proliferation by NADPH oxidase-mediated signaling: potential roles in tissue repair, regenerative medicine and tissue engineering. *Pharmacology & Therapeutics, 122*(2), 97-108.

Chan, S. S., Chen, J. H., Hwang, S. M., Wang, I. J., Li, H. J., Lee, R. T., & Hsieh, P. C. (2009). Salvianolic acid B–vitamin C synergy in cardiac differentiation from embryonic stem cells. *Biochemical and Biophysical Research Communications, 387*(4), 723-728.

Cheedipudi, S. M., Matkovich, S. J., Coarfa, C., Hu, X., Robertson, M. J., Sweet, M., Taylor, M., Mestroni, L., Cleveland, J., & Willerson, J. T. (2019). Genomic Reorganization of Lamin-Associated Domains in Cardiac Myocytes Is Associated With Differential Gene Expression and DNA Methylation in Human Dilated Cardiomyopathy. *Circulation Research, 124*(8), 1198-1213.

Chen, L., Zhang, W., Yue, H., Han, Q., Chen, B., Shi, M., Li, J., Li, B., You, S., & Shi, Y. (2007). Effects of human mesenchymal stem cells on the differentiation of dendritic cells from CD34+ cells. *Stem Cells and Development, 16*(5), 719-732.

Chen, Q., Wang, Q., Zhu, J., Xiao, Q., & Zhang, L. (2018). Reactive oxygen species: key regulators in vascular health and diseases. *British Journal of Pharmacology, 175*(8), 1279-1292.

Cheung, P. C., Salt, I. P., Davies, S. P., Hardie, D. G., & Carling, D. (2000). Characterization of AMP-activated protein kinase γ-subunit isoforms and their role in AMP binding. *Biochemical Journal, 346*(3), 659-669.

Choi, S.-L., Kim, S.-J., Lee, K.-T., Kim, J., Mu, J., Birnbaum, M. J., Kim, S. S., & Ha, J. (2001). The regulation of AMP-activated protein kinase by H2O2. *Biochemical Biophysical Research Communications, 287*(1), 92-97.

Chung, J. W., Kim, G.-Y., Mun, Y.-C., Ahn, J.-Y., Seong, C.-M., & Kim, J.-H. (2005). Leukotriene B4 pathway regulates the fate of the hematopoietic stem cells. *Experimental & Molecular Medicine, 37*(1), 45-50.

Condic, M. L. (2013). Totipotency: what it is and what it is not. *Stem Cells Development, 23*(8), 796-812.

Cosby, K., Partovi, K. S., Crawford, J. H., Patel, R. P., Reiter, C. D., Martyr, S., Yang, B. K., Waclawiw, M. A., Zalos, G., & Xu, X. (2003). Nitrite reduction to nitric oxide by deoxyhemoglobin vasodilates the human circulation. *Nature Medicine, 9*(12), 1498-1505.

Cowart, L. A., Wei, S., Hsu, M.-H., Johnson, E. F., Krishna, M. U., Falck, J. R., & Capdevila, J. H. (2002). The CYP4A isoforms hydroxylate epoxyeicosatrienoic acids to form high affinity peroxisome proliferator-activated receptor ligands. *Journal of Biological Chemistry, 277*(38), 35105-35112.

Crespo, F. L., Sobrado, V. R., Gomez, L., Cervera, A. M., & McCreath, K. J. (2010). Mitochondrial reactive oxygen species mediate cardiomyocyte formation from embryonic stem cells in high glucose. *Stem Cells, 28*(7), 1132-1142.

Crnkovic, S., Riederer, M., Lechleitner, M., Hallstrom, S., Malli, R., Graier, W. F., Lindenmann, J., Popper, H., Olschewski, H., Olschewski, A., & Frank, S. (2012). Docosahexaenoic acid-induced unfolded protein response, cell cycle arrest, and apoptosis in vascular smooth muscle cells are triggered by Ca^{2+}-dependent induction of oxidative stress. *Free Radical Biology and Medicine, 52*(9), 1786-1795.

da Silva, E. P., Jr., Nachbar, R. T., Levada-Pires, A. C., Hirabara, S. M., & Lambertucci, R. H. (2016). Omega-3 fatty acids differentially modulate enzymatic anti-oxidant systems in skeletal muscle cells. *Cell Stress Chaperones, 21*(1), 87-95.

Das, U. N. (2006). Essential fatty acids-a review. *Current Pharmaceutical Biotechnology, 7*(6), 467-482.

Davidson, K. C., Mason, E. A., & Pera, M. F. (2015). The pluripotent state in mouse and human. *Development, 142*(18), 3090-3099.

Denic, V., & Weissman, J. S. (2007). A molecular caliper mechanism for determining very long-chain fatty acid length. *Cell, 130*(4), 663-677.

Der Sarkissian, S., Lévesque, T., & Noiseux, N. (2017). Optimizing stem cells for cardiac repair: current status and new frontiers in regenerative cardiology. *World Journal of Stem Cells, 9*(1), 9.

Ding, L., Liang, X., Zhu, D., & Lou, Y. (2007). Peroxisome proliferator-activated receptor α is involved in cardiomyocyte differentiation of murine embryonic stem cells in vitro. *Cell Biology International, 31*(9), 1002-1009.

Djinovic-Carugo, K., Young, P., Gautel, M., & Saraste, M. (1999). Structure of the a-actinin rod: molecular basis for cross-linking of actin filaments. *Cell, 98*(4), 537-546.

Doetschman, T. C., Eistetter, H., Katz, M., Schmidt, W., & Kemler, R. (1985). The in vitro development of blastocyst-derived embryonic stem cell lines: formation of visceral yolk sac, blood islands and myocardium. *Development, 87*(1), 27-45.

du Pré, B. C., Doevendans, P. A., & van Laake, L. W. (2013). Stem cells for cardiac repair: an introduction. *Journal of Geriatric Cardiology, 10*(2), 186-197.

Dumancas, G. G., Kimani, M., Purdie, N., & Reilly, L. (2010). Partial least squares (PLS1) algorithm for quantitating cholesterol and polyunsaturated fatty acids in human serum. *Journal of Biotech Research, 2*, 121-130.

Dunn, S.-J., Martello, G., Yordanov, B., Emmott, S., & Smith, A. (2014). Defining an essential transcription factor program for naive pluripotency. *Science, 344*(6188), 1156-1160.

Echeverría, F., Ortiz, M., Valenzuela, R., & Videla, L. A. (2016). Long-chain polyunsaturated fatty acids regulation of PPARs, signaling: Relationship to tissue development and aging. *Prostaglandins, Leukotrienes and Essential Fatty Acids, 114*, 28-34.

Ellen Kreipke, R., Wang, Y., Miklas, J. W., Mathieu, J., & Ruohola-Baker, H. (2016). Metabolic remodeling in early development and cardiomyocyte maturation. *Seminars in Cell & Developmental Biology, 52*, 84-92.

Engler, M. B., Ma, Y. H., & Engler, M. M. (1999). Calcium-mediated mechanisms of eicosapentaenoic acid-induced relaxation in hypertensive rat aorta. *American Journal of Hypertension, 12*(12), 1225-1235.

Enikolopov, G., Banerji, J., & Kuzin, B. (1999). Nitric oxide and Drosophila development. *Cell Death Differentiation, 6*(10), 956-963.

Evans, M. J., & Kaufman, M. H. (1981). Establishment in culture of pluripotential cells from mouse embryos. *Nature, 292*(5819), 154-156.

Ezashi, T., Das, P., & Roberts, R. M. (2005). Low O2 tensions and the prevention of differentiation of hES cells. *Proceedings of the National Academy of Sciences, 102*(13), 4783-4788.

Farvid, M. S., Ding, M., Pan, A., Sun, Q., Chiuve, S. E., Steffen, L. M., Willett, W. C., & Hu, F. B. (2014). Dietary linoleic acid and risk of coronary heart disease: a systematic review and meta-analysis of prospective cohort studies. *Circulation, 130*(18), 1568-1578.

Fassler, R., Rohwedel, J., Maltsev, V., Bloch, W., Lentini, S., Guan, K., Gullberg, D., Hescheler, J., Addicks, K., & Wobus, A. M. (1996). Differentiation and integrity of cardiac muscle cells are impaired in the absence of beta 1 integrin. *Journal of Cell Science, 109*(13), 2989-2999.

Feric, N. T., & Radisic, M. (2016). Towards adult-like human engineered cardiac tissue: Maturing human pluripotent stem cell-derived cardiomyocytes in human engineered cardiac tissues. *Advanced Drug Delivery Reviews, 96*, 110-134.

Fidaleo, M., & Sartori, C. (2008). Administration of ciprofibrate to lactating mothers induces PPARα-signaling pathway in the liver and kidney of suckling rats. *Experimental and Toxicologic Pathology, 60*(1), 33-41.

Figueroa, V., Saez, P. J., Salas, J. D., Salas, D., Jara, O., Martinez, A. D., Saez, J. C., & Retamal, M. A. (2013). Linoleic acid induces opening of connexin26 hemichannels through a PI3K/Akt/Ca^{2+}-dependent pathway. *Biochimica et Biophysica Acta - Biomembranes, 1828*(3), 1169-1179.

Forrester, S. J., Kikuchi, D. S., Hernandes, M. S., Xu, Q., & Griendling, K. K. (2018). Reactive oxygen species in metabolic and inflammatory signaling. *Circulation Research, 122*(6), 877-902.

Franekova, V., Angin, Y., Hoebers, N. T., Coumans, W. A., Simons, P. J., Glatz, J. F., Luiken, J. J., & Larsen, T. S. (2014). Marine omega-3 fatty acids prevent myocardial insulin resistance and metabolic remodeling as induced experimentally

by high insulin exposure. *American Journal of Physiology-Cell Physiology, 308*(4), C297-C307.

Friel, R., Van Der Sar, S., & Mee, P. J. (2005). Embryonic stem cells: understanding their history, cell biology and signalling. *Advanced Drug Delivery Reviews, 57*(13), 1894-1903.

Garcia, D., & Shaw, R. J. (2017). AMPK: mechanisms of cellular energy sensing and restoration of metabolic balance. *Molecular Cell, 66*(6), 789-800.

Gaspar, J. A., Doss, M. X., Hengstler, J. G., Cadenas, C., Hescheler, J., & Sachinidis, A. (2014). Unique metabolic features of stem cells, cardiomyocytes, and their progenitors. *Circulation Research, 114*(8), 1346-1360.

Gee, K. R., Brown, K., Chen, W. U., Bishop-Stewart, J., Gray, D., & Johnson, I. (2000). Chemical and physiological characterization of fluo-4 Ca^{2+}-indicator dyes. *Cell Calcium, 27*(2), 97-106.

Gentile, C., Muise-Helmericks, R. C., & Drake, C. J. (2013). VEGF-mediated phosphorylation of eNOS regulates angioblast and embryonic endothelial cell proliferation. *Developmental Biology, 373*(1), 163-175.

Gentillon, C., Li, D., Duan, M., Yu, W.-M., Preininger, M. K., Jha, R., Rampoldi, A., Saraf, A., Gibson, G. C., & Qu, C.-K. (2019). Targeting HIF-1α in combination with PPARα activation and postnatal factors promotes the metabolic maturation of human induced pluripotent stem cell-derived cardiomyocytes. *Journal of Molecular and Cellular Cardiology, 132*, 120-135.

Georgiadi, A., Boekschoten, M. V., Müller, M., & Kersten, S. (2012). Detailed transcriptomics analysis of the effect of dietary fatty acids on gene expression in the heart. *Physiological Genomics, 44*(6), 352-361.

Gibson, R. A., & Kneebone, G. M. (1981). Fatty acid composition of human colostrum and mature breast milk. *The American Journal of Clinical Nutrition, 34*(2), 252-257.

Gidàli, J., & Fehėr, I. (1977). The effect of E type prostaglandins on the proliferation of haemopoietic stem cells in vivo. *Cell Proliferation, 10*(4), 365-373.

Glatz, J. F., & Luiken, J. J. (2015). Fatty acids in cell signaling: historical perspective and future outlook. *Prostaglandins, Leukotrienes Essential Fatty Acids, 92*, 57-62.

Glatz, J. F., & Luiken, J. J. (2018). Dynamic role of the transmembrane glycoprotein CD36 (SR-B2) in cellular fatty acid uptake and utilization. *Journal of Lipid Research, 59*(7), 1084-1093.

Goessling, W., North, T. E., Loewer, S., Lord, A. M., Lee, S., Stoick-Cooper, C. L., Weidinger, G., Puder, M., Daley, G. Q., & Moon, R. T. (2009). Genetic interaction of PGE2 and Wnt signaling regulates developmental specification of stem cells and regeneration. *Cell, 136*(6), 1136-1147.

Gonzalez-Crussi, F. (1971). Vasculogenesis in the chick embryo. An ultrastructural study. *American Journal of Anatomy, 130*(4), 441-459.

Görlach, A., Bertram, K., Hudecova, S., & Krizanova, O. (2015). Calcium and ROS: a mutual interplay. *Redox Biology, 6*, 260-271.

Grabacka, M., Pierzchalska, M., & Reiss, K. (2013). Peroxisome proliferator activated receptor alpha ligands as anticancer drugs targeting mitochondrial metabolism. *Current Pharmaceutical Biotechnology, 14*(3), 342-356.

Guan, Y. (2002). Targeting peroxisome proliferator-activated receptors (PPARs) in kidney and urologic disease. *Minerva Urologica e Nefrologica = The Italian Journal of Urology and Nephrology, 54*(2), 65-79.

Guo, Y., & Pu, W. T. (2020). Cardiomyocyte maturation: new phase in development. *Circulation Research, 126*(8), 1086-1106.

Hansen, T., Galougahi, K.-K., Celermajer, D., Rasko, N., Tang, O., Bubb, K. J., & Figtree, G. (2016). Oxidative and nitrosative signalling in pulmonary arterial hypertension—implications for development of novel therapies. *Pharmacology & Therapeutics, 165*, 50-62.

Hardell, L. I., & Walldius, G. (1980). Fatty acid composition of human serum lipids at birth. *Upsala Journal of Medical Sciences, 85*(1), 45-58.

Hardie, D. G. (2015). AMPK: positive and negative regulation, and its role in whole-body energy homeostasis. *Current Opinion in Cell Biology, 33*, 1-7.

Hashimoto, T., Cook, W. S., Qi, C., Yeldandi, A. V., Reddy, J. K., & Rao, M. S. (2000). Defect in peroxisome proliferator-activated receptor α-inducible fatty acid oxidation determines the severity of hepatic steatosis in response to fasting. *Journal of Biological Chemistry, 275*(37), 28918-28928.

He, C., Qu, X., Cui, L., Wang, J., & Kang, J. X. (2009). Improved spatial learning performance of fat-1 mice is associated with enhanced neurogenesis and neuritogenesis by docosahexaenoic acid. *Proceedings of the National Academy of Sciences, 106*(27), 11370-11375.

Heinke, J., Patterson, C., & Moser, M. (2012). Life is a pattern: vascular assembly within the embryo. *Frontiers in Bioscience, 4*, 2269-2288.

Holmström, K. M., & Finkel, T. (2014). Cellular mechanisms and physiological consequences of redox-dependent signalling. *Nature Reviews Molecular Cell Biology, 15*(6), 411-421.

Holterman, C. E., Thibodeau, J.-F., Towaij, C., Gutsol, A., Montezano, A. C., Parks, R. J., Cooper, M. E., Touyz, R. M., & Kennedy, C. R. (2014). Nephropathy and elevated BP in mice with podocyte-specific NADPH oxidase 5 expression. *Journal of the American Society of Nephrology, 25*(4), 784-797.

Horie, M., Ito, A., Kawabe, Y., & Kamihira, M. (2011). A genetically engineered STO feeder system expressing E-cadherin and leukemia inhibitory factor for mouse pluripotent stem cell culture. *Journal of Bioprocessing & Biotechniques, 3*, 001.

Horrobin, D. (1990). Gamma linolenic acid: an intermediate in essential fatty acid metabolism with potential as an ethical pharmaceutical and as a food. *Reviews in Contemporary Pharmacotherapy., 1*, 1-45.

Hou, P., Li, Y., Zhang, X., Liu, C., Guan, J., Li, H., Zhao, T., Ye, J., Yang, W., & Liu, K. (2013). Pluripotent stem cells induced from mouse somatic cells by small-molecule compounds. *Science, 341*(6146), 651-654.

Høy, C. E., Hølmer, G., Kaur, N., Byrjalsen, I., & Kirstein, D. (1983). Acyl group distributions in tissue lipids of rats fed evening primrose oil (λ-linolenic plus linoleic acid) or soybean oil (α-linolenic plus linoleic acid). *Lipids, 18*(11), 760-771.

Hu, C., Fan, L., Cen, P., Chen, E., Jiang, Z., & Li, L. (2016). Energy metabolism plays a critical role in stem cell maintenance and differentiation. *International Journal of Molecular Sciences, 17*(2), 253.

Hu, J., Frömel, T., & Fleming, I. (2018). Angiogenesis and vascular stability in eicosanoids and cancer. *Cancer and Metastasis Reviews, 37*(2-3), 425-438.

Huang, N. F., Fleissner, F., Sun, J., & Cooke, J. P. (2010). Role of nitric oxide signaling in endothelial differentiation of embryonic stem cells. *Stem Cells and Development, 19*(10), 1617-1626.

Huang, Y. H., Sharifpanah, F., Becker, S., Wartenberg, M., & Sauer, H. (2016). Impact of Arachidonic Acid and the Leukotriene Signaling Pathway on Vasculogenesis of Mouse Embryonic Stem Cells. *Cells Tissues Organs, 201*(5), 319-332.

Hunter, J. E. (1990). n-3 fatty acids from vegetable oils. *The American Journal of Clinical Nutrition, 51*(5), 809-814.

Itoh, F., Watabe, T., & Miyazono, K. (2014). Roles of TGF-β family signals in the fate determination of pluripotent stem cells. *Seminars in Cell & Developmental Biology, 32*, 98-106.

Jakobsson, L., Kreuger, J., & Claesson-Welsh, L. (2007). Building blood vessels—stem cell models in vascular biology. *The Journal of Cell Biology, 177*(5), 751-755.

Jang, M. W., Yun, S. P., Park, J. H., Ryu, J. M., Lee, J. H., & Han, H. J. (2012). Cooperation of Epac1/Rap1/Akt and PKA in prostaglandin E2-induced proliferation of human umbilical cord blood derived mesenchymal stem cells: Involvement of c-Myc and VEGF expression. *Journal of Cellular Physiology, 227*(12), 3756-3767.

Jiang, F., Zhang, G., Hashimoto, I., Kumar, B., Bortolotto, S., Morrison, W., & Dusting, G. (2008). Neovascularization in an arterio-venous loop-containing tissue engineering chamber: role of NADPH oxidase. *Journal of Cellular Molecular Medicine, 12*(5b), 2062-2072.

Jump, D. B. (2002). The biochemistry of n-3 polyunsaturated fatty acids. *Journal of Biological Chemistry, 277*(11), 8755-8758.

Jump, D. B., Depner, C. M., & Tripathy, S. (2012). Omega-3 fatty acid supplementation and cardiovascular disease Thematic Review Series: New lipid and lipoprotein targets for the treatment of cardiometabolic diseases. *Journal of Lipid Research, 53*(12), 2525-2545.

Jung, K.-H., Chu, K., Lee, S.-T., Kim, J., Sinn, D.-I., Kim, J.-M., Park, D.-K., Lee, J.-J., Kim, S. U., & Kim, M. (2006). Cyclooxygenase-2 inhibitor, celecoxib, inhibits the altered hippocampal neurogenesis with attenuation of spontaneous recurrent seizures following pilocarpine-induced status epilepticus. *Neurobiology of Disease, 23*(2), 237-246.

Juntilla, M. M., Patil, V. D., Calamito, M., Joshi, R. P., Birnbaum, M. J., & Koretzky, G. A. (2010). AKT1 and AKT2 maintain hematopoietic stem cell function by regulating reactive oxygen species. *Blood, 115*(20), 4030-4038.

Kalra, K., & Tomar, P. (2014). Stem cell: basics, classification and applications. *American Journal of Phytomedicine and Clinical Therapeutics, 2*(7), 919-930.

Kan, I., Melamed, E., Offen, D., & Green, P. (2007). Docosahexaenoic acid and arachidonic acid are fundamental supplements for the induction of neuronal differentiation. *Journal of Lipid Research, 48*(3), 513-517.

Kanaan, G. N., & Harper, M. E. (2017). Cellular redox dysfunction in the development of cardiovascular diseases. *Biochimica et Biophysica Acta -General Subjects, 1861*(11 Pt A), 2822-2829.

Kang, J. X., Wan, J. B., & He, C. (2014). Concise review: regulation of stem cell proliferation and differentiation by essential fatty acids and their metabolites. *Stem Cells, 32*(5), 1092-1098.

Kanno, S., Kim, P. K., Sallam, K., Lei, J., Billiar, T. R., & Shears, L. L. (2004). Nitric oxide facilitates cardiomyogenesis in mouse embryonic stem cells. *Proceedings of the National Academy of Sciences, 101*(33), 12277-12281.

Karbassi, E., Fenix, A., Marchiano, S., Muraoka, N., Nakamura, K., Yang, X., & Murry, C. E. (2020). Cardiomyocyte maturation: advances in knowledge and implications for regenerative medicine. *Nature Reviews Cardiology, 17*(6), 341-359.

Katakura, M., Hashimoto, M., Shahdat, H., Gamoh, S., Okui, T., Matsuzaki, K., & Shido, O. (2009). Docosahexaenoic acid promotes neuronal differentiation by regulating basic helix–loop–helix transcription factors and cell cycle in neural stem cells. *Neuroscience, 160*(3), 651-660.

Katura, T., Moriya, T., & Nakahata, N. (2009). 15-deoxy-Δ12, 14-prostaglandin J2 biphasically regulates the proliferation of mouse hippocampal neural stem cells by modulating the redox state. *Neuroscience Research*(65), S155.

Katura, T., Moriya, T., & Nakahata, N. (2010). 15-deoxy-Δ12, 14-prostaglandin J2 regulates the proliferation of mouse hippocampal neural stem/progenitor cells. *Neuroscience Research*(68), e93.

Kaur, N., Chugh, V., & Gupta, A. K. (2014). Essential fatty acids as functional components of foods-a review. *Journal of Food Science Technology, 51*(10), 2289-2303.

Kersten, S. (2014). Integrated physiology and systems biology of PPARα. *Molecular Metabolism, 3*(4), 354-371.

Khan, F. A., Almohazey, D., Alomari, M., & Almofty, S. A. (2018). Isolation, Culture, and Functional Characterization of Human Embryonic Stem Cells: Current Trends and Challenges. *Stem Cells International, 2018*, 1429351.

Kim, J., Yang, G., Kim, Y., Kim, J., & Ha, J. (2016). AMPK activators: mechanisms of action and physiological activities. *Experimental & Molecular Medicine, 48*(4), e224.

Kim, J. M., Lee, K. P., Park, S. J., Kang, S., Huang, J., Lee, J. M., Sato, K., Chung, H. Y., Okajima, F., & Im, D. S. (2015). Omega-3 fatty acids induce Ca(2+) mobilization responses in human colon epithelial cell lines endogenously expressing FFA4. *Acta Pharmacologica Sinica, 36*(7), 813-820.

Kim, M. H., Kim, M. O., Kim, Y. H., Kim, J. S., & Han, H. J. (2009). Linoleic acid induces mouse embryonic stem cell proliferation via Ca^{2+}/PKC, PI3K/Akt, and MAPKs. *Cellular Physiology Biochemistry, 23*(1-3), 053-064.

Kim, M. H., Lee, Y. J., Kim, M. O., Kim, J. S., & Han, H. J. (2010). Effect of leukotriene D4 on mouse embryonic stem cell migration and proliferation: involvement of

PI3K/Akt as well as GSK-3β/β-catenin signaling pathways. *Journal of Cellular Biochemistry, 111*(3), 686-698.

Kim, M. R., Jeon, E. S., Kim, Y. M., Lee, J. S., & Kim, J. H. (2009). Thromboxane A2 Induces Differentiation of Human Mesenchymal Stem Cells to Smooth Muscle-Like Cells. *Stem Cells, 27*(1), 191-199.

Kinder, M., Wei, C., Shelat, S. G., Kundu, M., Zhao, L., Blair, I. A., & Puré, E. (2010). Hematopoietic stem cell function requires 12/15-lipoxygenase–dependent fatty acid metabolism. *Blood, 115*(24), 5012-5022.

Kinsella, J. (1990). Sources of omega-3 fatty acids in human diets. *Omega-3-Fatty Aicds in Health Disease*, 157-200.

Kitazawa, H., Miyamoto, Y., Shimamura, K., Nagumo, A., & Tokita, S. (2009). Development of a High-Density Assay for Long-Chain Fatty Acyl-CoA Elongases. *Lipids, 44*(8), 765-773.

Knight, W. E., Cao, Y., Lin, Y.-H., Chi, C., Bai, B., Sparagna, G. C., Zhao, Y., Du, Y., Londono, P., Reisz, J. A., Brown, B. C., Taylor, M. R. G., Ambardekar, A. V., Cleveland, J. C., McKinsey, T. A., Jeong, M. Y., Walker, L. A., Woulfe, K. C., D'Alessandro, A., Chatfield, K. C., Xu, H., Bristow, M. R., Buttrick, P. M., & Song, K. (2021). Maturation of Pluripotent Stem Cell-Derived Cardiomyocytes Enables Modeling of Human Hypertrophic Cardiomyopathy. *Stem Cell Reports, 16*(3), 519-533.

Kobayashi, H., & Kikyo, N. (2015). Epigenetic regulation of open chromatin in pluripotent stem cells. *Translational Research, 165*(1), 18-27.

Kojima, H., Hirata, M., Kudo, Y., Kikuchi, K., & Nagano, T. (2001). Visualization of oxygen-concentration-dependent production of nitric oxide in rat hippocampal slices during aglycemia. *Journal of Neurochemistry, 76*(5), 1404-1410.

Kolte, D., McClung, J. A., & Aronow, W. S. (2016). Vasculogenesis and angiogenesis. In *Translational Research in Coronary Artery Disease* (pp. 49-65): Elsevier.

Kota, B. P., Huang, T. H.-W., & Roufogalis, B. D. (2005). An overview on biological mechanisms of PPARs. *Pharmacological Research, 51*(2), 85-94.

Kraft, C., LeMoine, C., Lyons, C., Michaud, D., Mueller, C., & Moyes, C. (2006). Control of mitochondrial biogenesis during myogenesis. *American Journal of Physiology-Cell Physiology, 290*(4), C1119-C1127.

Krey, G., Braissant, O., L'Horset, F., Kalkhoven, E., Perroud, M., Parker, M. G., & Wahli, W. (1997). Fatty acids, eicosanoids, and hypolipidemic agents identified as ligands of peroxisome proliferator-activated receptors by coactivator-dependent receptor ligand assay. *Molecular Endocrinology, 11*(6), 779-791.

Kuda, O., Pietka, T. A., Demianova, Z., Kudova, E., Cvacka, J., Kopecky, J., & Abumrad, N. A. (2013). Sulfo-N-succinimidyl oleate (SSO) inhibits fatty acid uptake and signaling for intracellular calcium via binding CD36 lysine 164: SSO also inhibits oxidized low density lipoprotein uptake by macrophages. *Journal of Biological Chemistry, 288*(22), 15547-15555.

Kurland, J., Broxmeyer, H., Pelus, L., Bockman, R., & Moore, M. (1978). Role for monocyte-macrophage-derived colony-stimulating factor and. *Blood, 52*(2), 388-407.

Lakatos, D., Travis, E. D., Pierson, K. E., Vivian, J. L., & Czirok, A. (2014). Autocrine FGF feedback can establish distinct states of Nanog expression in pluripotent stem cells: a computational analysis. *BMC systems biology, 8*(1), 112.

Lawson, L. D., & Hughes, B. G. (1988). Triacylglycerol structure of plant and fungal oils containing ψ-linolenic acid. *Lipids, 23*(4), 313-317.

Lee, J.-E., Cho, K. E., Lee, K. E., Kim, J., & Bae, Y. S. (2014). Nox4-mediated cell signaling regulates differentiation and survival of neural crest stem cells. *Molecules Cells, 37*(12), 907-911.

Lee, M.-C., Park, J. C., Yoon, D.-S., Choi, H., Kim, H.-J., Shin, K.-H., Hagiwara, A., Han, J., Park, H. G., & Lee, J.-S. (2019). Genome-wide characterization and expression of the elongation of very long chain fatty acid genes (Elovl) and fatty acid profiles in the alga (Tetraselmis suecica) fed marine rotifer Brachionus koreanus. *Comparative Biochemistry and Physiology Part D: Genomics and Proteomics, 30*, 179-185.

Lee, M. Y., Lee, Y. J., Kim, Y. H., Lee, S. H., Park, J. H., Kim, M. O., Suh, H. N., Ryu, J. M., Yun, S. P., & Jang, M. W. (2009). Role of peroxisome proliferator-activated receptor (PPAR) δ in embryonic stem cell proliferation. *International Journal of Stem Cells, 2*(1), 28-34.

Leifert, W. R., McMurchie, E. J., & Saint, D. A. (1999). Inhibition of cardiac sodium currents in adult rat myocytes by n-3 polyunsaturated fatty acids. *The Journal of Physiology, 520*(3), 671-679.

Leonard, A. E., Bobik, E. G., Dorado, J., Kroeger, P. E., Chuang, L. T., Thurmond, J. M., Parker-Barnes, J. M., Das, T., Huang, Y. S., & Mukerji, P. (2000). Cloning of a human cDNA encoding a novel enzyme involved in the elongation of long-chain polyunsaturated fatty acids. *Biochemical Journal, 350 Pt 3*(3), 765-770.

Levental, K. R., Surma, M. A., Skinkle, A. D., Lorent, J. H., Zhou, Y., Klose, C., Chang, J. T., Hancock, J. F., & Levental, I. (2017). ω-3 polyunsaturated fatty acids direct differentiation of the membrane phenotype in mesenchymal stem cells to potentiate osteogenesis. *Science Advances, 3*(11), eaao1193.

Lewandowski, J. P., Sheehan, K. B., Bennett Jr, P. E., & Boswell, R. E. (2010). Mago Nashi, Tsunagi/Y14, and Ranshi form a complex that influences oocyte differentiation in Drosophila melanogaster. *Developmental Biology, 339*(2), 307-319.

Li, J., Stouffs, M., Serrander, L., Banfi, B., Bettiol, E., Charnay, Y., Steger, K., Krause, K.-H., & Jaconi, M. E. (2006). The NADPH oxidase NOX4 drives cardiac differentiation: role in regulating cardiac transcription factors and MAP kinase activation. *Molecular Biology of the Cell, 17*(9), 3978-3988.

Liin, S. I., Yazdi, S., Ramentol, R., Barro-Soria, R., & Larsson, H. P. (2018). Mechanisms underlying the dual effect of polyunsaturated fatty acid analogs on Kv7. 1. *Cell Reports, 24*(11), 2908-2918.

Liss, K. H., & Finck, B. N. (2017). PPARs and nonalcoholic fatty liver disease. *Biochimie, 136*, 65-74.

Liu, J., Chen, L., Tao, X., & Tang, K. (2013). Phosphoinositide 3-kinase/Akt signaling is essential for prostaglandin E2-induced osteogenic differentiation of rat tendon stem cells. *Biochemical and Biophysical Research Communications, 435*(4), 514-519.

Llames, S., García-Pérez, E., Meana, A., Larcher, F., & del Río, M. (2015). Feeder layer cell actions and applications. *Tissue Engineering Part B: Reviews, 21*(4), 345-353.

Long, Y. C., & Zierath, J. R. (2006). AMP-activated protein kinase signaling in metabolic regulation. *The Journal of Clinical Investigation, 116*(7), 1776-1783.

Lopaschuk, G. D., Ussher, J. R., Folmes, C. D., Jaswal, J. S., & Stanley, W. C. (2010). Myocardial fatty acid metabolism in health and disease. *Physiological Reviews, 90*(1), 207-258.

Lowry, O. H., Rosebrough, N. J., Farr, A. L., & Randall, R. J. (1951). Protein measurement with the Folin phenol reagent. *Journal of Biological Chemistry, 193*(1), 265-275.

Luiken, J. J., Chanda, D., Nabben, M., Neumann, D., & Glatz, J. F. (2016). Post-translational modifications of CD36 (SR-B2): Implications for regulation of myocellular fatty acid uptake. *Biochimica et Biophysica Acta -Molecular Basis of Disease, 1862*(12), 2253-2258.

Lundberg, J. O., & Weitzberg, E. (2009). NO generation from inorganic nitrate and nitrite: Role in physiology, nutrition and therapeutics. *Archives of Pharmacal Research, 32*(8), 1119-1126.

Lyons, C. L., & Roche, H. M. (2018). Nutritional modulation of AMPK-impact upon metabolic-inflammation. *International Journal of Molecular Sciences, 19*(10), 3092.

Ma, Y., Yang, F., Wang, Y., Du, Z., Liu, D., Guo, H., Shen, J., & Peng, H. (2012). CaMKKβ is involved in AMP-activated protein kinase activation by baicalin in LKB1 deficient cell lines. *PLos One, 7*(10), e47900.

Madonna, R., Van Laake, L. W., Botker, H. E., Davidson, S. M., De Caterina, R., Engel, F. B., Eschenhagen, T., Fernandez-Aviles, F., Hausenloy, D. J., Hulot, J. S., Lecour, S., Leor, J., Menasche, P., Pesce, M., Perrino, C., Prunier, F., Van Linthout, S., Ytrehus, K., Zimmermann, W. H., Ferdinandy, P., & Sluijter, J. P. G. (2019). ESC Working Group on Cellular Biology of the Heart: position paper for Cardiovascular Research: tissue engineering strategies combined with cell therapies for cardiac repair in ischaemic heart disease and heart failure. *Cardiovascular Research, 115*(3), 488-500.

Mahmoudi, R., Ghareghani, M., Zibara, K., Ardakani, M. T., Jand, Y., Azari, H., Nikbakht, J., & Ghanbari, A. (2019). Alyssum homolocarpum seed oil (AHSO), containing natural alpha linolenic acid, stearic acid, myristic acid and β-sitosterol, increases proliferation and differentiation of neural stem cells in vitro. *BMC Complementary and Alternative Medicine, 19*(1), 1-11.

Majo, F., Rochat, A., Nicolas, M., Jaoudé, G. A., & Barrandon, Y. (2008). Oligopotent stem cells are distributed throughout the mammalian ocular surface. *Nature, 456*(7219), 250.

Makinde, A.-O., Kantor, P. F., & Lopaschuk, G. D. (1998). Maturation of fatty acid and carbohydrate metabolism in the newborn heart. In *Molecular and Cellular Effects of Nutrition on Disease Processes* (pp. 49-56): Springer.

Malaguti, M., Nistor, P. A., Blin, G., Pegg, A., Zhou, X., & Lowell, S. (2013). Bone morphogenic protein signalling suppresses differentiation of pluripotent cells by maintaining expression of E-Cadherin. *Elife, 2*, e01197.

Malandraki-Miller, S., Lopez, C. A., Al-Siddiqi, H., & Carr, C. A. (2018). Changing Metabolism in Differentiating Cardiac Progenitor Cells—Can Stem Cells Become Metabolically Flexible Cardiomyocytes? *Frontiers in Cardiovascular Medicine, 5*, 119.

Mao, Y., Varoglu, M., & Sherman, D. H. (1999). Molecular characterization and analysis of the biosynthetic gene cluster for the antitumor antibiotic mitomycin C from Streptomyces lavendulae NRRL 2564. *Chemistry & Biology, 6*(4), 251-263.

Marletta, M. A. (1994). Nitric oxide synthase: aspects concerning structure and catalysis. *Cell, 78*(6), 927-930.

Marvin, M. J., Di Rocco, G., Gardiner, A., Bush, S. M., & Lassar, A. B. (2001). Inhibition of Wnt activity induces heart formation from posterior mesoderm. *Genes Development, 15*(3), 316-327.

Marx, N., Libby, P., & Plutzky, J. (2001). Peroxisome proliferator-activated receptors (PPARs) and their role in the vessel wall: possible mediators of cardiovascular risk? *Journal of Cardiovascular Risk, 8*(4), 203-210.

Mascheck, L., Sharifpanah, F., Tsang, S. Y., Wartenberg, M., & Sauer, H. (2015). Stimulation of cardiomyogenesis from mouse embryonic stem cells by nuclear translocation of cardiotrophin-1. *International Journal of Cardiology, 193*, 23-33.

Mazrouei, S., Sharifpanah, F., Bekhite, M., Figulla, H., Sauer, H., & Wartenberg, M. (2015). Cardiomyogenesis of embryonic stem cells upon purinergic receptor activation by ADP and ATP. *Purinergic Signalling, 11*(4), 491-506.

Mena, J., Manosalva, C., Ramirez, R., Chandia, L., Carroza, D., Loaiza, A., Burgos, R. A., & Hidalgo, M. A. (2013). Linoleic acid increases adhesion, chemotaxis, granule release, intracellular calcium mobilisation, MAPK phosphorylation and gene expression in bovine neutrophils. *Veterinary Immunology and Immunopathology, 151*(3-4), 275-284.

Mobraten, K., Haug, T. M., Kleiveland, C. R., & Lea, T. (2013). Omega-3 and omega-6 PUFAs induce the same GPR120-mediated signalling events, but with different kinetics and intensity in Caco-2 cells. *Lipids in Health and Disease, 12*(1), 101.

Moon, Y.-A., Shah, N. A., Mohapatra, S., Warrington, J. A., & Horton, J. D. (2001). Identification of a mammalian long chain fatty acyl elongase regulated by sterol regulatory element-binding proteins. *Journal of Biological Chemistry, 276*(48), 45358-45366.

Mora-Castilla, S., Tejedo, J., Hmadcha, A., Cahuana, G. M., Martín, F., Soria, B., & Bedoya, F. (2010). Nitric oxide repression of Nanog promotes mouse embryonic stem cell differentiation. *Cell Death & Differentiation, 17*(6), 1025-1033.

Morey, L., Santanach, A., & Di Croce, L. (2015). Pluripotency and epigenetic factors in mouse embryonic stem cell fate regulation. *Molecular Cellular Biology, 35*(16), 2716-2728.

Motomura, S., & Dexter, T. M. (1980). The effect of prostaglandin E1 on hemopoiesis in long-term bone marrow cultures. *Experimental Hematology, 8*(3), 298-303.

Murphy, M. P. (2009). How mitochondria produce reactive oxygen species. *Biochemical Journal, 417*(1), 1-13.

Murray, T. V., Smyrnias, I., Shah, A. M., & Brewer, A. C. (2013). NADPH oxidase 4 regulates cardiomyocyte differentiation via redox activation of c-Jun protein and

the cis-regulation of GATA-4 gene transcription. *Journal of Biological Chemistry, 288*(22), 15745-15759.

Nakamura, M. T., & Nara, T. Y. (2004). Structure, function, and dietary regulation of Δ6, Δ5, and Δ9 desaturases. *Annual Review of Nutrition, 24*, 345-376.

Nakamura, M. T., Yudell, B. E., & Loor, J. J. (2014). Regulation of energy metabolism by long-chain fatty acids. *Progress in Lipid Research, 53*, 124-144.

Nathan, C., & Cunningham-Bussel, A. (2013). Beyond oxidative stress: an immunologist's guide to reactive oxygen species. *Nature Reviews Immunology, 13*(5), 349-361.

Nicola, N. A., & Babon, J. J. (2015). Leukemia inhibitory factor (LIF). *Cytokine Growth Factor Reviews, 26*(5), 533-544.

Niwa, H. (2007). How is pluripotency determined and maintained? *Development, 134*(4), 635-646.

Oh, C.-S., Toke, D. A., Mandala, S., & Martin, C. E. (1997). ELO2 and ELO3, Homologues of theSaccharomyces cerevisiae ELO1 Gene, Function in Fatty Acid Elongation and Are Required for Sphingolipid Formation. *Journal of Biological Chemistry, 272*(28), 17376-17384.

Okada, T., Morino, K., Nakagawa, F., Tawa, M., Kondo, K., Sekine, O., Imamura, T., Okamura, T., Ugi, S., & Maegawa, H. (2017). N-3 Polyunsaturated Fatty Acids Decrease the Protein Expression of Soluble Epoxide Hydrolase via Oxidative Stress-Induced P38 Kinase in Rat Endothelial Cells. *Nutrients, 9*(7), 654.

Okuda, Y., Ezure, M., Tsukahara, K., Sawada, T., Mizutani, M., Katori, T., Bannai, C., & Yamashita, K. (1994). Eicosapentaenoic Acid Enhances Intracellular Free Calcium in Cultured Human EndothelialCells. *Biochemical Medicine and Metabolic Biology, 51*(2), 166-168.

Okuda, Y., Kawashima, K., Sawada, T., Tsurumaru, K., Asano, M., Suzuki, S., Soma, M., Nakajima, T., & Yamashita, K. (1997). Eicosapentaenoic acid enhances nitric oxide production by cultured human endothelial cells. *Biochemical and Biophysical Research Communications, 232*(2), 487-491.

Omura, M., Kobayashi, S., Mizukami, Y., Mogami, K., Todoroki-Ikeda, N., Miyake, T., & Matsuzaki, M. (2001). Eicosapentaenoic acid (EPA) induces Ca^{2+}-independent activation and translocation of endothelial nitric oxide synthase and endothelium-dependent vasorelaxation. *FEBS Letters, 487*(3), 361-366.

Oner, T., Ozdemir, R., Doksöz, O., Genc, D. B., Guven, B., Demirpence, S., Yilmazer, M. M., Yozgat, Y., Mese, T., & Tavli, V. (2018). Cardiac function in children with premature ventricular contractions: the effect of omega-3 polyunsaturated fatty acid supplementation. *Cardiology in the Young, 28*(7), 949-954.

Owusu-Ansah, E., & Banerjee, U. (2009). Reactive oxygen species prime Drosophila haematopoietic progenitors for differentiation. *Nature, 461*(7263), 537-541.

Padmasekar, M., Sharifpanah, F., Finkensieper, A., Wartenberg, M., & Sauer, H. (2011). Stimulation of cardiomyogenesis of embryonic stem cells by nitric oxide downstream of AMP-activated protein kinase and mTOR signaling pathways. *Stem Cells Development, 20*(12), 2163-2175.

Papatsenko, D., Waghray, A., & Lemischka, I. R. (2018). Feedback control of pluripotency in embryonic stem cells: Signaling, transcription and epigenetics. *Stem Cell Research & Therapy, 29*, 180-188.

Park, M., & Yoon, Y.-s. (2018). Cardiac regeneration with human pluripotent stem cell-derived cardiomyocytes. *Korean Circulation Journal, 48*(11), 974-988.

Park, Y.-G., Lee, S.-E., Kim, E.-Y., Hyun, H., Shin, M.-Y., Son, Y.-J., Kim, S.-Y., & Park, S.-P. (2015). Effects of feeder cell types on culture of mouse embryonic stem cell in vitro. *Development Reproduction, 19*(3), 119-126.

Pawlak, M., Lefebvre, P., & Staels, B. (2015). Molecular mechanism of PPARα action and its impact on lipid metabolism, inflammation and fibrosis in non-alcoholic fatty liver disease. *Journal of Hepatology, 62*(3), 720-733.

Pelus, L. M., Broxmeyer, H. E., Kurland, J. I., & Moore, M. A. (1979). Regulation of macrophage and granulocyte proliferation. Specificities of prostaglandin E and lactoferrin. *The Journal of Experimental Medicine, 150*(2), 277-292.

Pettersen, K., Monsen, V. T., Hakvag Pettersen, C. H., Overland, H. B., Pettersen, G., Samdal, H., Tesfahun, A. N., Lundemo, A. G., Bjorkoy, G., & Schonberg, S. A. (2016). DHA-induced stress response in human colon cancer cells - Focus on oxidative stress and autophagy. *Free Radical Biology and Medicine, 90*, 158-172.

Pietka, T. A., Sulkin, M. S., Kuda, O., Wang, W., Zhou, D., Yamada, K. A., Yang, K., Su, X., Gross, R. W., Nerbonne, J. M., Efimov, I. R., & Abumrad, N. A. (2012). CD36 protein influences myocardial Ca^{2+} homeostasis and phospholipid metabolism: conduction anomalies in CD36-deficient mice during fasting. *Journal of Biological Chemistry, 287*(46), 38901-38912.

Platt, D. H., Bartoli, M., El-Remessy, A. B., Al-Shabrawey, M., Lemtalsi, T., Fulton, D., & Caldwell, R. B. (2005). Peroxynitrite increases VEGF expression in vascular endothelial cells via STAT3. *Free Radical Biology and Medicine, 39*(10), 1353-1361.

Poon, E., Keung, W., Liang, Y., Ramalingam, R., Yan, B., Zhang, S., Chopra, A., Moore, J., Herren, A., Lieu, D. K., Wong, H. S., Weng, Z., Wong, O. T., Lam, Y. W., Tomaselli, G. F., Chen, C., Boheler, K. R., & Li, R. A. (2015). Proteomic Analysis of Human Pluripotent Stem Cell-Derived, Fetal, and Adult Ventricular Cardiomyocytes Reveals Pathways Crucial for Cardiac Metabolism and Maturation. *Circulation: Cardiovascular Genetics, 8*(3), 427-436.

PrabhuDas, M., Bowdish, D., Drickamer, K., Febbraio, M., Herz, J., Kobzik, L., Krieger, M., Loike, J., Means, T. K., Moestrup, S. K., Post, S., Sawamura, T., Silverstein, S., Wang, X.-Y., & El Khoury, J. (2014). Standardizing Scavenger Receptor Nomenclature. *The Journal of Immunology, 192*(5), 1997-2006.

Prakash, R., Somanath, P. R., El-Remessy, A. B., Kelly-Cobbs, A., Stern, J. E., Dore-Duffy, P., Johnson, M., Fagan, S. C., & Ergul, A. (2012). Enhanced cerebral but not peripheral angiogenesis in the Goto-Kakizaki model of type 2 diabetes involves VEGF and peroxynitrite signaling. *Diabetes, 61*(6), 1533-1542.

Quintana, A., & Grosveld, G. (2011). Zebrafish as a model to characterize TEL2 function during development and cancer. *Journal of Carcinogenesis & Mutagenesis*(S1), 1.

Quintero, M., Colombo, S. L., Godfrey, A., & Moncada, S. (2006). Mitochondria as signaling organelles in the vascular endothelium. *Proceedings of the National Academy of Sciences, 103*(14), 5379-5384.

Rajabzadeh, N., Fathi, E., & Farahzadi, R. (2019). Stem cell-based regenerative medicine. *Stem Cell Investigation, 6*, 19.

Rajala, K., Pekkanen-Mattila, M., & Aalto-Setälä, K. (2011). Cardiac differentiation of pluripotent stem cells. *Stem Cells International, 2011*, 383709.

Rajasingh, J., & Bright, J. J. (2006). 15-Deoxy-Δ12, 14-Prostaglandin J2 regulates leukemia inhibitory factor signaling through JAK-STAT pathway in mouse embryonic stem cells. *Experimental Cell Research, 312*(13), 2538-2546.

Ratajczak, M. Z., Bujko, K., Mack, A., Kucia, M., & Ratajczak, J. (2018). Cancer from the perspective of stem cells and misappropriated tissue regeneration mechanisms. *Leukemia, 32*(12), 2519-2526.

Rimm, E. B., Appel, L. J., Chiuve, S. E., Djousse, L., Engler, M. B., Kris-Etherton, P. M., Mozaffarian, D., Siscovick, D. S., Lichtenstein, A. H., American Heart Association Nutrition Committee of the Council on, L., Cardiometabolic, H., Council on, E., Prevention, Council on Cardiovascular Disease in the, Y., Council on, C., Stroke, N., & Council on Clinical, C. (2018). Seafood Long-Chain n-3 Polyunsaturated Fatty Acids and Cardiovascular Disease: A Science Advisory From the American Heart Association. *Circulation, 138*(1), e35-e47.

Risau, W. (1997). Mechanisms of angiogenesis. *Nature, 386*(6626), 671-674.

Risau, W., & Flamme, I. (1995). Vasculogenesis. *Annual Review of Cell and Developmental Biology, 11*(1), 73-91.

Risha, M. A., Siengdee, P., Dannenberger, D., Wimmers, K., & Ponsuksili, S. (2021). PUFA Treatment Affects C2C12 Myocyte Differentiation, Myogenesis Related Genes and Energy Metabolism. *Genes, 12*(2), 192.

Robertson, E., Bradley, A., Kuehn, M., & Evans, M. (1986). Germ-line transmission of genes introduced into cultured pluripotential cells by retroviral vector. *Nature, 323*(6087), 445.

Rochette, L., Lorin, J., Zeller, M., Guilland, J.-C., Lorgis, L., Cottin, Y., & Vergely, C. (2013). Nitric oxide synthase inhibition and oxidative stress in cardiovascular diseases: possible therapeutic targets? *Pharmacology Therapeutics, 140*(3), 239-257.

Roy, K., Wu, Y., Meitzler, J. L., Juhasz, A., Liu, H., Jiang, G., Lu, J., Antony, S., & Doroshow, J. H. (2015). NADPH oxidases and cancer. *Clinical Science, 128*(12), 863-875.

Rustan, A. C., & Drevon, C. A. (2001). Fatty acids: structures and properties. *In: Encyclopedia of Life Sciences. Nature Publishing, London.*

Sachinidis, A., Fleischmann, B. K., Kolossov, E., Wartenberg, M., Sauer, H., & Hescheler, J. (2003). Cardiac specific differentiation of mouse embryonic stem cells. *Cardiovascular Research, 58*(2), 278-291.

Sakamoto, T., Cansev, M., & Wurtman, R. J. (2007). Oral supplementation with docosahexaenoic acid and uridine-5′-monophosphate increases dendritic spine density in adult gerbil hippocampus. *Brain Research, 1182*, 50-59.

Samovski, D., Sun, J., Pietka, T., Gross, R. W., Eckel, R. H., Su, X., Stahl, P. D., & Abumrad, N. A. (2015). Regulation of AMPK activation by CD36 links fatty acid uptake to β-oxidation. *Diabetes, 64*(2), 353-359.

Sandalio, L. M., Rodríguez-Serrano, M., Romero-Puertas, M. C., & del Río, L. A. (2013). Role of peroxisomes as a source of reactive oxygen species (ROS) signaling molecules. In L. A. del Río (Ed.), *Peroxisomes and their Key Role in Cellular*

Signaling and Metabolism (Vol. 69, pp. 231-255). Dordrecht: Springer Netherlands.

Sander, P. R., Hau, P., Koch, S., Schütze, K., Bogdahn, U., Kalbitzer, H. R., & Aigner, L. (2013). Stem cell metabolic and spectroscopic profiling. *Trends in Biotechnology, 31*(3), 204-213.

Sasaki, T., Kitagawa, K., Sugiura, S., Omura-Matsuoka, E., Tanaka, S., Yagita, Y., Okano, H., Matsumoto, M., & Hori, M. (2003). Implication of cyclooxygenase-2 on enhanced proliferation of neural progenitor cells in the adult mouse hippocampus after ischemia. *Journal of Neuroscience Research, 72*(4), 461-471.

Sauer, H., Neukirchen, W., Rahimi, G., Grünbeck, F., Hescheler, J., & Wartenberg, M. (2004). Involvement of reactive oxygen species in cardiotropin-1 (CT-1)-induced cell proliferation of cardiomyocytes differentiated from murine embryonic stem cells. *Experimental Cell Research, 294*(2), 313-324.

Sauer, H., Rahimi, G., Hescheler, J., & Wartenberg, M. (2000). Role of reactive oxygen species and phosphatidylinositol 3-kinase in cardiomyocyte differentiation of embryonic stem cells. *FEBS Letters, 476*(3), 218-223.

Sauer, H., & Wartenberg, M. (2005). Reactive oxygen species as signaling molecules in cardiovascular differentiation of embryonic stem cells and tumor-induced angiogenesis. *Antioxidants Redox Signaling, 7*(11-12), 1423-1434.

Sauer, H., Wartenberg, M., & Hescheler, J. (2001). Reactive oxygen species as intracellular messengers during cell growth and differentiation. *Cellular Physiology and Biochemistry, 11*(4), 173-186.

Schmelter, M., Ateghang, B., Helmig, S., Wartenberg, M., & Sauer, H. (2006). Embryonic stem cells utilize reactive oxygen species as transducers of mechanical strain-induced cardiovascular differentiation. *The FASEB Journal, 20*(8), 1182-1184.

Shabani, P., Ghazizadeh, Z., Gorgani-Firuzjaee, S., Molazem, M., Rajabi, S., Vahdat, S., Azizi, Y., Doosti, M., Aghdami, N., & Baharvand, H. (2019). Cardioprotective effects of omega-3 fatty acids and ascorbic acid improve regenerative capacity of embryonic stem cell-derived cardiac lineage cells. *BioFactors, 45*(3), 427-438.

Shabani, P., Ghazizadeh, Z., Pahlavan, S., Hashemizadeh, S., Baharvand, H., Aghdami, N., & Doosti, M. (2015). Exogenous treatment with eicosapentaenoic acid supports maturation of cardiomyocytes derived from embryonic stem cells. *Biochemical Biophysical Research Communications, 461*(2), 281-286.

Shackelford, D. B., & Shaw, R. J. (2009). The LKB1-AMPK pathway: metabolism and growth control in tumour suppression. *Nature Reviews Cancer, 9*(8), 563-575.

Shah, S., & Cox, A. G. (2009). Article Commentary: A Role for IR-β in the Free Fatty Acid Mediated Development of Hepatic Insulin Resistance? *Biochemistry Insights, 2*, BCI. S2996.

Shamblott, M. J., Axelman, J., Wang, S., Bugg, E. M., Littlefield, J. W., Donovan, P. J., Blumenthal, P. D., Huggins, G. R., & Gearhart, J. D. (1998). Derivation of pluripotent stem cells from cultured human primordial germ cells. *Proceedings of the National Academy of Sciences, 95*(23), 13726-13731.

Sharifpanah, F., Ali, E. H., Wartenberg, M., & Sauer, H. (2019). The milk thistle (Silybum marianum) compound Silibinin stimulates leukopoiesis from mouse embryonic stem cells. *Phytotherapy Research, 33*(2), 452-460.

Sharifpanah, F., Behr, S., Wartenberg, M., & Sauer, H. (2016). Mechanical strain stimulates vasculogenesis and expression of angiogenesis guidance molecules of embryonic stem cells through elevation of intracellular calcium, reactive oxygen species and nitric oxide generation. *Biochimica et Biophysica Acta -Molecular Cell Research, 1863*(12), 3096-3105.

Sharifpanah, F., Wartenberg, M., Hannig, M., Piper, H. M., & Sauer, H. (2008). Peroxisome proliferator-activated receptor alpha agonists enhance cardiomyogenesis of mouse ES cells by utilization of a reactive oxygen species-dependent mechanism. *Stem Cells, 26*(1), 64-71.

Shen, N., Knopf, A., Westendorf, C., Kraushaar, U., Riedl, J., Bauer, H., Poschel, S., Layland, S. L., Holeiter, M., Knolle, S., Brauchle, E., Nsair, A., Hinderer, S., & Schenke-Layland, K. (2017). Steps toward Maturation of Embryonic Stem Cell-Derived Cardiomyocytes by Defined Physical Signals. *Stem Cell Reports, 9*(1), 122-135.

Shireman, R. (2003). Essential fatty acids. In B. Caballero (Ed.), *Encyclopedia of Food Sciences and Nutrition (Second Edition)* (pp. 2169-2176). Oxford: Academic Press.

Skonieczna, M., Hejmo, T., Poterala-Hejmo, A., Cieslar-Pobuda, A., & Buldak, R. J. (2017). NADPH oxidases: insights into selected functions and mechanisms of action in cancer and stem cells. *Oxidative Medicine Cellular Longevity, 2017*, 9420539.

Sokoła-Wysoczańska, E., Wysoczański, T., Wagner, J., Czyż, K., Bodkowski, R., Lochyński, S., & Patkowska-Sokoła, B. (2018). Polyunsaturated fatty acids and their potential therapeutic role in cardiovascular system disorders—A review. *Nutrients, 10*(10), 1561.

Stapleton, D., Mitchelhill, K. I., Gao, G., Widmer, J., Michell, B. J., Teh, T., House, C. M., Fernandez, C. S., Cox, T., Witters, L. A., & Kemp, B. E. (1996). Mammalian AMP-activated protein kinase subfamily. *Journal of Biological Chemistry, 271*(2), 611-614.

Steinbusch, L. K., Schwenk, R. W., Ouwens, D. M., Diamant, M., Glatz, J. F., & Luiken, J. J. (2011). Subcellular trafficking of the substrate transporters GLUT4 and CD36 in cardiomyocytes. *Cellular and Molecular Life Sciences, 68*(15), 2525-2538.

Stratman, A. N., Malotte, K. M., Mahan, R. D., Davis, M. J., & Davis, G. E. (2009). Pericyte recruitment during vasculogenic tube assembly stimulates endothelial basement membrane matrix formation. *Blood, 114*(24), 5091-5101.

Sun, S., Liu, Y., Lipsky, S., & Cho, M. (2007). Physical manipulation of calcium oscillations facilitates osteodifferentiation of human mesenchymal stem cells. *The FASEB Journal, 21*(7), 1472-1480.

Sweeney, M., & Foldes, G. (2018). It takes two: Endothelial-perivascular cell cross-talk in vascular development and disease. *Frontiers in Cardiovascular Medicine, 5*, 154.

Taha, A., Sharifpanah, F., Wartenberg, M., & Sauer, H. (2020). Omega-3 and Omega-6 polyunsaturated fatty acids stimulate vascular differentiation of mouse embryonic stem cells. *Journal of Cellular Physiology, 235*(10), 7094-7106.

Tahara, E. B., Navarete, F. D., & Kowaltowski, A. J. (2009). Tissue-, substrate-, and site-specific characteristics of mitochondrial reactive oxygen species generation. *Free Radical Biology Medicine, 46*(9), 1283-1297.

Tai, C.-I., & Ying, Q.-L. (2013). Gbx2, a LIF/Stat3 target, promotes reprogramming to and retention of the pluripotent ground state. *Journal of Cell Science, 126*(5), 1093-1098.

Takahashi, K., & Yamanaka, S. (2006). Induction of pluripotent stem cells from mouse embryonic and adult fibroblast cultures by defined factors. *Cell, 126*(4), 663-676.

Tamura, K., Makino, A., Hullin-Matsuda, F., Kobayashi, T., Furihata, M., Chung, S., Ashida, S., Miki, T., Fujioka, T., & Shuin, T. (2009). Novel lipogenic enzyme ELOVL7 is involved in prostate cancer growth through saturated long-chain fatty acid metabolism. *Cancer Research, 69*(20), 8133-8140.

Tejedo, J., Tapia-Limonchi, R., Mora-Castilla, S., Cahuana, G., Hmadcha, A., Martin, F., Bedoya, F., & Soria, B. (2010). Low concentrations of nitric oxide delay the differentiation of embryonic stem cells and promote their survival. *Cell Death & Disease, 1*(10), e80-e80.

Tejedo, J. R., Cahuana, G. M., Bedoya, F. J., & Tapia-Limonchi, R. (2012). Embryonic Stem Cells: The Role of Nitric Oxide in Regulating Cell Differentiation, Self-Renewal, and Apoptosis. In *Stem Cells and Cancer Stem Cells* (Vol. 3, pp. 359-369): Springer, Dordrecht.

Thomas, D. D., Ridnour, L. A., Isenberg, J. S., Flores-Santana, W., Switzer, C. H., Donzelli, S., Hussain, P., Vecoli, C., Paolocci, N., Ambs, S., Colton, C. A., Harris, C. C., Roberts, D. D., & Wink, D. A. (2008). The chemical biology of nitric oxide: implications in cellular signaling. *Free Radical Biology Medicine, 45*(1), 18-31.

Thompson, E., Eldstrom, J., & Fedida, D. (2021). Hormonal Signaling Actions on Kv7.1 (KCNQ1) Channels. *Annual Review of Pharmacology and Toxicology, 61*(1), 381-400.

Thomson, J. A., Itskovitz-Eldor, J., Shapiro, S. S., Waknitz, M. A., Swiergiel, J. J., Marshall, V. S., & Jones, J. M. (1998). Embryonic stem cell lines derived from human blastocysts. *Science, 282*(5391), 1145-1147.

Thornton, C., Snowden, M. A., & Carling, D. (1998). Identification of a novel AMP-activated protein kinase β subunit isoform that is highly expressed in skeletal muscle. *Journal of Biological Chemistry, 273*(20), 12443-12450.

Tonelli, F. M., Santos, A. K., Gomes, D. A., da Silva, S. L., Gomes, K. N., Ladeira, L. O., & Resende, R. R. (2012). Stem cells and calcium signaling. *Calcium Signaling, 740*, 891-916.

Tumelty, J., Scholfield, N., Stewart, M., Curtis, T., & McGeown, G. (2007). Ca^{2+}-sparks constitute elementary building blocks for global Ca^{2+}-signals in myocytes of retinal arterioles. *Cell Calcium, 41*(5), 451-466.

Tvrdik, P., Westerberg, R., Silve, S., Asadi, A., Jakobsson, A., Cannon, B., Loison, G., & Jacobsson, A. (2000). Role of a new mammalian gene family in the biosynthesis of very long chain fatty acids and sphingolipids. *The Journal of Cell Biology, 149*(3), 707-718.

Ulmer, B. M., Stoehr, A., Schulze, M. L., Patel, S., Gucek, M., Mannhardt, I., Funcke, S., Murphy, E., Eschenhagen, T., & Hansen, A. (2018). Contractile work contributes to maturation of energy metabolism in hiPSC-derived cardiomyocytes. *Stem Cell Reports, 10*(3), 834-847.

Van Oosten, A. L., Costa, Y., Smith, A., & Silva, J. C. (2012). JAK/STAT3 signalling is sufficient and dominant over antagonistic cues for the establishment of naive pluripotency. *Nature Communications, 3*, 817.

Vanhoutte, P. M., Zhao, Y., Xu, A., & Leung, S. W. (2016). Thirty Years of Saying NO: Sources, Fate, Actions, and Misfortunes of the Endothelium-Derived Vasodilator Mediator. *Circulation Research, 119*(2), 375-396.

Verweij, J., & Pinedo, H. M. (1990). Mitomycin C: mechanism of action, usefulness and limitations. *Anticancer Drugs, 1*(1), 5-13.

Wada, K., Arita, M., Nakajima, A., Katayama, K., Kudo, C., Kamisaki, Y., & Serhan, C. N. (2006). Leukotriene B4 and lipoxin A4 are regulatory signals for neural stem cell proliferation and differentiation. *The FASEB Journal, 20*(11), 1785-1792.

Wallis, J. G., Watts, J. L., & Browse, J. (2002). Polyunsaturated fatty acid synthesis: what will they think of next? *Trends in Biochemical Sciences, 27*(9), 467-473.

Wang, S., Hannafon, B. N., Zhou, J., & Ding, W.-Q. (2013). Clofibrate induces heme oxygenase 1 expression through a PPARα-independent mechanism in human cancer cells. *Cellular Physiology and Biochemistry, 32*(5), 1255-1264.

Wang, Y., Botolin, D., Christian, B., Busik, J., Xu, J., & Jump, D. B. (2005). Tissue-specific, nutritional, and developmental regulation of rat fatty acid elongases. *Journal of Lipid Research, 46*(4), 706-715.

Wei, H., Juhasz, O., Li, J., Tarasova, Y. S., & Boheler, K. R. (2005). Embryonic stem cells and cardiomyocyte differentiation: phenotypic and molecular analyses. *Journal of Cellular Molecular Medicine, 9*(4), 804-817.

Weissman, I. L. (2000). Stem cells: units of development, units of regeneration, and units in evolution. *Cell, 100*(1), 157-168.

Westfall, M. V., Pasyk, K. A., Yule, D. I., Samuelson, L. C., & Metzger, J. M. (1997). Ultrastructure and cell-cell coupling of cardiac myocytes differentiating in embryonic stem cell cultures. *Cell Motility the Cytoskeleton, 36*(1), 43-54.

Willems, E., Bushway, P. J., & Mercola, M. (2009). Natural and synthetic regulators of embryonic stem cell cardiogenesis. *Pediatric Cardiology, 30*(5), 635-642.

Wo, Y. b., Zhu, D. y., Hu, Y., Wang, Z. Q., Liu, J., & Lou, Y. J. (2008). Reactive oxygen species involved in prenylflavonoids, icariin and icaritin, initiating cardiac differentiation of mouse embryonic stem cells. *Journal of Cellular Biochemistry, 103*(5), 1536-1550.

Wong, J. L., Créton, R., & Wessel, G. M. (2004). The oxidative burst at fertilization is dependent upon activation of the dual oxidase Udx1. *Developmental Cell, 7*(6), 801-814.

World Health Organization. (2014). Global health estimates: deaths by cause, age, sex and country, 2000-2012. In (Vol. 9). Geneva: World Health Organization.

Wu, K. C., Wong, K. L., Wang, M. L., Shiao, L. R., Leong, I. L., Gong, C. L., Cheng, K. S., Chan, P., & Leung, Y. M. (2018). Eicosapentaenoic acid triggers Ca 2+ release and Ca 2+ influx in mouse cerebral cortex endothelial bEND. 3 cells. *The Journal of Physiological Sciences, 68*(1), 33-41.

Wu, Y., Viana, M., Thirumangalathu, S., & Loeken, M. (2012). AMP-activated protein kinase mediates effects of oxidative stress on embryo gene expression in a mouse model of diabetic embryopathy. *Diabetologia, 55*(1), 245-254.

Xiao, Y.-F., Ke, Q., Wang, S.-Y., Auktor, K., Yang, Y., Wang, G. K., Morgan, J. P., & Leaf, A. (2001). Single point mutations affect fatty acid block of human myocardial sodium channel α subunit Na+ channels. *Proceedings of the National Academy of Sciences, 98*(6), 3606-3611.

Xu, H., Ang, Y.-S., Sevilla, A., Lemischka, I. R., & Ma'ayan, A. (2014). Construction and validation of a regulatory network for pluripotency and self-renewal of mouse embryonic stem cells. *PLos Computational Biology, 10*(8), e1003777.

Xu, H. E., Stanley, T. B., Montana, V. G., Lambert, M. H., Shearer, B. G., Cobb, J. E., McKee, D. D., Galardi, C. M., Plunket, K. D., & Nolte, R. T. (2002). Structural basis for antagonist-mediated recruitment of nuclear co-repressors by PPAR α. *Nature, 415*(6873), 813-817.

Xu, J., Xiao, G., Trujillo, C., Chang, V., Blanco, L., Joseph, S. B., Bassilian, S., Saad, M. F., Tontonoz, P., Lee, W. N., & Kurland, I. J. (2002). Peroxisome proliferator-activated receptor alpha (PPARalpha) influences substrate utilization for hepatic glucose production. *Journal of Biological Chemistry, 277*(52), 50237-50244.

Y Kots, A., Bian, K., & Murad, F. (2011). Nitric oxide and cyclic GMP signaling pathway as a focus for drug development. *Current Medicinal Chemistry, 18*(22), 3299-3305.

Yanes, O., Clark, J., Wong, D. M., Patti, G. J., Sanchez-Ruiz, A., Benton, H. P., Trauger, S. A., Desponts, C., Ding, S., & Siuzdak, G. (2010). Metabolic oxidation regulates embryonic stem cell differentiation. *Nature Chemical Biology, 6*(6), 411-417.

Yang, X., Pabon, L., & Murry, C. E. (2014). Engineering adolescence: maturation of human pluripotent stem cell–derived cardiomyocytes. *Circulation Research, 114*(3), 511-523.

Yang, X., Rodriguez, M. L., Leonard, A., Sun, L., Fischer, K. A., Wang, Y., Ritterhoff, J., Zhao, L., Kolwicz, S. C., Jr., Pabon, L., Reinecke, H., Sniadecki, N. J., Tian, R., Ruohola-Baker, H., Xu, H., & Murry, C. E. (2019). Fatty Acids Enhance the Maturation of Cardiomyocytes Derived from Human Pluripotent Stem Cells. *Stem Cell Reports, 13*(4), 657-668.

Yun, D. H., Song, H. Y., Lee, M. J., Kim, M. R., Kim, M. Y., Lee, J. S., & Kim, J. H. (2009). Thromboxane A 2 modulates migration, proliferation, and differentiation of adipose tissue-derived mesenchymal stem cells. *Experimental & Molecular Medicine, 41*(1), 17-24.

Yun, S., Lee, M., Ryu, J., & Han, H. (2009). Interaction between PGE 2 and EGF receptor through MAPKs in mouse embryonic stem cell proliferation. *Cellular and Molecular Life Sciences, 66*(9), 1603-1616.

Yun, S. P., Ryu, J. M., Jang, M. W., & Han, H. J. (2011). Interaction of profilin-1 and F-actin via a β-arrestin-1/JNK signaling pathway involved in prostaglandin E2-induced human mesenchymal stem cells migration and proliferation. *Journal of Cellular Physiology, 226*(2), 559-571.

Zajdel, A., Wilczok, A., Chodurek, E., Gruchlik, A., & Dzierzewicz, Z. (2013). Polyunsaturated fatty acids inhibit melanoma cell growth in vitro. *Acta Poloniae Pharmaceutica, 70*(2), 365-369.

Zajdel, A., Wilczok, A., & Tarkowski, M. (2015). Toxic effects of n-3 polyunsaturated fatty acids in human lung A549 cells. *Toxicol In Vitro, 30*(1 Pt B), 486-491.

Zakrzewski, W., Dobrzyński, M., Szymonowicz, M., & Rybak, Z. (2019). Stem cells: past, present, and future. *Stem Cell Research & Therapy, 10*(1), 68.

Zandbergen, F., & Plutzky, J. (2007). PPARα in atherosclerosis and inflammation. *Biochimica et Biophysica Acta-Molecular and Cell Biology of Lipids, 1771*(8), 972-982.

Zhang, H., Badur, M. G., Spiering, S., Divakaruni, A., Meurs, N. E., Michael, S. Y., Colas, A. R., Murphy, A. N., Mercola, M., & Metallo, C. M. (2020). Lipid availability influences the metabolic maturation of human pluripotent stem cell-derived cardiomyocytes. *bioRxiv*, 2020.2003.2014.991927.

Zhang, H., & Bradley, A. (1996). Mice deficient for BMP2 are nonviable and have defects in amnion/chorion and cardiac development. *Development, 122*(10), 2977-2986.

Zhao, Y., Wang, L., Qiu, J., Zha, D., Sun, Q., & Chen, C. (2013). Linoleic acid stimulates [Ca2+]i increase in rat pancreatic beta-cells through both membrane receptor- and intracellular metabolite-mediated pathways. *PLos One, 8*(4), e60255.

Zhou, D., Shao, L., & Spitz, D. R. (2014). Reactive oxygen species in normal and tumor stem cells. *Advances in Cancer Research, 122*, 1-67.

Zhu, Z., Fu, C., Li, X., Song, Y., Li, C., Zou, M., Guan, Y., & Zhu, Y. (2011). Prostaglandin E2 promotes endothelial differentiation from bone marrow-derived cells through AMPK activation. *PLos One, 6*(8).

Zmijewski, J. W., Banerjee, S., Bae, H., Friggeri, A., Lazarowski, E. R., & Abraham, E. (2010). Exposure to hydrogen peroxide induces oxidation and activation of AMP-activated protein kinase. *Journal of Biological Chemistry, 285*(43), 33154-33164.

Zuk, P. A., Zhu, M., Ashjian, P., De Ugarte, D. A., Huang, J. I., Mizuno, H., Alfonso, Z. C., Fraser, J. K., Benhaim, P., & Hedrick, M. H. (2002). Human adipose tissue is a source of multipotent stem cells. *Molecular Biology of the Cell, 13*(12), 4279-4295.

Publications

Parts of this thesis have been published in:

- **Taha, A.,** Sharifpanah, F., Wartenberg, M., & Sauer, H. (2020). Omega-3 and Omega-6 polyunsaturated fatty acids stimulate vascular differentiation of mouse embryonic stem cells. *Journal of Cellular Physiology* 235(10), 7094-7106. doi: 10.1002/jcp.29606.
- Ali, E. H., Sharifpanah, F., **Taha, A.,** Tsang, S. Y., Wartenberg, M., & Sauer, H. (2018). The Milk Thistle (Silybum marianum) Compound Silibinin Inhibits Cardiomyogenesis of Embryonic Stem Cells by Interfering with Angiotensin II Signaling. *Stem cells International* 2018:9215792. doi: 10.1155/2018/9215792.

Poster Presentations

- **Amer Taha, Fatemeh Sharifpanah, Maria Wartenberg & Heinrich Sauer.** Omega-6 and Omega-3 polyunsaturated fatty acids stimulate vascular differentiation of mouse embryonic stem cells. Excellence Cluster Cardio-Pulmonary System ECCPS Retreat 2016. Hotel Dolce Bad Nauheim 07th 08th Jul. 2016. Germany.

- **Amer Taha, Fatemeh Sharifpanah, Maria Wartenberg & Heinrich Sauer.** Omega-6 and Omega-3 polyunsaturated fatty acids stimulate vascular differentiation of mouse embryonic stem cells. Joint International Meeting in vascular Biology 26th - 28th Sept. 2016. Goethe University Hospital, Frankfurt. Germany.

- **Amer Taha, Fatemeh Sharifpanah, Yu-Han Huang, Maria Wartenberg & Heinrich Sauer.** Omega-6 and Omega-3 polyunsaturated fatty acids stimulate vasculogenesis and cardiomyogenesis of embryonic stem cells. The annual meeting of the German Physiology Society (DPG) 16th – 18th Mar. 2017. The University of Greifswald, Institute of Physiology, Greifswald. Germany.

- **Amer Taha, Fatemeh Sharifpanah, Yu-Han Huang, Maria Wartenberg & Heinrich Sauer.** Omega-6 and Omega-3 polyunsaturated fatty acids stimulate vasculogenesis and cardiomyogenesis of embryonic stem cells. ECCPS Symposium Poster Presentation-Area Cellular Plasticity and Heterogeneity 7th – 8th June 2017. Bad Nauheim, Germany.

Declaration

I declare that I have completed this dissertation single-handedly without the unauthorized help of a second party and only with the assistance acknowledged therein. I have appropriately acknowledged and referenced all text passages that are derived literally from or are based on the content of published or unpublished work of others, and all information that relates to verbal communications. I have abided by the principles of good scientific conduct laid down in the charter of the Justus Liebig University of Giessen in carrying out the investigations described in the dissertation.

Amer Hussein Taha

Ehrenwörtliche Erklärung

„Hiermit erkläre ich, dass ich die vorliegende Arbeit selbständig und ohne unzulässige Hilfe oder Benutzung anderer als der angegebenen Hilfsmittel angefertigt habe. Alle Textstellen, die wörtlich oder sinngemäß aus veröffentlichten oder nichtveröffentlichten Schriften entnommen sind, und alle Angaben, die auf mündlichen Auskünften beruhen, sind als solche kenntlich gemacht. Bei den von mir durchgeführten und in der Dissertation erwähnten Untersuchungen habe ich die Grundsätze guter wissenschaftlicher Praxis, wie sie in der „Satzung der Justus-Liebig-Universität Gießen zur Sicherung guter wissenschaftlicher Praxis“ niedergelegt sind, eingehalten. Ich versichere, dass Dritte von mir weder unmittelbar noch mittelbar geldwerte Leistungen für Arbeiten erhalten haben, die im Zusammenhang mit dem Inhalt der vorgelegten Dissertation stehen, und dass die vorgelegte Arbeit weder im Inland noch im Ausland in gleicher oder ähnlicher Form einer anderen Prüfungsbehörde zum Zweck einer Promotion oder eines anderen Prüfungsverfahrens vorgelegt wurde. Alles aus anderen Quellen und von anderen Personen übernommene Material, das in der Arbeit verwendet wurde oder auf das direkt Bezug genommen wird, wurde als solches kenntlich gemacht. Insbesondere wurden alle Personen genannt, die direkt an der Entstehung der vorliegenden Arbeit beteiligt waren.
Mit der Überprüfung meiner Arbeit durch eine Plagiatserkennungssoftware bzw. ein internetbasiertes Softwareprogramm erkläre ich mich einverstanden.“

Datum

Unterschrift

Acknowledgements

Above all, I am grateful to my God for everything, first and foremost, I would like to extend my deepest gratitude to the **DAAD (German: Deutscher Akademischer Austauschdienst)**, who gave me this chance to do my PhD in Germany. I also thank the **Reinhard and Barbara Bretzel Foundation** for financially supporting this study.

During the preparation of this thesis "**Impact of polyunsaturated omega-6 and omega-3 fatty acids on cardiomyogenesis and vasculogenesis of mouse embryonic stem cells**" I was deeply indebted to many persons who have helped me at various stages of the completion of the thesis.

I owe a debt of gratitude to my supervisor **Prof. Dr. Heinrich Sauer** for his initial encouragement for me to undertake PhD work in his group and guidance over the past years, for the interest and the time he devoted for critical reading. I also thank for his constant encouragement and sincere help that enabled me to complete this research work. Also, I would like to thank **Prof. Dr. Maria Wartenberg** for her valuable comments and support.

I express my sincere thanks to **Dr. Fatemeh Sharifpanah**, to her support during my research's time.

My special thanks to **Mrs. Barbara Arnold** for the supply of materials and her technical advice.

I express my sincere thanks to **Prof. Dr. Rainer Schulz** Head of the Department and all members of this institute.

Thanks to **my colleagues**, for all your positivity, help and encouragement.

Special Thanks to **my colleague Dr. Enas Ali** for her support, help chat and laughs over the years.

I am very grateful to the **Ministry of Higher Education and Scientific Research, University of Mosul, College of Veterinary Medicine and Department of Internal and Preventive Veterinary Medicine**.

Lastly, the biggest thank you must go to **my family** for their continuous support. Thank you for always believing in me and encouraging me to do my best, when I stumble and fall, I will always try to overcome. Sorry if I've missed anyone here, I'm sure you'll be mentioned in the thesis elsewhere! All the help given is much appreciated.